Agonist and antagonist peptide ligands of CXCR4 receptor as marker for the anticancer drugs or diagnostic agents delivery

Dr. Luca Monfregola

Dottorato in Scienze Biotecnologiche – XXIII ciclo
Indirizzo Biotecnologie Industriali e Molecolari
Università di Napoli Federico II

Dottorato in Scienze Biotecnologiche – XXIII ciclo
Indirizzo Biotecnologie Industriali e Molecolari
Università di Napoli Federico II

Agonist and antagonist peptide ligands of CXCR4 receptor as marker for the anticancer drugs or diagnostic agents delivery

Dr. Luca Monfregola

Dottorando:	Dr. Luca Monfregola
Relatore:	Prof. Ettore Benedetti
Correlatore:	Dr. Stefania De Luca
Coordinatore:	Prof. Giovanni Sannia

A chi quotidianamente ha condiviso con me questa esperienza, ma soprattutto a chi mi ha messo al mondo.

INDEX

Riassunto pag. 1

Summary pag. 10

Abbrevations pag. 12

1 Introduction pag. 14

1.1 The biological role of chemokines pag. 14

1.2 The chemokines involvement in cancers pag. 16

1.2.1 A role for chemokine recptors in cancer metastasis pag. 17

1.2.2 The role of the CXCR4-CXCL12 axis in cancer pag. 19

1.3 Structure of SDF-1 and hypothesized molecular mechanism of its interaction with CXCR4 receptor pag. 22

1.4 CXCR4 antagonists: AMD3100 and T-140 pag. 24

1.4.1 AMD 3100 pag. 25

1.4.2 T140 pag. 28

1.5 Aims of the project pag. 31

2 Rational design and synthesis of peptide ligands pag. 32

2.1 Rational design pag. 32

2.2 Peptide synthesis pag. 35

3 Biological evaluation pag. 37

3.1 Discussion pag. 41

4 Synthesis of peptide-chelating agent conjugates pag. 43

5 Peptidomimetics design pag. 45

5.1 New N-alkylation procedure of Fmoc-amino acid derivatives pag. 45

5.2 Synthetic strategy to incorporate amino-alkylated building blocks into a peptide sequence pag. 48

6 Conclusion pag. 50

7 Material and methods pag. 51

7.1 Computational methods pag. 51

7.2 Peptide synthesis pag. 51

7.3 Biological test pag. 52

7.4 N-alkylation reaction pag. 54

References pag. 62

Comunications pag. 76

Publications pag. 77

Agonisti ed antagonisti peptidici o peptidomimetici per il recettore delle chemochine CXCR4 come marcatore biologico e target diagnostico-terapeutico

Riassunto

1. Introduzione

Le chemochine costituiscono una famiglia di piccole proteine (8-10 kDa) con attività chemotattica. Esse si dividono in quattro sottofamiglie: CXC (alpha), CC (beta), C (gamma) e CXXXC(delta), a seconda della posizione delle prime due cisteine (Fig. 1) [1]. Il meccanismo d'azione delle chemochine prevede il legame a specifici recettori transmembrana accoppiati a proteine G (GPCR).

Classe	**Dominio N-terminale**	***Nome***
CX3C:	.....CXXXC.....	CX3CL1
CXC:	.....CX__C.....	CXCL#
CC:	.....C___C.....	CCL#
C:	.....C.....	XCL#

Fig.1 Classificazione delle chemochine endogene.

I GPCR sono caratterizzati da un comune dominio centrale costituito da sette eliche transmembranarie, connesse da tre loop intracellulari (i1, i2 ed i3) e da tre loop extracellulari (e1, e2 ed e3) (Fig 2). Due residui di cisteina (uno sull'elica 3 e l'altro sul loop e2), che sono conservati nella maggior parte dei GPCR, formano un ponte disolfuro importante per l'impacchettamento e la stabilizzazione del dominio elicoidale. A parte la variabilità di sequenza, i GPCR differiscono nella lunghezza e nella funzione del dominio extracellulare N-terminale, del dominio C-terminale intracelullare e dei loop intracellulari.

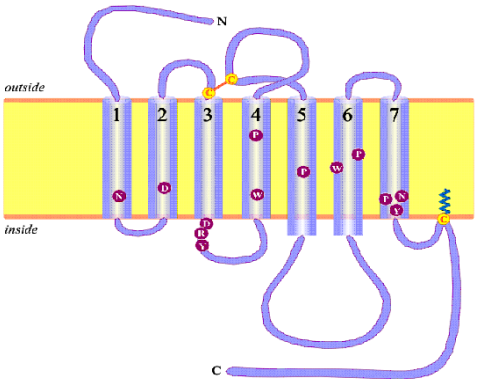

Fig. 2 Rappresentazione schematica dei recettori GPCR.

Le chemochine sono prodotte e rilasciate da una grande varietà di cellule durante la fase iniziale della risposta immunitaria a lesioni, allergeni, antigeni e microorganismi patogeni. Esse svolgono un ruolo centrale nei processi infiammatori, promuovendo l'attivazione e la migrazione dei leucociti presso i focolai di infiammazione. Le chemochine sono altresì coinvolte nell'angiogenesi e nell'ematopoiesi. Il CXCL-12 (o “Stromal Derived Factor” SDF-1α), un membro della famiglia CXC (Cys-X-Cys), è prodotto nei linfonodi, polmoni, fegato e nel midollo osseo ed è un potente chemoattrattore dei linfociti T, neutrofili e cellule staminali ematopoietiche CD34+ e rappresenta l'unico ligando naturale noto del recettore CXCR4, appartenente alla classe della rodopsina della superfamiglia dei recettori GPCR.

Recentemente è stato trovato che le cellule tumorali sovraesprimenti una serie di recettori per chemochine, attraverso l’interazione con specifici ligandi prodotti nei siti di sviluppo delle metastasi, determinano la progressione sia del tumore primario che la destinazione finale delle metastasi. Diversi lavori descrivono la presenza del recettore CXCR4 e della relativa chemochina SDF-1α in numerose neoplasie umane, quali il tumore mammario, il melanoma, il carcinoma del colon, il carcinoma renale, del colon retto, del polmone [2]. In particolare, è stato enfatizzato il ruolo dell’asse CXCR4-CXCL12 nell’homing midollare e quindi nella mobilizzazione di precursori ematopoietici. Nel midollo osseo e nei tessuti linfoidi le cellule tumorali sono in diretto contatto con le cellule stromali (stromal cells and/or “nurselike cells”) che costituiscono il microambiente relativo a diversi stadi della malattia. CXCL12 ha un ampio spettro di effetti in relazione allo sviluppo delle neoplasie,

ma il ruolo primario del CXCL12 è nella mobilizzazione di precursori ematopoietici e nella definizione di una nicchia di cellule staminali neoplastiche in cui l'elevata concentrazione di CXCL12 richiama una sottopopolazione di cellule altamente tumorigeniche e ne promuove sopravvivenza, proliferazione, angiogenesi e diffusione metastatica.
L'importanza dei recettori delle chemochine *in vivo* è stata dimostrata dall'utilizzo di anticorpi specifici per il recettore CXCR4 che significativamente riducono la formazione di metastasi nei linfonodi e nei polmoni in topi immunodeficienti [3].
CXCR4 è espresso costitutivamente in maniera diffusa in una varietà di tessuti sani, tra cui il tessuto linfatico, il tessuto cerebrale, la milza e lo stomaco. Inoltre tale recettore è anche espresso in cellule staminali normali di diversi tessuti incluse le cellule staminali mammarie. Questo suggerisce che CXCR4 è essenziale per quelle cellule staminali che sembrano essere le progenitrici delle cellule tumorali. Il segnale prodotto dall'interazione di questo recettore produce tutta una serie di molecole coinvolte in processi chiave come il controllo del ciclo cellulare e l' apoptosi.
La formazione di metastasi richiede diversi passaggi distinti, tra cui il raggiungimento dei vasi sanguigni da parte di cellule tumorali, la sopravvivenza nella circolazione, il movimento verso un organo secondario, l'adesione e la proliferazione delle cellule tumorali nell'organo e tessuto bersaglio. Secondo studi effettuati in vitro ognuno di questi stadi è potenzialmente regolato da segnali da parte di CXCR4. L'asse CXCR4/ SDF-1α, infatti, attiva una serie di cascate metaboliche che portano alla produzione di molecole che giocano un ruolo chiave nei processi appena elencati. Ad esempio tale interazione stimola la via del fosfatidilinositolo-3-chinasi che attiva la proteina chinasi AKT che porta all'inibizione dell'apoptosi e al prolungamento della vita cellulare in numerosi tipi di cranco. Tale proteina è anche implicata nella proliferazione cellulare e nella migrazione attraverso un gradiente di SDF-1α. La polimerizzazione dell'actina, che determina la mobilità cellulare, e l'attivazione di alcune proteine tiroxina chinasi della famiglia delle src, che attivano l'adesione della cellula a componenti esterne, derivano dall' interazione CXCR4/ SDF-1α. Infine, anche il processo di angiogenesi sembra scaturire da tale interazione attraverso la non regolata produzione di VEGF (Vascular Endothelial Growth Factor) [4].
Da tali evidenze consegue che l'asse CXCR4/ SDF-1α gioca un ruolo fondamentale nella diffusione e nella progressione di numerosi tipi di tumore, quindi, sia SDF-1 che CXCR4 potrebbero essere utili bersagli di nuovi agenti terapeutici e diagnostici nell'ambito delle patologie tumorali.

2. Premesse scientifiche ed obiettivi del progetto di dottorato

Le strutture delle chemochine finora risolte sono molto simili e sono caratterizzate da un dominio centrale formato da tre β-strand con sopra adagiata un'elica C-terminale. Gli strand sono preceduti da una regione N-terminale, il motivo CXC o CC ed un loop esteso (chiamato N-loop). Diversi studi di relazione struttura-attività hanno evidenziato l'importanza del dominio N-terminale, del motivo disolfuro e dell'N-loop che precede il caratteristico dominio CXC della chemochina SDF1 per il legame e l'attivazione del recettore [5]. E' stato infatti ipotizzato un meccanismo di interazione a due stadi compatibile con le relazioni struttura-funzione trovate per altre chemochine, dove il motivo RFFESH (12-17) costituisce il primo contatto tra il recettore e il suo ligando permettendo cosi l'accesso ad un sito più ingombrato. Infatti nel secondo stadio del processo di interazione i residui N-terminali 1-8, determinanti per l'attivazione del recettore, interagiscono con le eliche transmembrana inducendo un cambiamento nella conformazione del recettore e, quindi, consentendo la trasmissione del segnale (Fig. 3) [6].

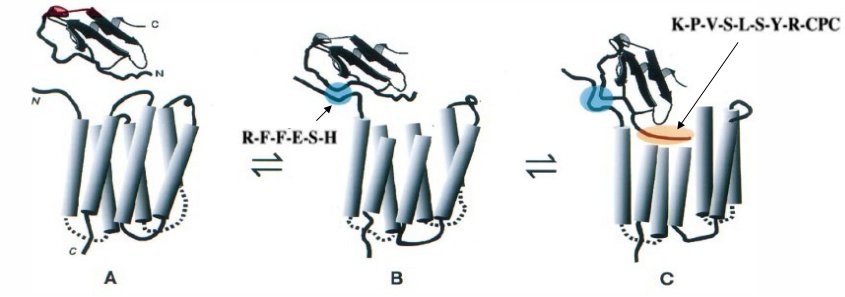

Fig. 3 Meccanismo di interazione ipotizzato per il complesso CXCR4/CXCL12.

Il CXCR4 è stato inoltre identificato come co-recettore per la fusione ed infezione delle cellule T da parte del virus HIV-1 [7]. L'ingresso del virus nella cellula ospite è mediato dall'interazione di alcune glicoproteine dell'involucro virale (gp120 e gp41) con recettori della cellula ospite (CD4 e CCR5 o CXCR4), attraverso una complessa sequenza di eventi molecolari.
L'antagonista più diffuso per il recettore CXCR4 è l' AMD3100 [8], una molecola biciclica inizialmente utilizzata nel trattamento dell' HIV. Sebbene l'AMD3100 risulti un rapido ed efficiente agente mobilizzante, esso ha, tuttavia, rivelato in precedenti studi scarsa biodisponibilità, tossicità epatica, cardiaca e cerebrale. Inoltre sono stati descritti diversi peptidi, quali il T140 e i suoi derivati, che mostrano una discreta attività antagonista verso il recettore CXCR4. Recentemente sono stati anche sviluppati peptidi ciclici, quali FC130, in modo da ottenere antagonisti a più basso peso molecolare rispetto al T140 [9].
Poiché CXCR4 e altri recettori per chemochine omologhi rappresentano bersagli promettenti e al momento è disponibile un numero limitato di molecole attive, spesso dotate di considerevoli effetti collaterali negativi, esiste una forte richiesta di nuove molecole dotate di incrementata attività biologica, azione selettiva sui differenti pathway associati ai recettori e, quindi, minori effetti collaterali.
Sulla base di tali considerazioni, l'attività di ricerca è stata focalizzata sulla progettazione, sintesi e valutazione dell'attività biologica di nuovi ligandi peptidici dotati di una buona affinità verso il recettore CXCR4, in modo da essere utilizzati come agenti terapeutici, in grado di modulare le caratteristiche funzionali del recettore target, o come marker diagnostici per patologie tumorali. Individuato un motivo strutturale dotato di una buona affinità col recettore target e che possa essere utilizzato come templato per lo sviluppo di ligandi biologicamente attivi verso il CXCR4, come passo successivo, è stato elaborata una nuova strategia sintetica per la preparazione di aminoacidi modificati in catena laterale da usare come building block nella sintesi di peptidomimetici.

3. Progettazione e sintesi di ligandi peptidici

Il sarcoma di Kaposi (KS) è una lesione tumorale che insorge frequentemente negli individui immunodeficienti. L'herpesvirus associato al KS è l'agente infettivo responsabile della malattia e, sorprendentemente, codifica diverse proteine che possiedono una diretta controparte nel sistema immunitario, in particolare proteine "chemokine-like" che hanno approssimativamente una identità del 40% rispetto alle chemochine umane. Per una di queste, vMIP-II, è stato dimostrato che lega ed inibisce recettori appartenenti alla classe CXC, CC e XC, bloccando il flusso di calcio attivato dai recettori CCR1, CCR2, CCR5, CCR8, CXCR4 e XCR1 [10]. Come per SDF-1α, la regione N-terminale e l'N-loop sono essenziali per l'interazione recettoriale. In particolare è stato dimostrato che la regione N-terminale (residui 1-10) da sola è sufficiente per legare il recettore CXCR4 e per esplicare l'attività antagonista [11].

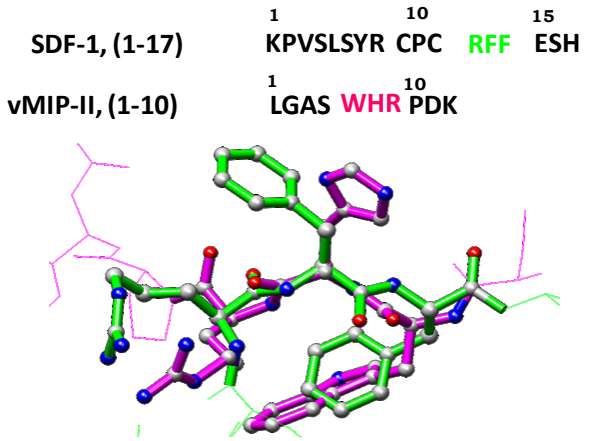

Fig.4 Sovrapposizione della struttura tridimensionale del motivo analogo di SDF-1α (verde) e vMIP-II (magenta).

Il confronto sequenza-struttura fra le regioni N-termiale di SDF1 e vMIP-II mostra la conservazione per un motivo strutturale associato ad una sequenza omologa, seppur invertita di senso (Fig.4). Tale motivo prevede i residui Ar-X-R (riferito al senso di vMIP-II), dove Ar è un residuo aromatico e X è un anello aromatico o insaturo. In particolare la sequenza è R^{12}-F-F^{14} per SDF1 e W^{5}-H-R^{7} per vMIP-II.

Ipotizzando per questa associazione sequenza-struttura un ruolo fondamentale nel binding e traendo spunto dalle sequenze e strutture disponibili, sono stati disegnati 18 peptidi al fine di:

- convalidare le ipotesi sulle relazioni sequenza-struttura-attività e, in particolare, sull'invarianza del senso della sequenza,
- determinare i requisiti minimi di sequenza per l'attività biologica;
- individuare e misurare le influenze sul binding complessivo di singoli residui e/o gruppi terminali.

Un'analisi preliminare dei motivi individuati in SDF-1a e vMIP-II ha condotto al design di una prima generazione di peptidi in cui la conformazione desiderata sia favorita dalla formazione di ponti disolfuro, e il motivo di binding sia limitato a soli residui aromatici, o anelli insaturi, e uno o due basici (Fig. 5). I motivi di residui aromatici sono stati derivati dalle sequenze di SDF-1α e vMIP-II, introducendo variazioni sulla natura del secondo residuo aromatico nelle sequenze di vMIP-II e variando anche il verso del peptide e la terminazione ai due estremi.

Tutti i peptidi sono stati sintetizzati in fase solida utilizzando i protocolli della chimica Fmoc. Il primo amminoacido è stato legato alla resina seguendo i protocolli standard riportati in letteratura [12] e l'efficienza di tale reazione è stata valutata mediante test Fmoc. Le reazioni di accoppiamento di tutti gli aminoacidi sono state effettuate due volte per 30 minuti in DMF, utilizzando un eccesso di quattro equivalenti per ogni amminoacido, PyBop e HOBt come attivanti e DIPEA come base.

Il distacco dei peptidi dal supporto solido e la contemporanea rimozione di gruppi protettori presenti in catena laterale di ciascun aminoacido è stata eseguita sospendendo il peptide-resina in una soluzione di acido trifluoroacetico contenente acqua ed etandiolo come scavinger. A

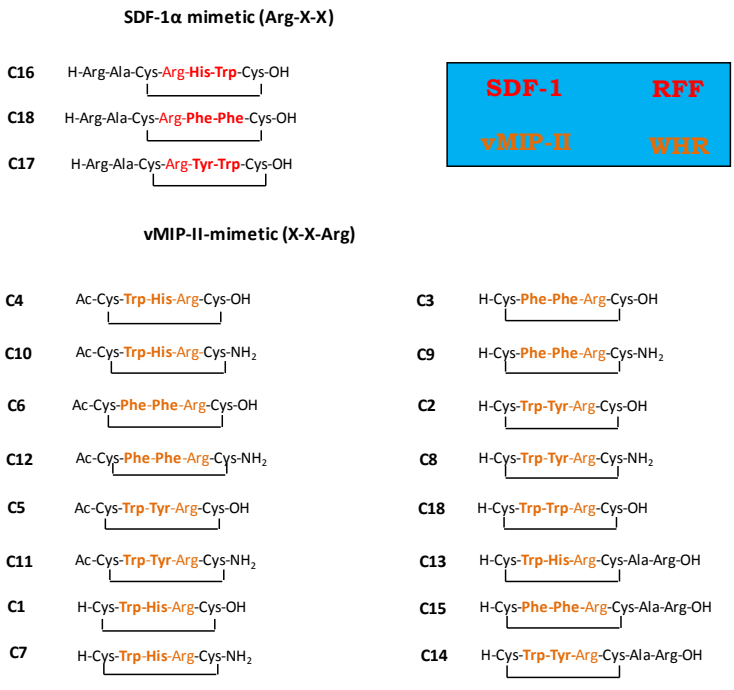

Fig.5 Sequenze aminoacidiche dei peptidi sintetizzati.

tale reazione, durata circa tre ore, è seguita un filtrazione allo scopo di eliminare le particelle di resina. Il filtrato è stato quindi concentrato ed il prodotto grezzo desiderato è stato isolato per precipitazione in etere freddo. La reazione di ciclizzazione, attraverso la formazione di un ponte disolfuro tra due residui di cisteina, è avvenuta sospendendo il peptide grezzo in una soluzione acquosa 0.1 M di NH_4HCO_3. Dopo quattro ore la miscela di reazione è stata concentrata e il prodotto desiderato è stato isolato, con buone rese e con alta purezza, attraverso l'utilizzo di tecniche cromatografiche in fase inversa.
I peptidi ammidati al C-terminale sono stati ottenuti utilizzando un resina Rink Amide come supporto solido, mentre i peptidi Acetilati all' N-terminale sono stati ottenuti effettuando la reazione di acetilazione con anidride acetica e piridina prima di distaccare il peptide dalla resina.

4. Saggi Biologici

Allo scopo di valutare la capacità dei peptidi sintetizzati di modulare la funzionalità dell'asse CXCR4/SDF-1α, sono stati effettuati una serie di saggi biologici volti alla valutazione dei singoli eventi legati all'attivazione del recettore. Tali saggi hanno rilevato un'attività biologica in vitro dei peptidi saggiati sia antagonista che agonista sull'attivazione del recettore. In particolare i saggi effettuati sono i seguenti: a) la valutazione citofluorimetrica della liberazione di Ca^{2+} in seguito alla stimolazione con SDF-1α; b) la modulazione della capacità migratoria cellulare in presenza o assenza dello specifico ligando SDF-1α; c) la modulazione dell'attivazione di ERK-1,2; d) l'inibizione del legame al recettore target da parte di specifici anticorpi coniugati a sonde fluorescenti. In particolare, alcuni dei peptidi sviluppati hanno mostrato azione antagonista, rispetto all'induzione di migrazione indotta dal ligando, quasi comparabile all'inibitore meglio caratterizzato, AMD3100.
I peptidi candidati che si sono rivelati inibenti in misura maggiore in tutti i saggi eseguiti sono: **C16**, **C18** e **C1**. Su tali sequenze peptidiche è stato eseguito un saggio *in vivo,* adoperando un modello murino di cellule di melanoma B16 precedentemente trasdotte con il recettore CXCR4 ed inoculate in un sistema di topo immunocompetente C57 Black.
L'analisi macroscopica e microscopica ha dimostrato un numero significativamente ridotto di metastasi polmonari nei gruppi di topi trattati con i peptidi **C18**, **C16**, **C1**. Nel dettaglio però la sequenza peptidica che ha mostrato maggiore capacità di ridurre il numero delle metastasi è **C 18** (Fig. 6)**.**
Pertanto, i peptidi sviluppati, opportunamente selezionati, potrebbero essere impiegati come agenti antitumorali o per la diagnosi di neoplasie.

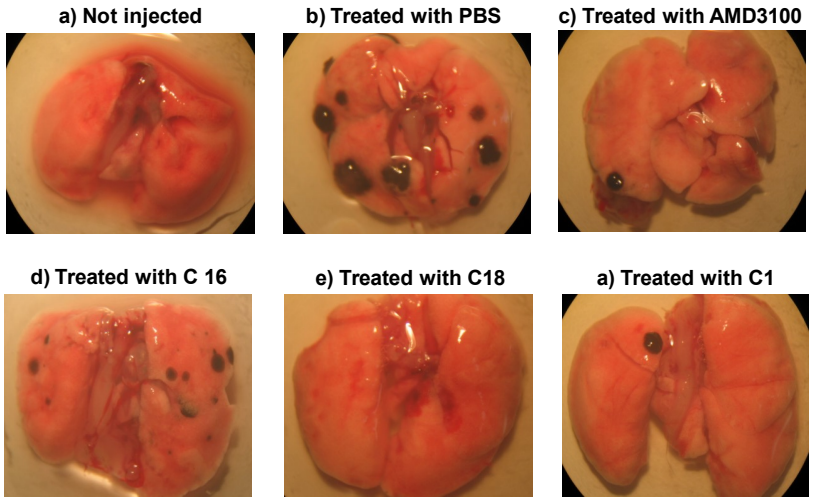

Fig.6 Metastasi polmonari dei topi trattati con i peptidi C18, C16, C1.

5. Sintesi di Coniugati chelante-peptide

Al fine di effettuare studi di imaging paramagnetico ed eventualmente radioattivo, sono stati progettati e sintetizzati coniugati in cui la sequenza di **C18** è covalentemente legata ad un agente chelante.

Allo scopo di esplorare la posizione di funzionalizzazione della sequenza peptidica più attiva, senza disturbare l'interazione del peptide col recettore target, l'agente chelante è stato inserito in due posizioni diverse della sequenza di **C18**: la catena laterale di un residuo di lisina inserito nel segmento peptidico (**C19**) e la sua estremità N-terminale (**C20**) (Schema 1).

L'agente chelante scelto è il DTPA (Acido dietilentriamminopentacetico). Tale chelante è in grado di formare complessi stabili sia con il radioisotopo $^{111}In^{+3}$, per applicazioni in medicina nucleare, sia con lo ione metallico Gd^{+3} per applicazioni come agente di contrasto NMRI.

La sequenza peptidica di Ciclo-Phe 7 INV è stata modificata mediante sostituzione di Ala2 con un residuo di Lys. L'obiettivo è stato quello di legare il DTPA in catena laterale al residuo di lisina, in modo da essere sufficientemente distante dal backbone peptidico e quindi non influenzarne il binding con il recettore.

Il DTPA-tetra (t-Bu estere) è stato coniugato, attraverso il suo gruppo carbossilico libero, all' ε-NH_2 della Lys2. Tale residuo di lisina è stato introdotto nella catena peptidica protetto con gruppo Fmoc sull'alfa-NH2 e con un gruppo Mtt sull' ε-NH2 (Schema 1). Ciò ha consentito la rimozione selettiva del gruppo Mtt sull' ε-NH2 effettuata con ripetuti lavaggi della resina-peptide con una soluzione di 1%TFA in DCM, in presenza di TIS come scavenger. L'ancoraggio del chelante è stato successivamente eseguito utilizzando lo stesso protocollo di attivazione (HBTU/HOBt/DIPEA) impiegato per gli accoppiamenti in fase solida.

Successivamente, la sequenza di **C18** è stata funzionalizzata con il chelante DTPA sull' NH_2 terminale. Terminata la sintesi del segmento peptidico, dopo rimozione del gruppo Fmoc, l'ancoraggio del chelante è stato eseguito utilizzando il protocollo di attivazione (HBTU/HOBt/DIPEA) impiegato per gli accoppiamenti degli aminoacidi (Schema 1).

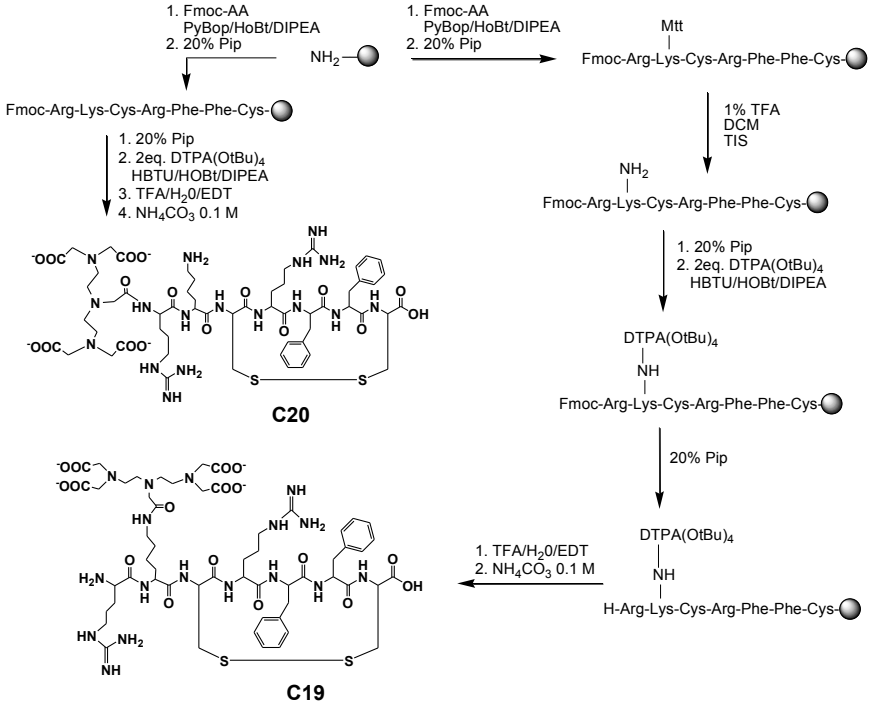

Schema 1. Strategia sintetica dei coniugati C19 e C20.

I coniugati ottenuti **C19** e **C20**, dopo essere stati ciclizzati e purificati con l'utilizzo di tecniche cromatografiche in fase inversa, sono stati saggiati mediante saggio di inibizione

del legame al recettore target di anticorpi fluorescenti. I risultai di tali studi hanno purtroppo evidenziato una ridotta affinità del coniutato **C19** per il CXCR4 rispetto all'affinità mostrata dal solo peptide **C18**. Per ciò che riguarda il coniugato **C20**, sono attualmente in corso gli esperimenti di binding che ci consentiranno di valutare se il composto conserva un'affinità per il recettore utile agli scopi di utilizzo dello stesso coniugato come sonda in esami di imaging diagnostico.

6. Progettazione e sintesi di peptidomimetici

La sequenza peptidica di **C18** si è rivelata la più attiva nei saggi biologici effettuati sia in vivo che in vitro. In particolare, il motivo Arg-Phe-Phe del peptide in oggetto è stato individuato come nucleo farmacoforico, ossia principale motivo strutturale responsabile dell'interazione con il recettore target. Ciò ha suggerito la possibilità di sintetizzare peptidomimetici di **C18**, che consentano di variare la disposizione spaziale dei residui aromatici del nucleo farmacoforico, in modo da stabilizzarne la conformazione bioattiva.

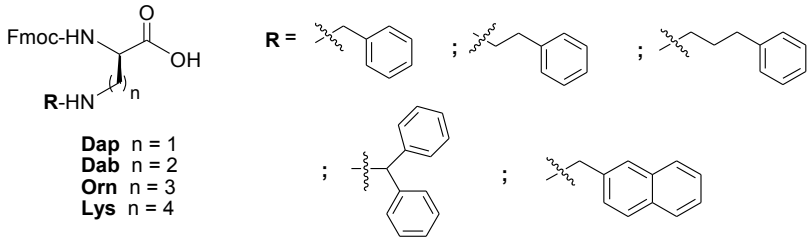

Fig. 7 Derivati N-alchilati di Dap, Dab, Orn e Lys

E' stata progettata una libreria di peptidomimetici in cui i residui di Phe3 e Phe4 di **C18** sono sostituiti con derivati di vari aminoacidi, quali Lys e i suoi omologhi inferiori, modificati in catena laterale mediante reazioni di N-alchilazione, che hanno consentito di introdurre diversi sostituenti aromatici (Fig. 7). La realizzazione di tali obiettivi ha previsto innanzitutto la messa a punto di una strategia di sintesi di building block da inserire nella sequenza peptidica.

E' stata, quindi, elaborata una efficiente procedura sintetitica che permette di ottenere amminoacidi basici N-alchilati in catena laterale [13]. In particolare, Lys, Orn, Dab a Dap sono stati funzionalizzati in catena laterale mediante una procedura di N-alchilazione. Tale procedura risulta semplice, efficiente e riproducibile su scale superiori, in modo da poter utilizzare gli N^{α}-Fmoc amminoacidi alchilati ottenuti come building blocks da inserire nella sintesi dei peptidomimetici desiderati. Lo scopo è quello di sviluppare una procedura generale con condizione blande di N-alchilazione, che non influenzino né la stereochimica dell' aminoacido, né gli altri gruppi funzionali e/o protettori presenti sul substrato da alchilare (α-COOH e Fmoc/Boc).

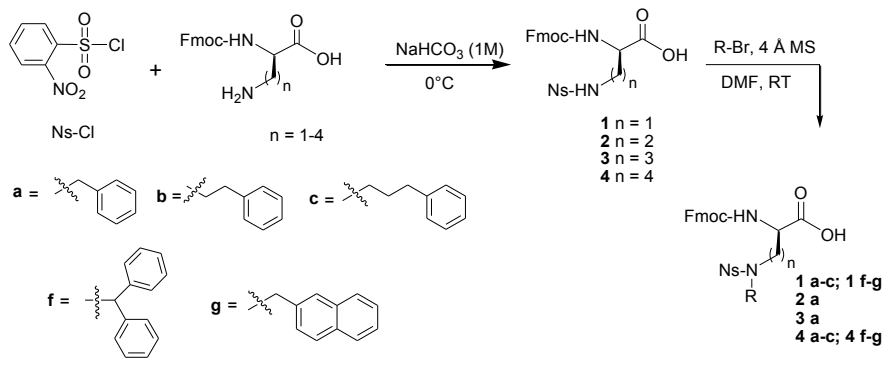

Schema 2 Strategia sintetica dei building block N-alchilati

Come mostrato nello schema 2, la strategia sintetica impiegata prevede il trattamento di ogni N^{α}-Fmoc amminoacido, opportunamente attivato in catena laterale col gruppo o-NBS e sciolto in DMF, solo con l'appropiato alogenuro alchilico e in presenza di setacci molecolari di 4 Å come base blanda. Tale procedura porta a rese quantitative, permettendo così di utilizzare il composto ottenuto direttamente (senza passaggi di purificazione) per la fase successiva di assemblaggio del peptidomimetico. Al fine di rendere generale l'utilizzo di tale metodologia, la procedura è

stata impiegata utilizzando diversi agenti alchilanti; la resa e i tempi di reazione sono descritti nella Tab.1.

Composto	Tempo (h)	Resa (%)	R-X	Composto	Tempo (h)	Resa (%)	R-X
1a	15	>95	Br-Bn	**3a**	18	>95	Br-Bn
1b	15	95	Br-$(CH_2)_2$-Ph	**4a**	22	>95	Br-Bn
1c	15	95	Br-$(CH_2)_3$-Ph	**4b**	22	90	Br-$(CH_2)_2$-Ph
1f	38	70	Br-$CH(Ph)_2$	**4c**	24	<70	Br-$(CH_2)_3$-Ph
1g	18	95	Br-CH_2-Naph	**4f**	48	50	Br-$CH(Ph)_2$
2a	18	>95	Br-Bn	**4g**	22	90	Br-CH_2-Naph

Tab 1. Rese e tempi di reazione dei building block sintetizzati.

7. Conclusioni e prospettive future

Il lavoro svolto durante il corso di dottorato ha portato allo sviluppo di ligandi peptidici alcuni dei quali hanno esibito un'azione antagonista, rispetto all'induzione di migrazione indotta dal ligando, quasi comparabile all'inibitore meglio caratterizzato (AMD3100) del recettore target CXCR4. Lo studio condotto in vivo relativo al saggio di metastasi polmonari di melanoma ha dimostrato un numero significativamente ridotto di metastasi polmonari nei gruppi di topi trattati con alcuni dei peptidi sviluppati. Pertanto, essi, opportunamente selezionati, potrebbero in futuro essere impiegati come agenti antitumorali o per la diagnosi di neoplasie.

Inoltre, sono state messe a punto strategie di sintesi allo scopo di preparare aminoacidi modificati da utilizzare per la sintesi di una libreria di peptidomimetici. Lo scopo, infatti, è quello di introdurre motivi strutturali in grado di stabilizzare la conformazione bioattiva del peptide che si è rivelato più attivo nei saggi biologici eseguiti. Parallelamente, in futuro il lavoro di progettazione e sintesi sarà focalizzato sullo sviluppo di una seconda generazione di peptidi caratterizzati da strutture omo- o eterodimeriche. Tale obiettivo nasce dalle numerose evidenze sperimentali che hanno rilevato che frammenti peptidici della porzione N-terminale di SDF-1, già da soli attivi verso il recettore CXCR4, mostrano maggiore affinità ed attività se inseriti in omodimeri [5]. Su tali basi sarà quindi possibile utilizzare le sequenze più attive dei peptidi di prima generazione per sintetizzare una seconda generazione di antagonisti del recettore CXCR4 di natura omo- o etero dimerica.

Bibliografia

[1] Zlotnik, A. & Yoshie, O. Chemokines: a new classification system and their role in immunity. *Immunity* 12:121–127 (**2000**).

[2] Burger, J.A. Kipps, T.J. CXCR4: a key receptor in the crosstalk between tumor cells and their microenvironment. *Blood* 107:1761–1767 (**2006**).

[3] Muller, A. *et al.* Involvement of chemokine receptors in breast cancer metastasis. *Nature* 410:50–56 (**2001**).

[4] Luker, K.E. and Luker G.D. Functions of CXCL12 and CXCR4 in breast cancer. *Cancer Letters* 238:30-41(**2006**).

[5] Loetscher, P. Gong, J.H. Dewald, B. Baggiolini, M. and Clark-Lewis, I.N-terminal Peptides of Stromal Cell-derived Factor-1 with CXC Chemokine Receptor 4 Agonist and Antagonist Activities. *J Biol Chem.* 273(35):22279-22283 (**1998**).

[6] Crump, M.P. Gong, J.H. Loetscher, P. Rajarathnam, K. Amara, A. Arenzana-Seisdedos, F. Virelizier, J.L. Baggiolini. M. Solution structure and basis for functional activity of stromal cell-derived factor-1; dissociation of CXCR4 activation from binding and inhibition of HIV-1. *EMBO J.* 16:6996-7007 (**1997**).
[7] Feng, Y. Broder, C.C. Kennedy, P.E. Berger, E.A. HIV-1 entry cofactor: functional cDNA cloning of a seven-transmembrane, G protein-coupled receptor. *Science* 272:872-877 (**1996**).
[8] Rosenkilde, M.M. Gerlach, L.O. Hatse, S. Skerlj, R.T. Schols, D. Bridger, G.J. and. Schwartz, T.W. Molecular Mechanism of Action of Monocyclam *Versus* Bicyclam Non-peptide Antagonists in the CXCR4 Chemokine Receptor. *The Journal of Biological Chemistry* 282:27354–27365 (**2007**).
[9] Tamamura, H. Tsutsumi, H. Nomura, W. and Fujii, N. Exploratory Studies on Development of the Chemokine Receptor CXCR4 Antagonists Toward Downsizing. *Perspectives in Medicinal Chemistry* 2:1–9 (**2008**).
[10] Shan, L. Qiao, X. Oldham, E. Catron, D. Kaminski, H. Lundell, D. Zlotnik, A. Gustafson, E. and Hedrick, J.A.. Identification of viral macrophage inflammatory protein (vMIP)-II as a ligand for GPR5/XCR1. *Biochem. Biophys. Res. Commun.* 268(3):938-41 (**2000**).
[11] Crump, M.P. Elisseeva, E. Gong, J.H. Clark-Lewis, I. Sykes, B.D. Structure/function of human herpesvirus-8 MIP-II (1–71) and the antagonist N-terminal segment (1–10). *FEBS Lett.* 489(2-3):171-5 (**2001**).
[12] Sheppard, R.C. and Williams, B.J. Acid-labile resin linkage agents for use in solid phase peptide synthesis. *Int. J. Peptide Protein Res*. 20:451–454 (**1982**).
[13] Monfregola, L. and De Luca, S. Synthetic Strategy for Side Chain mono-N-Alkylation of Fmoc-amino Acids Promoted by Molecular Sieves. *Amino Acids* In press (**2010**)

Summary

Chemokines are a family of small low molecular weight secreted cytokines that regulate cell migration by activating a set of G-protein-coupled receptors (GPCRs). Beside the physiologic role, chemokines and their receptors participate in numerous disease states, including HIV/AIDS, asthma, autoimmune diseases, and cancer. Over expression of CXCR4 receptor and over production of its only ligand, the chemokine CXCL12 (also called stromal cell-derived factor-1, SDF-1), was described in brain neoplasm, neuroblastoma cells, colorectal cancer, prostate cancer, melanoma,renal cell cancer, ovarian cancer, and others. Because it directs stem-cell homing and participates in nearly every aspect of cancer progressions, growth, metastasis and neovascularization, the CXCL12/CXCR4 signaling axis is of increasing interest for drug discovery. Among the CXCR4 inhibitors there are two major classes of CXCR4 antagonists, small-molecule antagonists (AMD3100 and its analogs) and peptidomimetics (T140 and its analogs).
As for other chemokines, structure-activity studies of SDF-1 have shown the critical role of the N-terminal region for both receptor binding and activation and in particular the residues 1-8 and 12-17, these last being located in the loop region.
vMIP-II, a CC chemokine-like protein encoded by Kaposi's sarcoma-associated herpesvirus, binds and blocks chemokine receptors belonging to the CXC, CC and XC class, such as CCR1, CCR2. CCR5, CCR8, XCR1 and CXCR4. As for SDF-1, the N-terminus and the N-loop are essential for receptor binding. In particular it was demonstrated that the N-terminus alone, encompassing residues 1-10, is sufficient for binding and antagonizing CXCR4 receptor. Therefore in this study we have focused on a sequence-structure comparison between the N-terminal regions of SDF-1 and vMIP-II, with the aim of looking for a possible common motif responsible for the binding to CXCR4. On the basis of this comparison, several cyclic peptides containing a putative common motif have been designed, studied by molecular dynamics simulations and then synthesized. The peptides differ in: a) nature of the aromatic residues; b) sequence sense; c) N- and C-termination, as all combinations of free, single- and double-protected (by acetylation and amidation) termini were tested on selected peptides; d) possible elongation at either peptide termini by a Arg-Ala sequence. Their activity has been tested by different essays addressing some of the many physiological and pathological functions of CXCR4 receptor: Binding through flow cytometry, modulation of intracellular Ca^{2+} release, modulation of cell migration in presence or without specific ligand SDF-1 and Modulation of P-Erk activation.
The pattern of biological responses elicited by these peptides was, heterogeneous demonstrating agonism, antagonism and no interference for the same peptide in different assays. These results cannot be explained simple models interaction receptor activation/inhibition and suggest more complex scenario considering direct CXCL12-peptide interactions and/or influence on symmetry, stoichiometry or structural variations of the homo- or hetero-oligomeric state of CXCR4 receptor. Among the peptides with consistent inhibitory activity on CXCR4 four peptides were identified: peptides C1, C16, C17 and C18. In particular peptide C16 is inhibitor in all the evaluated *in vitro* assays performed. Based on these results, the *in vivo* effect on metastases formation was tested. The peptides (C1, C16 and C18) significantly inhibited melanoma metastases and preliminary results showed that renal cancer cells xenograft SN12C-pEGFP was significantly reduced in growth in the presence of peptides C1, C16 and C18.
As a subsequent step, it was evaluated the possibility to develop peptide C18 derivative bearing a chelating agent able to coordinate radioactive metals for applications in cancer diagnosis by nuclear medicine techniques. In order to investigate the chelating agent site of linkage which does not interfere on the peptide-receptor interaction, two

diethylentriaminopentacetic acid (DTPA)-C18 conjugates were synthesized: one carrying DTPA moiety covalently bound to petide N-terminus (C20) and one carrying the chelating moiety DTPA covalently bound to the epsilon-NH2 of a lysine residue which replaced Ala2 of C18 (C19).
Before performing nuclear medicine imaging studies, C19 and C20 were evaluated for their ability to inhibit the specific antibody binding to CXCR4. Both conjugates exhibited a reduced inhibiting activity, compared with that exerted by the only peptide sequence (C18). These results highlighted that the introduction of the chelating agent on the N-terminus, as well as on the lysine epsilon-NH2 group, can affect the binding process with the receptor target. We are currently exploring other peptide positions where to anchor the DTPA moiety.
Since the pharmacophoric motif of the most active peptide sequence (C18) is characterized by aromatic rings and idrofobic residues, it is possible to project peptidomimetics in order to modulate the aromatic rings distance from the peptide backbone. In particular, Phe3 and Phe4 residues of C18 can be replaced by aminobenzilic derivatives, such as Nε-benzylated Lys and its shorter homologues, in order to evaluate the influence of the more flexible pharmacoforic motif on the binding process. The final goal has been to introduce conformational constraint into the peptide sequence by which it would be possible to stabilize the so-called 'bioactive' conformation, that is the peptide conformation required for receptor binding and activation.
On these basis, we focused on an alternative and more practical synthetic strategy in solution and in solid phase in order to obtain modified amino acids to be used as a building block in peptidomimetic synthesis. In particular we performed the alkylation reaction on several Fmoc-amino acids, protected on their side chain, (Fmoc-Lys(P)-OH, Fmoc-Orn(P)-OH, Fmoc-Dab(P)-OH Fmoc-Dap(P)-OH) only in presence of 4 Å molecular sieves and alkyl halides. This methodology was validated for different amino protecting groups, but the best results were obtained by using *o*-Ns protected Fmoc-amino acids. Furthermore, for the majority of the employed halides, the procedure is a one-pot synthesis which avoids the purification after each reaction step. As final step we verified the applicability of building block synthesized by introducing one of them into a peptide sequence using the standard Fmoc-based solid phase protocol.
Data complied and the methodology developed open new perspectives in obtaining more selective compounds toward different biological pathways involving CXCR4 receptor. In this regard, the forthcoming activity will be focused on the development of peptidomimetics that allow stabilizing conformation required for receptor binding and activation. Moreover, dimers of the most active peptides will be also synthesized and tested for their biological activity, in order to evaluate any potential improvement of it compared with the activity exerted by the corresponding monomeric peptide sequence.

Abbreviation

Ac_2O	Acetic anhydride
AKT	Adenosine kinasi transfer
AIDS	Acquired immune deficiency syndrome
Alloc	Allyloxycarbonyl
Boc	Butossicarbonyl
BSA	Bovine serum albumin
cf	Amide group C-terminations
cf	Free carboxylate C-terminations
CLL	Chronic lymphocytic leukaemia
DBU	1,8- Diazabicyclo[5.4.0]undec-7-ene
DCM	Dicloromethan
DIPEA	Diisopropilethylammina
DTPA	Diethylentriaminopentacetic
DMF	Dimethylformammide
DMSO	Dimethyl sulfoxide
ECM	Extracellular matrix
EDT	Ethanedithiol
EDTA	Ethylenediaminetetraacetic acid
EGTA	Ethylene glycol tetraacetic acid
Env	Viral envelope
ERK	Extracellular Signal-Regulated Protein kinase
ESI-MS	Electrospray Ionization-Mass Spectrometry
FCS	Fetal calf serum
FBS	Precolostral bovine Serum
Fmoc	9-Fluorenilmetossicarbonyl
GPCRs	G protein coupled receptors
HATU	2-(1H-9-Azobenzotriazole-1-yl)-1,1,3,3,-tetramethyluronium
HCl	Cloridric acid
HBTU	2-(1H-Benzotriazole-1-ile)-1,1,3,3-tetramethyluronium esafluoro phosphate
HIF	Hypoxia-inducible factor
HIV-1	Human immunodeficiency virus
HL-60 cells	Human promyelocytic leukemia cells
HOBt	Hydroxybenzotriazole
HRMS	High resolution mass spectrometry
HSC	Haematopoietic stem cells
IMDM	Iscove's Modified Dulbecco's Media
K_2CO_3	Potassium carbonate
LC-ES-MS	Liquid chromatography-electrospray mas
LC-MS	Liquid chromatography-mass spectrometry
LiOH	Lithium hydroxide
MAPKinase	Mitogen-Activated Protein Kinase
MBHA	4-methylbenzhydrylamine
MD	Molecular dynamics
MEK	Mitogen extracellular signal regulated kinase
MMP	Matrix Metalloproteinases
MS	Molecular sieves
Mtt	Methyl trityl group
nac	Acetyl group peptide N-terminations
naf	Free amino group peptide N-terminations

NaH	Sodium hydrure
NAMD	Not Another Molecular Dynamics program
NaOH	Sodium hydroxide
NK	Natural killer
NH_4HCO_3	Ammonium Bicarbonate
NMR	Nuclear magnetic resonance spectroscopy
NOE	Nuclear Overhauser Effect.
Ns	Nitrobenzensulfonyl
OtBu	O-tert-Butyl
PDB	Protein data bank
Pbf	2,2,4,6,7-pentamethyl-2,3-dihydrobenzofuran-5-ylsulfonyl
Pip	Piperidine
PyBop	benzotriazol-1-yl-oxytripyrrolidinophosphonium hexafluorophosphate
QTOF	Quadrupole time-of-flight
RAFT	Related adhesion focal tyrosine kinase
r.m.s.d.	Root mean square deviation
RP-HPLC	Reversed phase high performance liquid chromatography
RPMI	Roswell Park Memorial Institute medium
SDF-1	Stromal cell-derived factor-1
tBu	t-Butyl
TIS	Triisopropylsilane
TFA	Trifluoroacetic acid
TH2	T-helper 2
Trt	Trityl
VEGF	Vascular Endothelial Growth factor
vMIP-II	Viral macrophage inflammatory protein-II

1. Introduction

1.1 The biological role of chemokines

Chemokines comprise a family of low molecular weight chemotactic cytokines, which are implicated in many biological processes, such as migration of leukocytes, embryogenesis, angiogenesis, hematopoiesis and atherosclerosis [1-3]. Chemokine signalling results in the transcription of target genes that are involved in cell invasion, motility, interactions with the extracellular matrix (ECM) and survival [4]. These chemotactic cytokines can be classified into two main groups based on their function and pattern of expression: homeostatic and inflammatory chemokines. The homeostatic chemokines (examples in this group include CCL21, CCL19, CXCL13, CXCL12 and TECK) are constitutively expressed in certain cell types and tissues, and play a vital role in the development and maintenance (homeostasis) of the hematopoietic and the immune system. In contrast, the inflammatory chemokines (typical examples include CXCL8, CCL24, CCL2, CXCL10, CCL4 and CCL5) are not constitutively expressed but are inducible and up-regulated by inflammatory stimuli. Their expression is tightly controlled by the local pro-inflammatory cytokine milieu. Directed migration of cells that express the appropriate chemokine receptor occurs along a chemical gradient of ligand — known as the chemokine gradient — allowing cells to move towards high local concentrations of chemokines (Fig. 1).

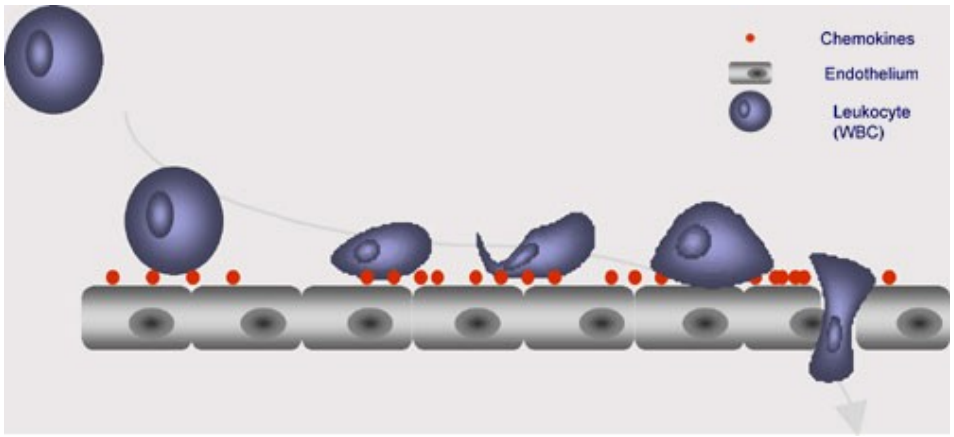

Figure 1 Leukocyte (immune cell) adhesion and migration along and penetration through the wall of a blood vessel under the influence of a CK gradient and vascular sheer flow.

The small (8–10 kDa) chemokine proteins are classified into four highly conserved groups — CXC, CC, C and CX3C — depending on the positioning of the conserved cysteines in the aminoterminal part of these small inducible proteins [3]. The CXC or α subgroup is further subdivided in ELR+ and ELR- chemokines, based on the presence or absence of the tripeptide glutamic acid-leucine-arginine (the 'ELR' motif) preceding the CXC domain. The ELR+ CXC chemokines, such as interleukin-8 (CXCL8/IL-8), are angiogenic, whereas most ELR- CXC chemokines, like platelet factor-4 (CXCL4/PF-4) inhibit angiogenesis [5]. This 'ELR' motif appears to be important in ligand/receptor interactions on neutrophils [6–8]. An exception of the relation between the 'ELR' motif and angiogenesis is CXCL12/SDF-1, an angiogenic ELR- CXC chemokine.

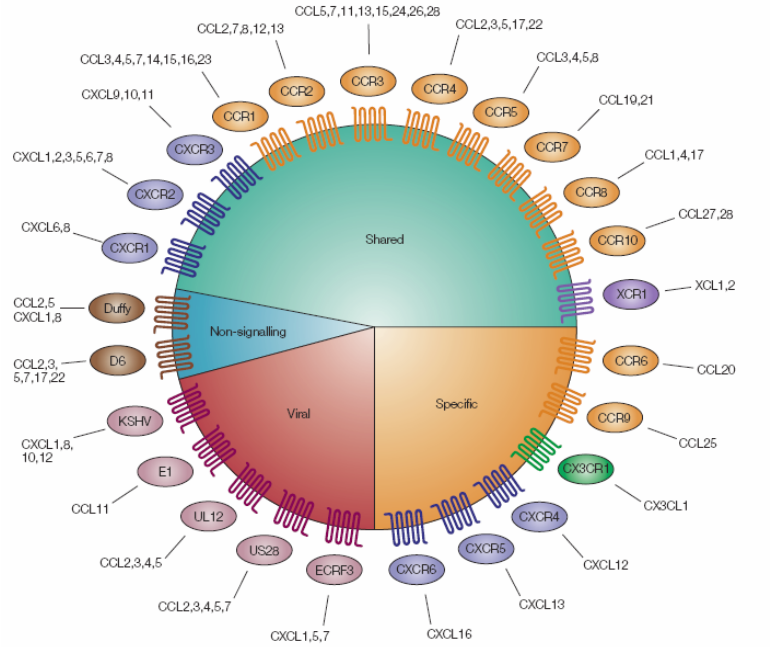

Figure 2 The chemokine wheel. This illustration explains the ligand-binding patterns of the seven-transmembrane domain G-protein-coupled human chemokine receptors. Receptors CXCR1–CXCR3, CCR1–CCR5, CCR7, CCR8, CCR10 and XCR1 all bind several chemokines. By contrast, CCR6, CCR9, CX3CR1 and CXCR4–CXCR6 bind only one ligand each. Duffy and D6 are considered to be 'deceptors', as they bind ligands but do not signal, thereby acting as a negative feedback for chemokine responses.

More than 50 chemokines have been discovered so far (Fig. 2); most, if not all chemokines activate leukocytes through binding to G protein-coupled seven transmembrane-domain receptors (GPCR) designated CXCR or CCR [9,10]. There are approximately 20 chemokine receptors identified [2]. In general, these receptors, which belong to the G-protein-coupled receptor family, bind to more than one type of chemokine (FIG. 2). However, six receptors bind to only one cytokine: CXCR4, CXCR5, CXCR6, CCR6, CCR9 and CX3CR1. The profile of chemokine-receptor expression on an individual cell is determined by its lineage, stage of differentiation, and microenvironmental factors such as chemokine concentration, the presence of inflammatory cytokines and HYPOXIA.

Chemokine receptors are present on many different cell types. Initially, these receptors were identified on leukocytes, where they were found to play an important role in the homing of such cells to sites of inflammation [11]. However, during the past few years, hematopoietic and nonhematopoietic cells have been found to express receptors for various chemokines that are constitutively expressed in distinct tissue microenvironments. The interactions between such receptors and their respective chemokines help coordinate the trafficking and organization of cells within various tissue compartments [12,13]. Lymphocytes trafficking between blood and secondary lymphoid tissues, for example, is a nonrandom process that is regulated by tissue-specific expression of chemokines [14]. Circulating blood lymphocytes interact transiently and reversibly with vascular endothelium through adhesion molecules (selectins, integrins) in a process called rolling. Chemokines on the luminal endothelial surface can activate chemokine receptors on the rolling cells, which triggers integrin activation[15]. This results in the arrest, firm adhesion, and transendothelial migration into tissues where chemokine gradients direct localization and retention of the cells [16]. These steps, collectively referred to as "homing," are essential for normal development of the organism, organization and function of the immune system, and tissue replacement. There is growing evidence that these physiologic mechanisms of tissue-specific recruitment also are functional in neoplastic cells.

In addition, these GPCRs may account for the angiogenic or angiostatic action of chemokines. Indeed, triggering of CXCR2 by ELR+ CXC chemokines or CXCR4 by CXCL12/SDF-1 causes angiogenesis, whereas CXCR3 is an 'angiostatic' receptor for some ELR- CXC chemokines [17,18].

1.2 The chemokines involvement in cancers

Chemokines are best known for inducing directional cellular migration, particularly of leukocytes during inflammation. Prolonged inflammation is thought to facilitate carcinogenesis by providing a microenvironment that is ideal for tumor cell development and growth.

The pattern of chemokine receptor and ligand expression in a tissue generally correlates with the numbers and types of infiltrating cell that are present. The chemokine gradient that attracts infiltrating cells can be created by different cell populations in a tissue. In infections, the first cells that produce chemokines are probably tissue leukocytes, but fibroblasts, endothelial cells and epithelial cells (both normal and malignant) are all able to produce chemokines and generate a chemokine gradient. Although originally identified on leukocytes, functional chemokine receptors are also found on endothelial cells [19] and on some epithelial cells, particularly those that have been malignantly transformed [20-22].

Chemokines affect tumor development indirectly by influencing angiogenesis, tumor–leukocyte interactions, as well as directly by influencing tumor transformation, survival and growth, invasion and metastasis. The role played by chemokines is rather complex as some chemokines may favor tumor growth and progression, while others may enhance anti-tumor immunity. Solid tumors contain in addition to tumor cells, also various types of stromal cells, such as fibroblasts and endothelial cells. Moreover, tumors are infiltrated by inflammatory cells, including neutrophils, macrophages and lymphocytes. Tumor cells, stromal cells, as well as the tumor-associated leukocytes contribute to the local production of chemokines inside the tumor. In addition, tumor-derived chemokines further determine the influx of leukocytes into the tumor [23]. In this way, chemokines can stimulate or inhibit tumor development in an autocrine fashion by attracting cells with pro- or anti-tumoral activities, respectively (Figure. 3). Tumor-associated neutrophils and macrophages may favor tumor progression by secreting matrix degrading enzymes and growth factors, respectively [24,25]. In addition, macrophages have a remarkable degree of plasticity with a ‘switch’ in phenotype during tumor progression [26]. Alternatively, tumor infiltrating cytotoxic T lymphocytes and NK cells are rather detrimental for tumor development [27].

Chemokines can also indirectly affect tumor growth by their angiogenic or angiostatic activity. Angiogenesis, the formation of new blood vessels from established ones, is an essential biological event during physiological and pathological processes, like embryogenesis, wound repair and tumor growth [28]. Angiogenesis is a complex process in which numerous stimulatory and inhibitory signals, such as integrins, angiopoietins, chemokines, oxygen sensors, growth factors, extracellular matrix proteins, and many other molecules are involved [29–31]. This delicate balance between angiostatic and angiogenic factors is strictly regulated. Tumor growth occurs when the equilibrium between angiogenic and angiostatic factors is disturbed in favor of the angiogenic factors.

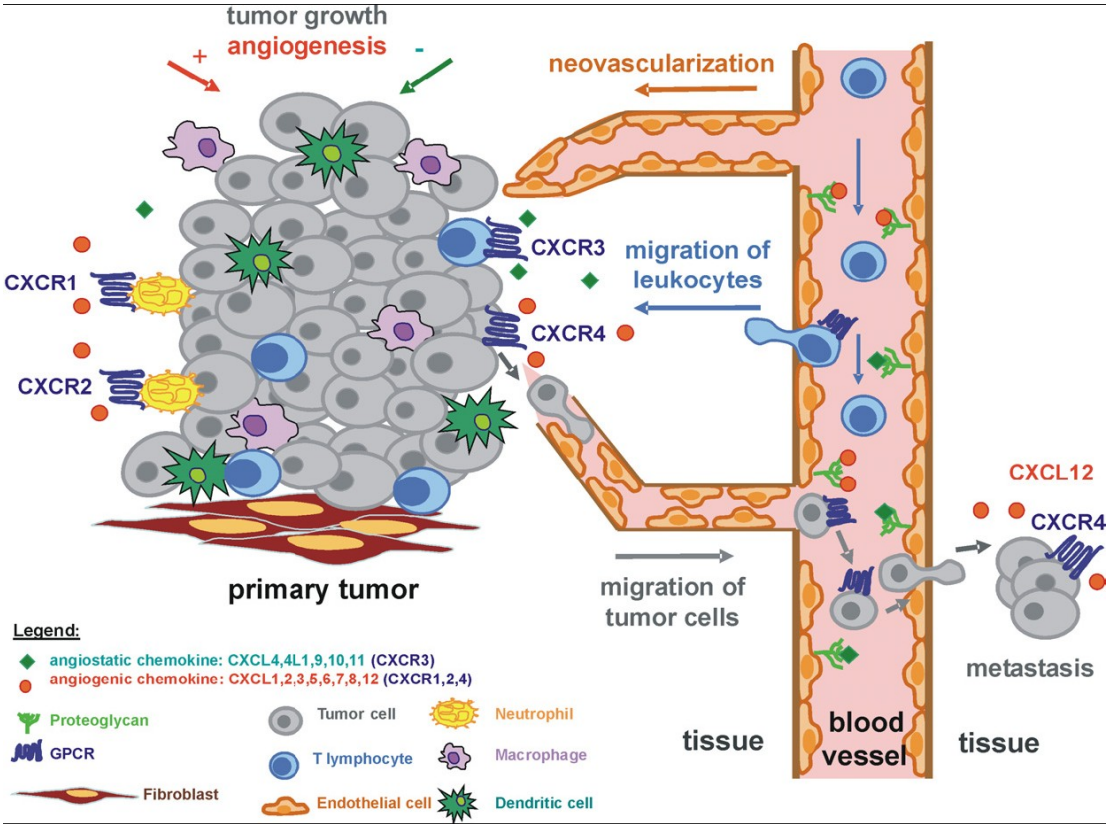

Figure 3 Role of chemokines and their receptors in the tumor environment. Solid tumors contain various types of stromal cells, such as fibroblasts and endothelial cells. All these cell types are good producers of chemokines, regulating the migration of leukocytes. Leukocyte traffic is a highly coordinated multistep process. Briefly, leukocytes roll along the endothelium and chemokines bind leukocytes via their Gprotein-coupled receptor. As a result, the leukocytes firmly attach to the endothelial cell layer. Finally, leukocytes transgress the endothelium and migrate into the underlying chemokine producing tissue in response to the chemokine gradient. As a result the tumor is infiltrated by inflammatory cells, including neutrophils, macrophages, T lymphocytes and dendritic cells. Indeed, all the ELR+ CXC chemokines attract CXCR2 expressing pro-tumoral neutrophils, loaded with proteases. In contrast, some ELR- CXC chemokines, like the CXCR3 ligands CXCL9/Mig, CXCL10/IP-10 and CXCL11/I-TAC, attract activated CXCR3 T lymphocytes and NK cells, which might exert anti-tumoral (cytotoxic) activity. The production of chemokines by tumor cells, normal stroma and leukocytes also affects the process of angiogenesis by their angiogenic (the CXCR2 ligands CXCL1,2,3/GRO-,a,b,c CXCL5/ENA-78, CXCL6/GCP-2, CXCL7/NAP-2, CXCL8/IL-8 and the CXCR4 agonist CXCL12/SDF) or angiostatic (CXCL4/PF-4, CXCL4L1/PF-4var, CXCL9/Mig, CXCL10/IP-10, CXCL11/I-TAC) properties. The formation of new blood vessels is important in tumorigenesis to provide oxygen and nutrients and to stimulate the process of metastasis. Further, the CXCR4-CXCL12/SDF-1 receptor–ligand axis is involved in the directed migration of tumor cells into metastatic sites.

1.2.1 A role for chemokine receptors in cancer metastasis

In many cancers, metastasis is the leading cause of mortality. Despite extensive research, the precise mechanisms by which cancer cells are disseminated to sites distant from the primary tumor are not fully understood. While the chemokine-mediated cell migration of leukocytes has long been known, it has only recently been found that tumor cells may utilize similar mechanisms during cancer metastasis [32]. It has been proposed that subsets of chemokine receptors are expressed by certain tumor cells and that specific chemokines are highly expressed at sites of cancer metastasis, thus suggesting that specific combinations of chemokines and chemokine receptors determine the final destination of metastatic tumor cells [23,33,34].

Infiltrating leukocytes are not the only cells that respond to chemokine gradients in cancers; cancer cells themselves can express chemokine receptors and respond to

chemokine gradients[16,34]. In fact, organ-specific metastasis might be governed, in part, by interactions between chemokine receptors on cancer cells with metastatic potential and chemokine gradients in target organs. There are similarities, for instance, between the transport of dendritic cells to lymph nodes, which is regulated by chemokine gradients, and the lymphatic spread of cancer cells [35]. This concept is supported by several reports, which describe the expression of a distinct non-random pattern of subsets of functionally active chemokine receptors, such as CXCR3 and CXCR4 in human melanoma cells[36, 37] CXCR4 in metastatic breast cancer cells [20], and CCR7 and CCR10 in skin metastases [20].

Other evidence for the role of chemokine receptors in cancer metastasis include the findings that CCR5 is expressed on stromal cells and thereby promotes pulmonary metastasis [38] and that the upregulation of CXCR4 is essential for HER2-mediated breast tumor metastasis [39]. Moreover, the relevance of chemokine receptors *in vivo* was demonstrated by using CXCR4- specific antibodies, which significantly reduced the formation of lymph node and lung metastases in immunodeficient mice [20] and by studying CCR5 knockout mice (CCR5-/-), which developed fewer metastases[38].

However, the chemokine receptor that is most commonly found on human and murine cancer cells is the CXC receptor CXCR4 (Table 1).

Table 1. Some of the chemokine receptors that are expressed on cancer cell

Chemokine receptor	Cancer cell expression	Normal-cell expression
CXCR4	23 different haematopoietic and solid cancers*	HSC, thymocytes, T cells, B cells, immature and mature dendritic cells, some endothelium, macrophages and neutrophils
CCR3	T-cell leukaemia	T cells, basophils, eosinophils and plasma cells
CCR4	T-cell leukaemia	Thymocytes, NK cell, immature dendritic cells, skin-homing T cells and T_H2 T cells
CCR5	Breast cancer cell line	Thymocytes, B lymphocites, immature and mature dendritic cells and macrophages
CCR7	Breast cancer, CCL, gastric cancer, non-small-cell lung and oesophageal cancer	B cells, T cells and mature dendritic cells
CCR10	Melanoma	Plasma cells and skin-homing T cells
CXCR2	Melanoma	Macrophages, eosinophils and neutrophils

*Breast cancer, ovarian cancer, glioma, pancreatic cancer, prostate cancer, acute myeloid leukaemia, B-chronic lymphocytic leukaemia, B-lineage acute lymphocytic leukaemia, non-Hodgkin's lymphoma, intraocular lymphoma, follicular centre lymphoma, chronic myelogenous leukaemia, multiple myeloma, thyroid cancer, colorectal cancer, squamous-cell carcinoma, neuroblastoma, renal cancer, astrocytoma, rhabdomyosarcoma, small-cell lung cancer, melanoma and cervical cancer. CLL, chronic lymphocytic leukaemia; HSC, haematopoietic stem cells; NK, natural killer; TH2, T-helper 2.

T. CXCR4 plays a critical role in the homing of cancer cells to distant sites [40, 20] by binding to its ligand CXCL12, which is highly expressed where metastastic lesions are commonly observed (Figure 4) [40, 41].

Increased CXCR4 expression is associated with an aggressive phenotype since metastases frequently exhibit increased CXCR4 receptor expression compared with the primary lesion [42, 43]. Similarly, elevated CXCR4 expression in estrogen and progestin receptor–negative breast cancers and triple negative breast cancers is closely associated with lymph node metastasis [44]**.** Preclinical and clinical studies have detected high concentrations of CXCR4 receptors in the primary brain tumors compared with normal brain parenchyma [45, 46]. The invading regions of glioblastomas and satellite tumors,

which are the primary foci of recurrence, have been observed to express high levels of CXCR4 [47]. Tissue microarray analyses of patient biopsies have shown that nuclear staining for CXCR4 increases with tumor grade [48] and that elevated CXCR4 expression levels are associated with poor survival in patients with breast cancer [49-51]. CXCR4 expression has therefore been proposed as a prognostic factor in several cancers including brain, breast, colon, prostate, kidney, melanoma, and osteosarcoma and considered a therapeutic target because of its role in tumor development, growth, and metastasis [52-56].

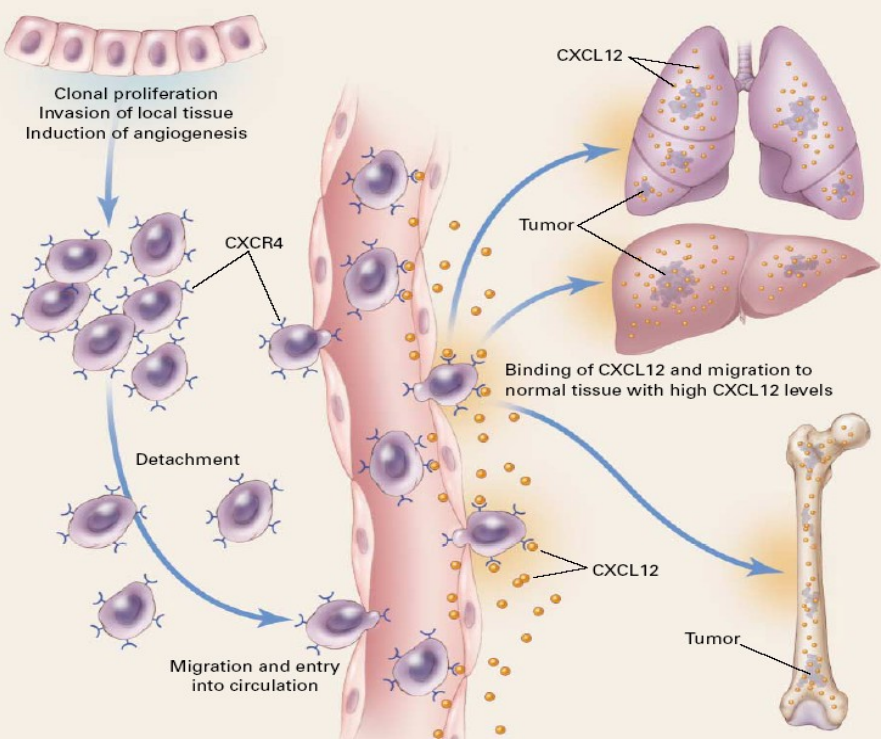

Figure 4 Different aspects of cancer progression where chemokines and their receptors may play a primary role: growth of the primary tumor, angiogenesis (cell migration of endothelial precursors), metastasis, and growth survival of the metastasized cells which is probably the least efficient step in the metastatic process.

1.2.2 The role of the CXCR4–CXCL12 axis in cancer

Tumour cells from at least 23 different types of human cancers of epithelial, mesenchymal and haematopoietic origin express CXCR4 (REF. 8).Not all cancerous cells in the primary tumour are CXCR4 positive. In ovarian and non-small-cell lung cancer, for instance, only a sub-population of cells expresses this receptor [57]. When it has been possible to study freshly isolated tumour cells — for example from leukaemias and cells that have been isolated from ovarian cancer ascites — the CXCR4 receptor is functional and various signalling pathways are activated.

CXCR4 is a member of the surface G protein–coupled seven-span transmembrane receptor class (Figure 5) that is expressed constitutively in a wide variety of normal tissues, including lymphatic tissues, thymus, brain, spleen, stomach, and small intestine [58]. This receptor is also expressed in normal stem cells from a variety of tissues, including mammary stem cells [59]. The fact that CXCR4 is present in normal mammary stem cells suggests that this molecule may be essential for stem cells that appear to be progenitors of carcinoma [60]. Signaling through CXCR4 activates a number of downstream effector molecules, including molecules that regulate key processes such as cell cycle control and apoptosis. The homeostatic chemokine stromal cell-derived factor-1 (CXCL12/SDF-1) is also expressed constitutively in a variety of tissues, including lung, liver, lymph nodes, bone marrow, and adrenal glands [20,58,61]. CXCL12 is highly

conserved between mice and humans with only a single amino acid substitution between the two species.

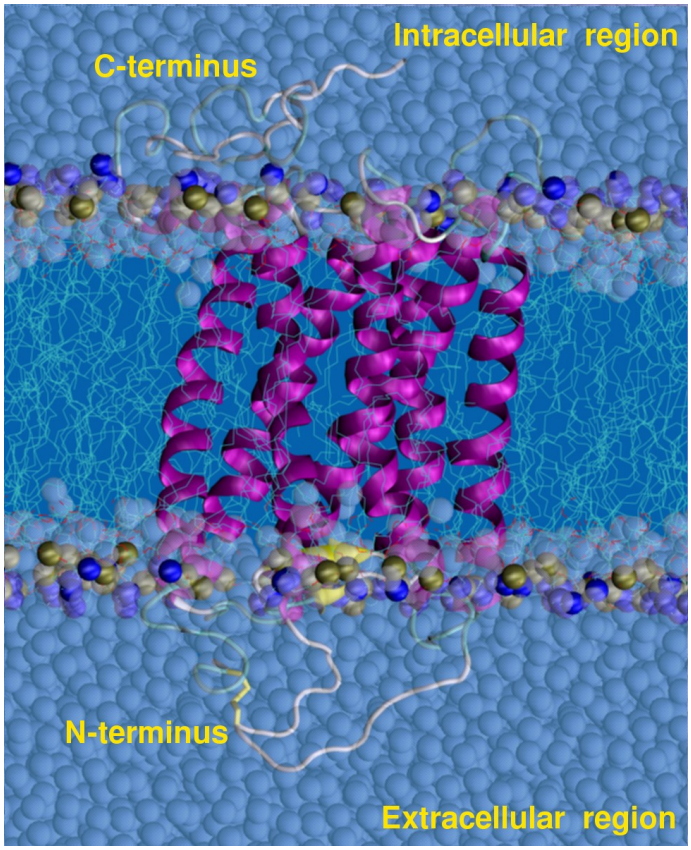

Figure 5 CXCR4 receptor structure model.

Two different isoforms of this chemokine have been identified in humans, CXCL12α and β. These isoforms are identical except for an additional four amino acids on the carboxyl terminus of CXCL12β. CXCL12α and β do not appear to differ in their functions as ligands for CXCR4, based on structure–function studies showing that the amino terminal region of CXCL12 is critical for activating the receptor [62]. CXCL12 binds to heparin and heparin sulfate glycosaminoglycans on the surfaces of cells and in the extracellular matrix, thereby increasing local concentrations of ligand to activate CXCR4 [63].The chemokine CXCL12 regulates many essential biological processes, including cardiac and neuronal development, stem cell motility, neovascularisation and tumorigenesis [64-68].

Besides the well known role of CXCR4 as a cofactor for human immunodeficiency virus infection of T lymphocytes [69], binding of CXCL12 to CXCR4 activates a variety of intracellular signal transduction pathways and effector molecules that regulate cell survival, proliferation, chemotaxis, migration, and adhesion. Briefly, the CXCL12/ SDF-1 – CXCR4 axis promotes angiogenesis and the migration of tumor cells into the metastatic sites in many cancers, like breast [20, 70], lung [61], ovarian [71], renal [72], prostate [73] cancer, and neuroblastoma [74]. These CXCR4 expressing tumors preferentially spread to tissues that highly express CXCL12/SDF-1, including lung, liver, lymph nodes and bone marrow. The involvement of this receptor–ligand interaction in the directed migration of cancer cells to metastatic sites has been reviewed by Balkwill [22].

The large number of downstream effector molecules regulated by CXCR4 likely account for the multiple effects of this receptor in the pathobiology of cancer. The extent to which various molecules activated by CXCR4 relate to specific functions, such as proliferation and chemoinvasion, remains to be established clearly. The roles of various effectors of CXCR4 at defined stages in primary and metastatic breast cancer also have not been well established. Defining downstream effectors of CXCR4 in vivo is important to establishing

molecular mechanisms through which CXCR4 promotes cancer. Moreover, identifying key mediators of CXCR4 function in cancer is expected to enable rational selection of other therapeutic agents for potential use with new compounds targeted against CXCR4.

CXCL12 and CXCR4 stimulate the phosphatidylinositol- 3-kinase pathway that subsequently activates the protein kinase AKT [75-77]. Activated AKT phosphorylates a wide variety of intracellular targets, functioning to inhibit apoptosis and prolong cell survival in many different types of cancer cells [78]. Beyond functions in promoting cell survival, AKT also has been implicated in effects of CXCR4 on proliferation of cells [76] and migration toward a chemotactic gradient of CXCL12 [79, 80].

The mitogen-activated protein kinase pathway (MAP kinase pathway) is another signal transduction pathway regulated by CXCR4. In response to CXCL12, CXCR4 activates the kinase MEK, the upstream activator of the p42/44 MAP kinases (also known as ERK 1/2). Because p42/44 activate the same downstream signal transduction pathway, these two related kinases generally are referred to as a single effector. Activated p42/44 MAP kinases phosphorylate transcription factors including Elk-1 to increase expression of genes that promote proliferation and survival of cancer cells (reviewed in [81, 82]. CXCR4 activates several different intracellular events such as chemotaxis, invasion, and adhesion, all of which are properties that correlate with metastatic behavior of cancer cells in vivo. CXCL12 binding to CXCR4 promotes polymerization of actin to promote cell motility. CXCR4 also activates members of the src family of protein tyrosine kinases, thereby producing phosphorylation and activation of components of focal adhesion complexes such as RAFTK/Pyk2, focal adhesion kinase, Crk, and paxillin [83]. CXCR4 also promotes adhesion to components of the extracellular matrix, including collagen and fibronectin, through integrins a2, a4, a5, and b1 [84]. Focal adhesion complexes and integrins have been shown to promote migration of cells and interactions with extracellular matrix molecules.

An important mechanism that alters the metastatic behavior of tumor cells in vivo is hypoxia. As the oxygen concentration decreases within a tumor, metastasis is favored, because hypoxia up-regulates CXCR4 in tumor cells via the hypoxia-inducible factor-1a (HIF-1a) [85, 86]. Hypoxic conditions in the tumor cell mass promote the transcription and translation of HIF-1a, whereas under physiological conditions, the tumor suppressor protein von Hippel– Lindau negatively regulates CXCR4 expression by the degradation of HIF-1a [87].

Further, CXCL12/SDF-1 is also involved in the invasion of tumor cells. Indeed, CXCL12/SDF-1 directed invasion of human basal carcinoma cells is mediated by the up-regulation of MMP-13 [88]. MMPs play an important role in the invasion process because their proteolytic activities assist in the degradation of the extracellular matrix and basement membranes and are essential in order to promote intravasation of cancer cells from the primary tumor into blood vessels and extravasation at sites of metastases [83]. In addition, Pro-angiogenic effects of CXCR4 signaling may be mediated through upregulation of vascular endothelial growth factor (VEGF), an established pro-angiogenic molecule [89]. VEGF itself has been shown to increase expression of CXCR4 in breast cancer cells, thereby forming a potential positive feedback loop for promoting angiogenesis [90]. Therefore, these data suggest that another potential function of CXCL12– CXCR4 signaling in cancer may be to directly or indirectly promote angiogenesis in primary and metastatic breast cancer.

Interruption of the interaction between CXCL12/SDF-1 and its receptor may inhibit the metastatic process. Therefore, the CXCR4 receptor could be an important therapeutic target for cancer treatment.

1.3 Structure of SDF-1 and hypothesized molecular mechanism of its interaction with CXCR4 receptor

The solution structure of SDF-1 provides the basis for addressing the structural features which are essential for function. Many aspects of the molecular biology and physiology of SDF-1 are unique, so we cannot assume that rules established for other chemokines apply.
The structure of SDF-1 is well defined except for the N- and C-terminal residues, 1–8 and 66–67, respectively. SDF-1 adopts a chemokine-like fold consisting of three anti-parallel β-strands and an overlying α-helix (Figure 6). The well ordered regions include an extended loop (Arg12 to Ala19) which leads into a 310 helix (Arg20 to Val23). The first β-strand (24 to 30) is connected by a type III turn (31 to 34) to the second β-strand (37 to 42) and the second and third β-strands (47 to 51) are connected by a type I turn (43 to 46). A type I turn (52 to 55) connects the third β-strand and the C-terminal α-helix (58 to 65) (Figure 7A).. SDF-1β, was also characterized by NMR and the data indicated that like SDF-1 it is well defined between residues 9 and 65. There was no significant change in either secondary or tertiary structure as a consequence of the five residue C-terminal extension that distinguishes SDF-1βfrom SDF-1.

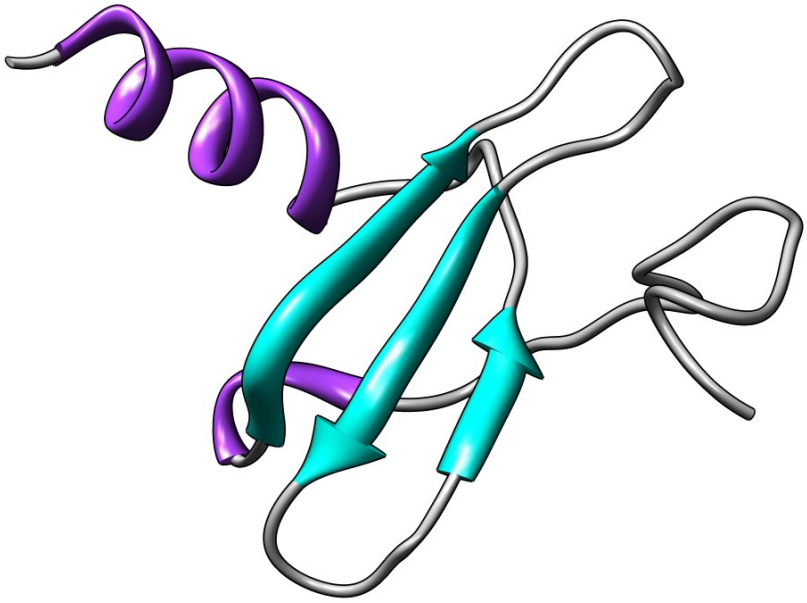

Figure 6. Crystallographic structure of the chemokine CXCL12

Chemokine structures that have been solved to date have a common tertiary fold that consists of an N-terminal region, a loop region that follows the CXC or CC motif, three antiparallel b-strands in a Greek key like arrangement, and a C-terminal a-helix. Several structural features are unique to SDF-1 and distinguish it from other chemokines (Figure 7). Differences are apparent in the packing of the hydrophobic core and this is evident when we consider Trp57 which is highly conserved among CC chemokines and also present in IL-8. In SDF-1, Trp57 makes extensive NOE contacts with residues of the 310 helix (Arg20, Val23), the first b-strand (Leu26), and the N-terminal loop (Val18). In contrast, in other chemokines, Trp57 is oriented away from the first β-strand and is packed predominantly against the side chains of residues in the N-terminal loop (Figure 7A). These differences in the hydrophobic core are reflected in the relative orientation of the α-helix to the rest of the protein: in SDF-1 it is aligned more parallel to the β-strands, whereas in all other chemokines it is orthogonal to the β-strands (Figure 7B, C and D).

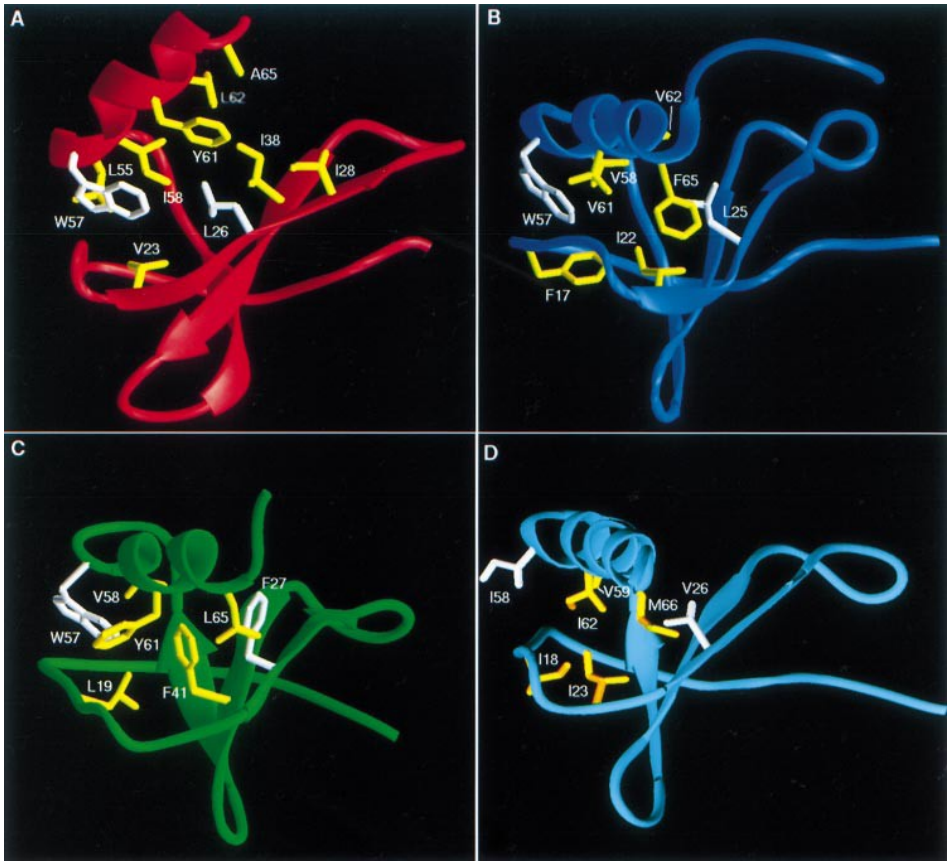

Figure 7 Comparison of SDF-1 with other chemokines. Ribbon outlines of: (**A**) SDF-1; (**B**) IL-8 (**C**) RANTES [91]and (**D**) GRO [92] Trp57 and the residue that corresponds to Leu26 of SDF-1 are shown in white to indicate the difference in their relative positions. Residues 1 to 8 in SDF-1, 1 to 3 in IL-8, 1 to 7 in RANTES and 1 to 5 in GRO, are not shown for clarity.

The packing requirements of the helix in SDF-1 are fulfilled by Trp57, Tyr61 and Leu62, which interact with residues of the first and second β-strands. Packing of the hydrophobic side chain of Leu55, which is part of the turn preceding the α-helix in SDF-1, also influences the hydrophobic core and the orientation of the helix.

SDF-1 is a highly basic protein with 21% of the total residues being arginine, lysine or histidine. Analysis of the electrostatic potential at the molecular surface revealed further differences between SDF-1 and other chemokines. In SDF-1, positive surface charges are clustered along the first and second β-strands and the α-helix displays a predominantly negative surface charge. With CXC chemokines, a positively charged surface is clustered in the C-terminal α-helix, whereas the CC chemokines show no obvious pattern in the clustering of charges. The positive surface charge in IL-8 has been proposed to be critical for heparin binding [93]. SDF-1 has been shown to bind heparin with higher affinity than either IL-8 or MCP-1 [94], suggesting that the surface charge distribution of SDF-1 could provide an optimal binding site for heparin or other cell-surface glycosaminoglycans.

To determine the SDF-1structural requirements for its biological function, a set of SDF-1 analogs have been synthesized and assayed for their ability to bind CXCR4 and to induce functional activation of the receptor by measuring induction of intracellular calcium levels [62]. These analogs consist in N-terminal truncations, single substitution analogs and chimeras of SDF-1 with other CXC chemokines.

Based on these results Crump proposed a two site model for SDF-1 binding to CXCR4 (Figure 8).

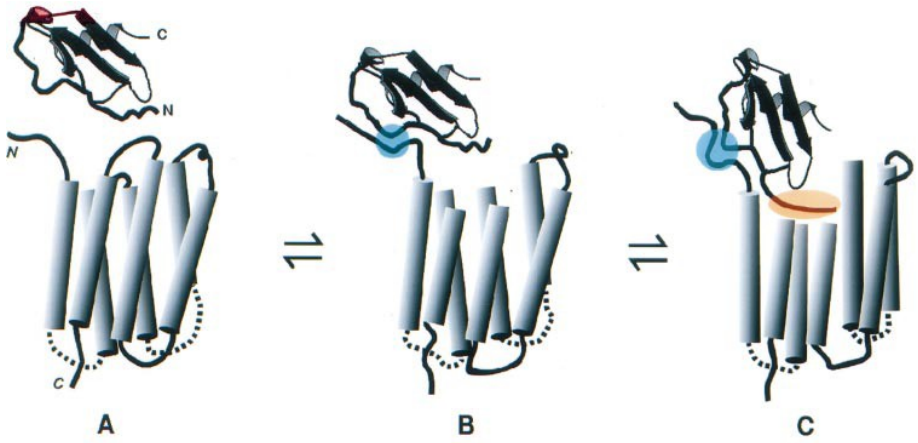

Figure 8 A model for interaction of SDF-1 with CXCR4. A schematic depicting the interaction of SDF-1 with the receptor is shown. (**A**) indicates the receptor and ligand separately. (**B**) indicates interaction of the SDF-1 RFFESH loop (site 1) with the N-terminal segment of the receptor. The contact region is shown in blue. Two (**C**) Shows the N-terminal region (site 2) of SDF-1 bound in groove at the top of the helices (orange). Binding of the N-terminal region results in activation of the receptor, which is depicted in (C) by the change in conformation of the receptor helices compared with (B).

The two receptor binding sites are contained in SDF-1 (1–17) that has the sequence: KPVSLSYR-CPC-RFFESH. The results show that the RFFESH site is important for optimal binding, but is not sufficient for receptor activation, and this region (site 1) makes the initial contact with the receptor (A to B).
In fact this step serves as an initial SDF-1 docking step, and this step could be like a key that permits access to the more buried receptor site. In the subsequent step (B to C), the N-terminal residues bind to a groove amongst the helices, which induces a change in the conformation of the receptor transmembrane helices that allows intracellular G-protein binding and signaling of cellular function [95]. The N-terminal region (site 2), which is disordered in solution, becomes structured during binding and establishes contacts with the receptor groove. Nevertheless, addition of a Gly residue to SDF-1 did not affect activity and some of the N-terminal residues could be modified with minimal change in function. This suggests that the bound form of the N-terminal region is not completely buried within the transmembrane region, but rather is bound in a shallow site. Receptor activation requires Lys-1 and Pro-2 within the N-terminal region. Modifications to Lys-1 and Pro-2 result in antagonists because the variants can no longer induce the conformational change in the receptor that is required for activation.
In conclusion, this hypothesized two-step mechanism for the interaction of SDF-1 with CXCR4 has provided the molecular basis for the design of SDF-1 analogs to be used as agonists or antagonists of the receptor target.

1.4 CXCR4 antagonists: AMD3100 and T-140

CXCR4 first drew attention as a major coreceptor for the infection of T cell line-tropic (X4) strains of human immunodeficiency virus 1 (HIV-1) [96, 97]. Interaction between the gp120/CD4 complex and a coreceptor, such as CXCR4 or CCR5, triggers conformational changes in the viral envelope (Env) that lead to membrane fusion and entry of the viral genome into the host cell cytoplasm (Figure 9) [98, 99].

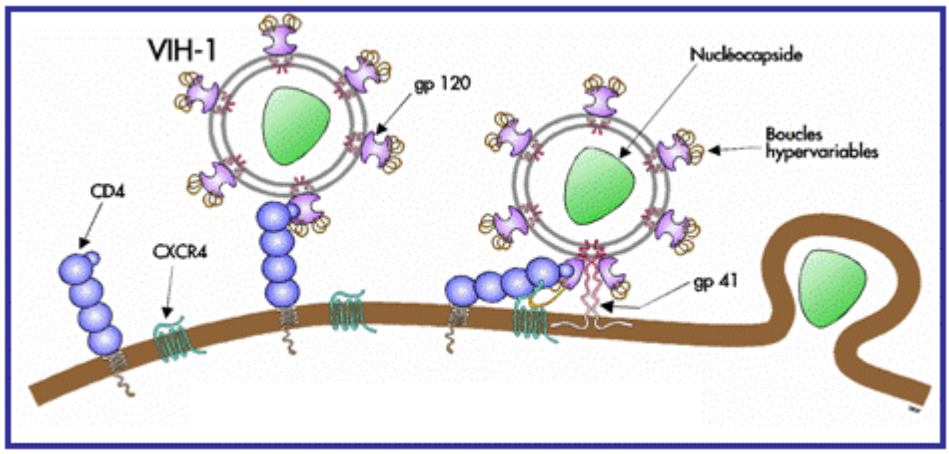

Figure 9 A model for the HIV-1 entry mechanism.

Importantly, the CXCR4 receptor is expressed much more broadly than chemokine receptors in general, that is, not only on a wide variety of leukocytes but also on cells outside the immune system. Compelling evidence is accumulating that the CXCR4 is far more than a coreceptor for HIV, playing an important role in cancer metastasis, regulation of stem cell trafficking, and neovascularization [100-103]. Consequently, therapeutic strategies to block the interaction between CXCR4 and SDF-1 hold promise for a variety of clinical applications. Since the identification of human immunodeficiency virus (HIV) as the causative agent of the acquired immune deficiency syndrome (AIDS) and the disclosure of CXCR4 as a coreceptor for HIV entry, various peptide CXCR4 antagonists, such as T140 and low molecular weight pseudopeptide CXCR4 antagonists, have been reported [104-108]. They have been proven to be efficient agents against HIV infection, as well as cancer metastasis, leukemia and rheumatoid arthritis. The bicyclam AMD3100 (plerixafor) is a nonpeptidic synthetic inhibitor of the CXCR4 receptor. Originally discovered as a potent and selective anti-HIV agent, it was found to be a strong inducer of "mobilization" of hematopoietic stem cells from the bone marrow to the bloodstream as peripheral blood stem cells [109]. Moreover, Plerixafor was seen to decrease metastasis in mice in several studies [70] and to decrease recurrence of glioblastoma in a mouse model after radiotherapy [110].

1.4.1 AMD3100

AMD3100 is composed of two 1,4,8,11-tetraazacyclotetradecane (cyclam) moieties connected by a conformationally constraining heteroaromatic phenylenebismethylene linker (Figure 10).

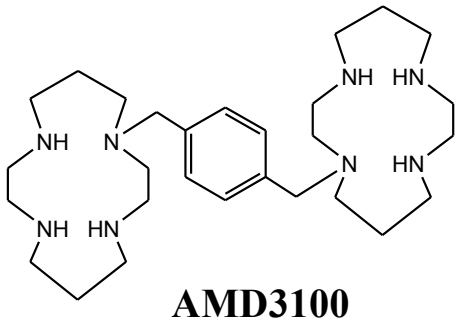

Figure 10 Structure formula of CXCR4 best known antagonist: AMD 3100.

AMD3100 is highly specific for CXCR4 and inhibits the binding and function of CXCL12 and the HIV cell entry with high affinity and potency [111, 112] through an electrostatic interaction with three acidic residues, Asp171 (AspIV:20), Asp262 (AspVI:23), and Glu288 (GluVII:06) located in the main ligand binding pocket of CXCR4 [113-115] (Figure 11). In more details, it has been supposed that one cyclam ring of AMD3100 interacts with Asp171 in TM-IV, whereas the other ring is sandwiched between the carboxylic acid groups of Asp262 and Glu288 from TM-VI and -VII, respectively [114]. Importantly, the high potency and efficacy of AMD3100 requires the presence of a rigid linker between the two cyclam moieties [113]. Previously described monocyclams as well as bicyclams with flexible linkers that were less potent were shown only to be dependent upon AspIV:20 [113].

AMD3100 binds with extreme specificity to CXCR4, independently of the cell type that carries this receptor: as monitored by chemokine-induced signalling, AMD3100 does not interact with a variety of chemokine receptors other than CXCR4, namely CXCR1–3 and CCR1–9 [116]. This prompts the prediction that AMD3100 would interfere with a number of pathophysiological processes mediated by CXCR4 but not any of the other CXCR or CCR receptors.

Gupta *et all.* have studied CXCR4 – AMD3100 interaction by evaluating inhibition of SDF-1α induced chemotaxis and Ca^{+2} flux inHL-60 cells and by evaluating the effect of AMD3100 on SDF-1α binding with CXCR4 in a radioligand binding assay [117]. Although, AMD3100 competed with [^{125}I]-SDF-1α for its CXCR4-specific binding in a dose dependent manner, significantly, its IC50 in the radioligand binding assay was upto 3000-fold less potent (15.2 μM vs 4.7 nM) as compared with its effect in the functional assays.

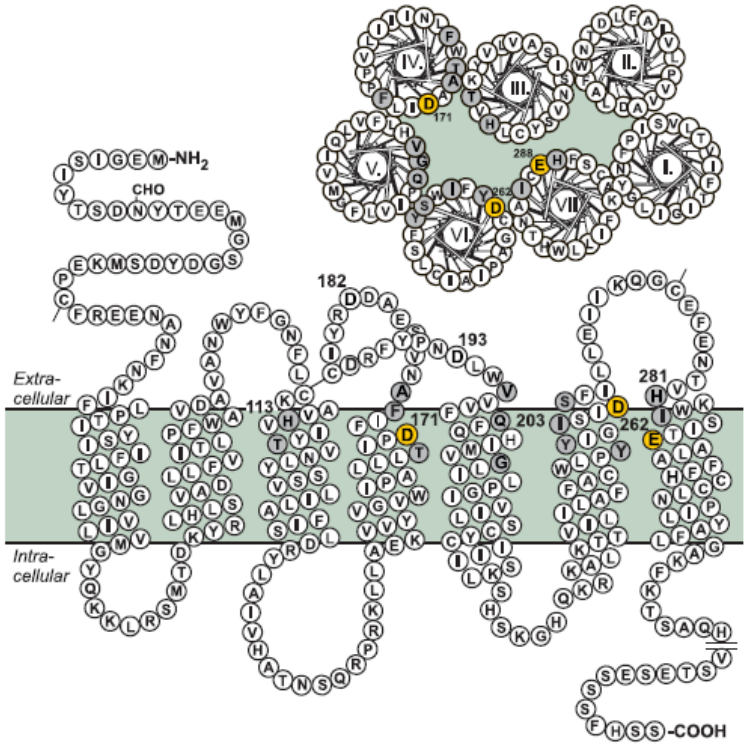

Figure 11 Serpentine and helical wheel diagram of the CXCR4 receptor. *Yellow* background indicates previously identified "hits" for the interaction of AMD3100 with CXCR4 [113, 114].

Taken together, these results reveal an apparent discrepancy between the effect of AMD3100-mediated functional antagonism versus radioligand binding. This discrepancy is best explained by invoking a two-site model for SDF-1-CXCR4 interaction [62] characterized byan initial docking step the N-terminal region of CXCR4 interacts with the R-F-F-E-S-H motif of SDF-1 (Figure 12A, B). and subsequent interaction of CXCR4 with the N-terminal residues (aa 1–11) of SDF-1 (K-P-V-S-L-S-Y-R-CPC-), thus triggering its

functional response (Figure 12C). Hence, in this two-site model, a receptor-specific CXCR4 antagonist like AMD3100 may be a potent functional antagonist by virtue of perturbing ligand interaction at one site, but without a concomitant effect on ligand displacement in a radioligand binding assay (Figure 12D).

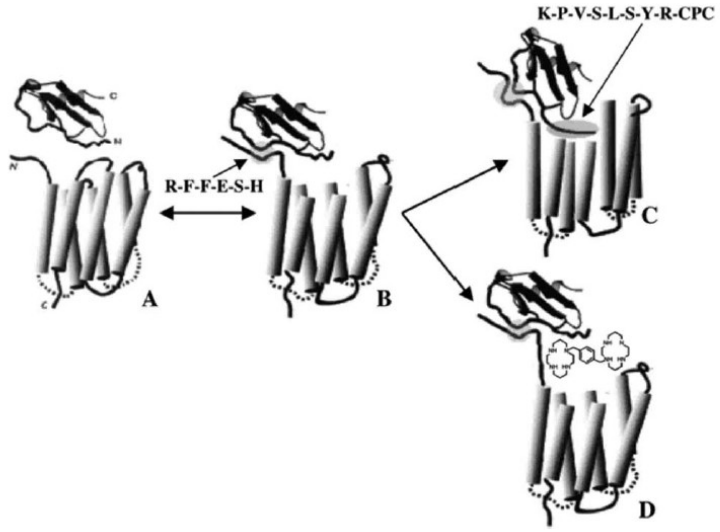

Figure 12 Pharmacological evidence for the schematic model from Crump et al. [62], depicting interaction of SDF-1 with CXCR4. (A) and (B) The intital docking step occurs between the N-terminal residues of CXCR4 and the R-F-F-E-S-H motif of SDF-1. (C) Conformational changes lead to interaction of the extracellular loops of CXCR4 with aa 1–11 of SDF-1. (D) Interaction of a small molecule antagonist like AMD3100 inhibits functional signal transduction without displacement of radiolabeled SDF-1.

Despite the fact that AMD3100 is a highly potent and specific CXCR4 antagonist, it does not exhibit oral bioavailability presumably due to the positive charge (+2) of each ring at physiological pH [118-120]. Long term treatment in HIV-infected persons may therefore be difficult. However, subcutaneous administration in combination with granulocyte-colony stimulating factor improves stem cell mobilization yields in patients undergoing transplantation [121].
In a recent study has been characterized the molecular mechanism of action of a novel series of monocyclam CXCR4 antagonists designed from the prototype symmetrical bicyclam AMD3100 (Figure 13).

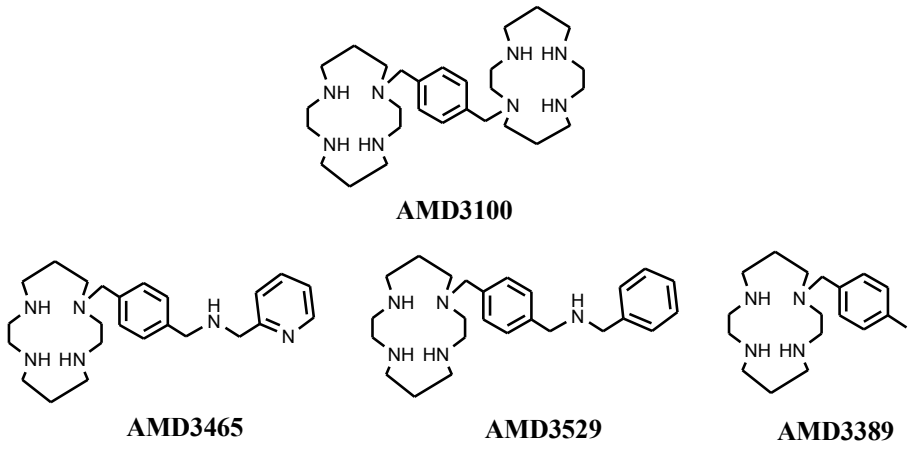

Figure 13 Different monocyclams, AMD3465, AMD3529 and AMD3389 direved from the bicyclam AMD3100.

In these compounds one of the cyclam rings was substituted with aromatic phenyl or pyridine rings (the “non-cyclam part”) linked by an *N*-substituted aliphatic chain and the original phenylenebismethylene linker to the remaining cyclam ring (*i.e.* the “cyclam part”). The binding of such analogs as well as its antagonistic properties was describe in respect of blocking CXCL12-induced activation and HIV cell entry. AMD3465, in which one of the

fournitrogen cyclam moieties has been replaced by a two-nitrogen *N* pyridinylmethylene moiety, binds with higher affinity and inhibits the CXCR4 signaling with higher potency than the classic, symmetrical bicyclam antagonist AMD3100. The low affinity of AMD3529 and AMD3389 (as compared with AMD3100 and AMD3465) indicates that the pyridine interaction of AMD3465 with the III-VI-VII pocket is necessary for high-affinity interaction with CXCR4. These interaction studies indicate that the pyridine ring of AMD3465 is interacting mainly with AspVI:23 and HisVII:-02 in a mode that cannot be mimicked by the corresponding phenyl group of AMD3529 (Figure 14).

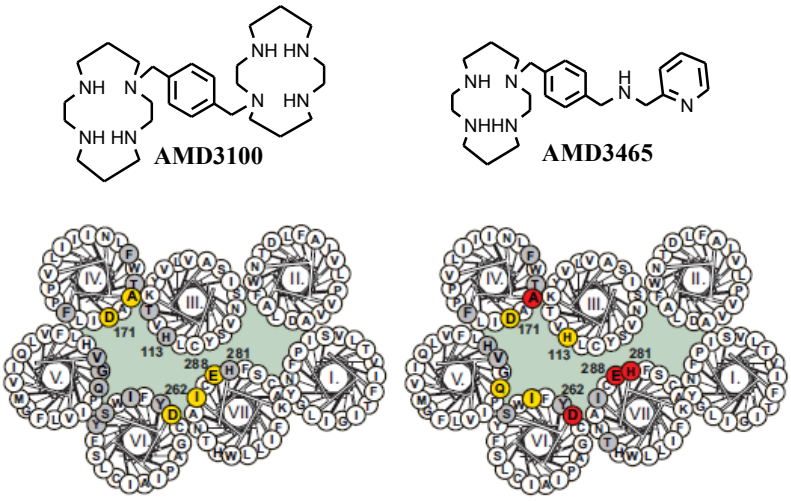

Figure 14 Residues identified through mutagenesis to be important for the binding of AMD3100 and AMD3465 shown in a helical wheel diagram of the CXCR4 receptor. The background color indicates the magnitude of the effect of the mutation on the binding of eitherAMD3100 (*left panel*) or AMD3465 (*right panel*). *Gray* background indicates <10-fold decrease in affinity; *yellow*, 10–50-fold decrease; *orange*, 50–500-fold decrease; and *red*, >500-fold decrease in affinity.

1.4.2 T140

Self-defense peptides with antibacterial and antiviral activities, tachyplesins and polyphemusins, have been isolated from the hemocyte debris of the Japanese horseshoe crab (*Tachypleus tridentatus*) and the American horseshoe crab (*Limulus polyphemus*), which are 17-mer and 18-mer peptides, respectively (Figure 15) [122, 123]. Preliminary structure-activity relationship studies of these peptides have led to the development of T22 ([Tyr5,12, Lys7]-polyphemusin II) [124, 125]. and its downsized 14-mer peptide, T140, which possess strong anti-HIV activity (Figure 15) [126]. T22 and T140 effectively block X4-HIV-1 entry into cells by binding specifically to CXCR4, and inhibit Ca2+ mobilization caused by CXCL12 stimulation against CXCR4 [127-129]. In addition, a T140 analog exhibited a remarkable and significant delaying of the appearance of drug resistant strains of HIV in passage experiments using cell cultures *in vitro* [130], and it was presumed that the T140 analogs would be useful for its suppressive effect against drug resistant strains.

Structural analysis revealed that T140 forms an antiparallel β-sheet structure supported by a disulfide bridge between Cys4 and Cys13, which is connected by a type II' β-turn [131]. Four amino acid residues that were contained in T140, Arg2, L-3- (2-naphthyl)alanine (Nal)3, Tyr5 and Arg14, were identified as residues indispensable for significant activity [132].

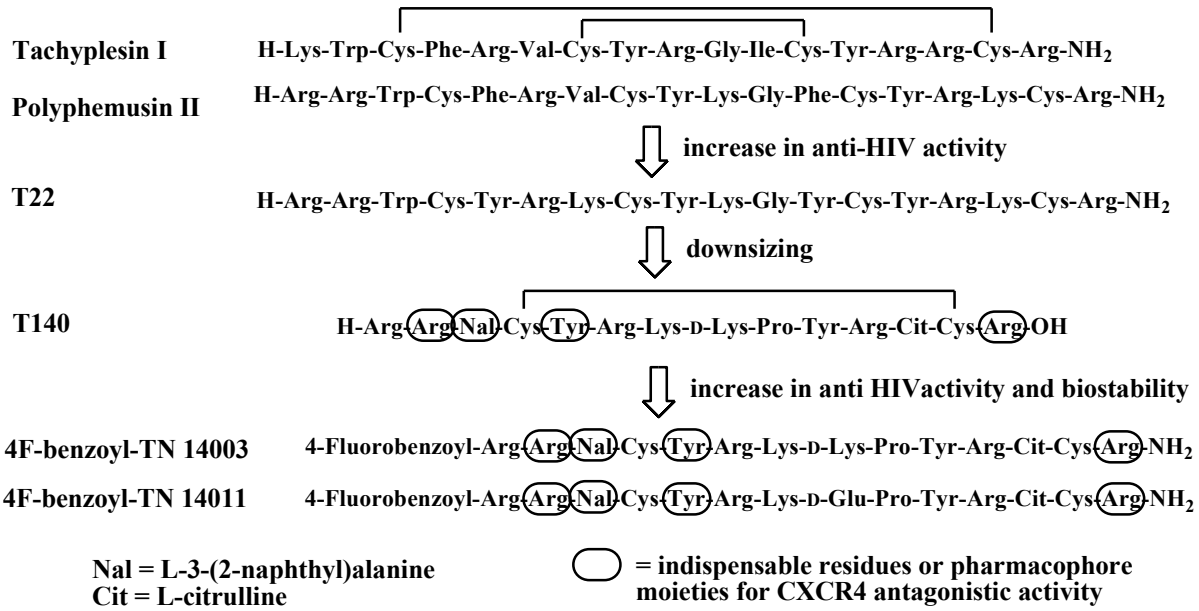

Figure 15 Structures of tachyplesin I, polyphemusin II, its analog T22, its downsized analog T140, its biostable analogs 4F-benzoyl-TN14003 and 4F-benzoyl-TE14011.

However, T140 is proven to be biologically unstable, and biodegradable in mouse/feline serum or in rat liver homogenate [133, 134]. When indispensable amino acid residues (Arg14 in serum; Arg2, Nal3 and Arg14 in liver homogenate) are deleted from the *N*- and the *C*-termini, the efficacy of degraded peptides is dramatically reduced.

Modification of T140 analogs at both termini efficiently suppresses the above biodegradations and leads to development of novel and effective compounds that show highly CXCR4-antagonistic activity as well as increased biological stability. Further studies on the *N*-terminal modifycation found an electron-deficient aromatic ring such as a 4-fluorobenzoyl moiety at the *N*-terminus to constitute a novel pharmacophore for strong anti-HIV activity. The T140 analogs, which contain an *N*-terminal 4-fluorobenzoyl moiety, 4F-benzoyl-TN14003 and 4F-benzoyl-TE14011, have anti-HIV activity two orders of magnitude higher than that of T140 and enhanced biostability in serum/ liver homogenates (Figure 15).

Arg2, Nal3, Tyr5 and Arg14 of T140, which are located in close proximity to each other in space, are indispensable to high antagonistic activity against CXCR4 as described above. For downsizing of T140 analogs, a pharmacophore-guided approach was performed using cyclic pentapeptide libraries, which were composed of two L/D-Arg, L/D-Nal and L/D-Tyr in addition to Gly as a spacer. This approach led to FC131 [*cyclo*(Arg1-Arg2-Nal3-Gly4-D-Tyr5-)], which showed strong CXCR4-antagonistic activity comparable to that of T140 (Figure 16) [135]. Structural analysis of FC131 by NMR and simulated annealing molecular dynamics revealed the near symmetrical pentagonal backbone structure.

A 4-fluorophenyl moiety found as a pharmacophoric moiety as described above was introduced into cyclic pentapeptides. Since replacement of the phenol group of D-Tyr5 by a 4-fluorophenyl group did not cause the maintenance of high potency, the 4-fluorophenyl group was incorporated into position 1. The resulting compound, FC401 ([Phe(4-F)1]-FC131), shows significant CXCR4-binding activity (Figure 16) [136]. Next, since a second Arg residue is thought to be indispensable for high potency and an aromatic residue [L/D-Phe(4-F)] has been incorporated into position 1, four analogs [L/D-Phe(4-F)1, L/D-Arg5]-FC131 were synthesized based on replacement of D-Tyr5 by L/D-Arg5.

Among these analogs, FC602, which is [D-Phe(4-F)1, Arg5]-FC131, shows the most potent activity, which is 10-fold greater than that of [D-Tyr1, Arg5]-FC131 (Figure 16). Thus, FC602 is a novel lead, which involves a pharmacophore moiety different from the pharmacophore groups of FC131.

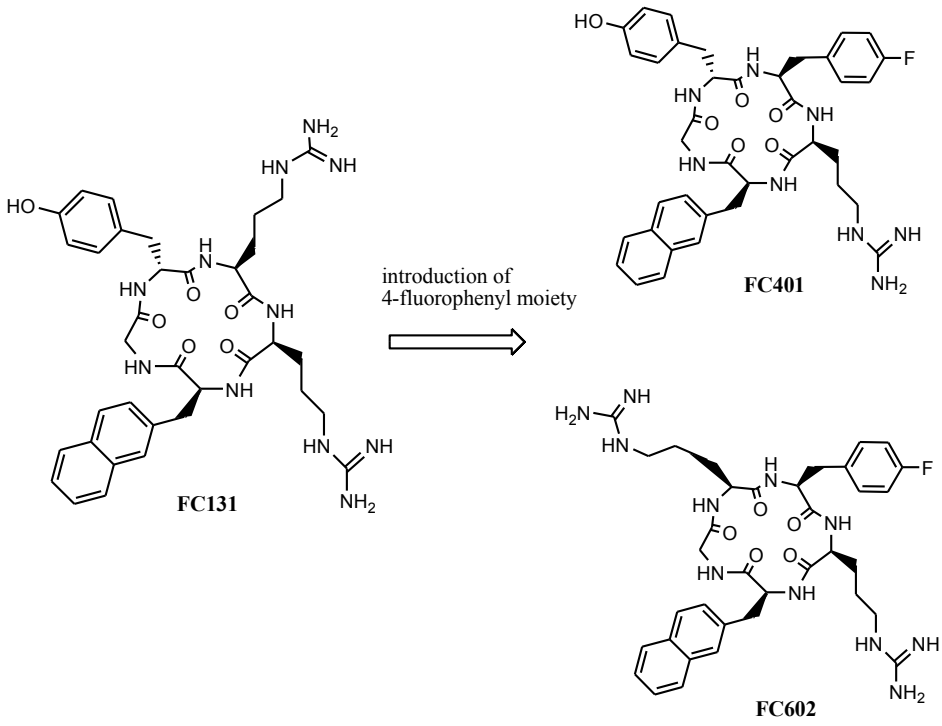

Figure 16 Structures of cyclic pentapetides FC131, FC401 and FC602.

Identification of a novel pharmacophore for CXCR4 antagonism, such as a 4 fluorobenzoyl or 4-fluorophenyl moiety, led to develop a linear type of low molecular weight CXCR4 antagonists. By combining substructure units of the T140 pharmacophore and new pharmacophore moieties, several compounds were designed and synthesized using combinatorial chemistry. As a result, several linear compounds were found as moderate CXCR4 antagonists, such as compounds **1**–**3** shown in Figure 17 [137]. These compounds are relatively weaker than a cyclic pentapeptide FC131. Thus, it is thought that conformational constriction based on a cyclic pentapeptide scaffold is critical for strong potency. Anthracene derivatives possessing two sets of zinc(II)-2,2'-dipicolylamine complex were previously found as useful chemosensors that can selectively bind to phosphorylated peptide surfaces [138]. Several low molecular weight compounds bearing the complex structure were identified as selective CXCR4 antagonists [139]. Molecular superposition of structures of the zinc(II)-2,2'-dipicolylamine complex compound 4 and the cyclic pentapeptide FC131 was investigated as it provided the best fit with the maintenance of local energy minimizations of both of the structures (Figure 17). The distance between two dipicolylamine moieties of compound 4 is estimated to be nearly equal to that between the two Arg side chains of FC131. Thus, the distance of these functional groups is thought to be essential for expression of CXCR4 antagonistic activity.

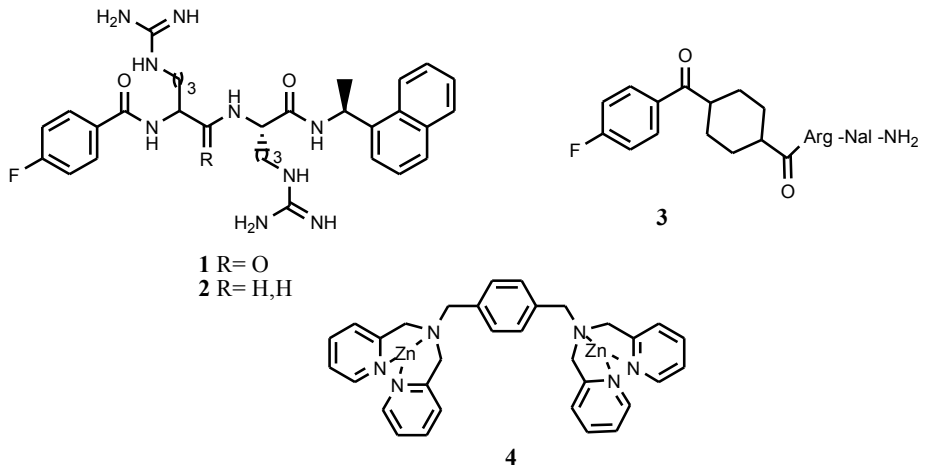

Figure 17 Structures of a linear type of low molecular weight CXCR4 antagonists

1.5 Aims of the project

The aim of this project is the design, synthesis and biological evaluation of new peptide analogues endowed with a good binding affinity toward the receptor CXCR4, in order to be used as therapeutic agents, if able to modulate the receptor target functional roles, or to be used as diagnostic markers.

Due to their involvement in several fundamental steps of inflammation and other immune response, as it was illustrated in the previous paragraph, chemokines in general represent an interesting target for many diagnostic or therapeutics approaches. However, the number of chemokines and of their different biological pathways requires considerable effort to correctly identify sequence or structure associated to different activities and responsible for observed specificities. To identify such relationships, we have been firstly focused on a compared analysis of sequences, whenever available, structures and, in particular, on locally conserved motifs, to be used both to verify hypothesized relationships, and as template to design and synthesize biologically active ligands of CXCR4 receptor. As next step, on the structural basis of the most active peptide sequence, we have developed new synthetic strategy in solution and in solid phase in order to prepare modified amino acids to be used as a building block in peptidomimetic synthesis. The final goal has been to introduce conformational constraint into the peptide sequence by which it would be possible to stabilize the so-called 'bioactive' conformation, that is the peptide conformation required for receptor binding and activation.

2. Rational design and synthesis of peptide ligands

2.1 Rational design

In general, chemokine structures presently solved share a high homology, all exhibiting a central core of three β-strands, with an overlying C-terminal α-helix [62]. Other common features are a disordered N-terminus, the CXC or CC disulphide motif and and extended loop (termed N-loop), preceding the strand region.
As for other chemokines, structure-activity studies of SDF-1 have shown the critical role of the N-terminal region for both receptor binding and activation and in particular the residues 1-8 and 12-17, these last being located in the loop region [62]. vMIP-II, a CC chemokine-like protein encoded by Kaposi's sarcoma-associated herpesvirus, binds and blocks chemokine receptors belonging to the CXC, CC and XC class, such as CCR1, CCR2. CCR5, CCR8, XCR1 and CXCR4 [140, 141]. As for SDF-1, the N-terminus and the N-loop are essential for receptor binding. In particular it was demonstrated that the N-terminus alone, encompassing residues 1-10, is sufficient for binding and antagonizing CXCR4 receptor [142]. Therefore in this study we have focused on a sequence-structure comparison between the N-terminal regions of SDF-1 and vMIP-II, with the aim of looking for a possible common motif responsible for the binding to CXCR4. As three-dimensional structures of both SDF-1 protein and vMIP-II N-terminal region are available (PDB entries, 2KED and 2FHT, respectively) a sequence-structure comparison between the N-terminal regions of the two proteins was performed, to look for a possible common motif responsible for their binding to CXCR4. Although a standard backbone superimposition shows apparently a local low sequence and structure similarity, the scenery changes dramatically when these regions are superimposed after reversing the direction of the backbone. In fact, this new comparison reveals a putative conserved motif, namely Ar-X-R (referred to vMIP-II backbone sense), where Ar1 is an aromatic residue and X is an aromatic or an unsaturated residue in which the orientation of the three sidechains is highly preserved. The sequence is R^{12}-F-F^{14} for SDF-1 and W^{5}-H-R^{7} for vMIP-II. In both cases the conformation of these stretches is well-ordered, falling in turn-like regions (Figure 18).

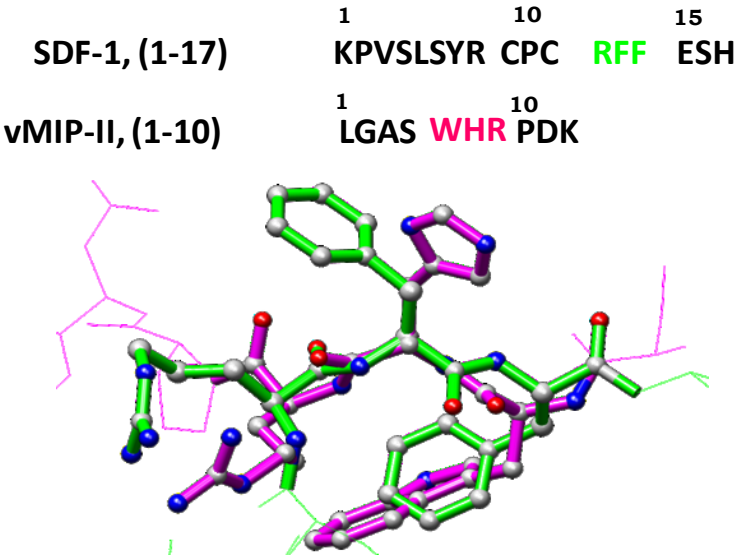

Figure 18. Tridimensional structure of the conserved amminoacidic motif shared by SDF-1α (green) e vMIP-II (purple).

In order to confirm this hypothesis, we designed, synthetized and tested a set of cyclic peptides enclosing this motif (Figure 19). The peptides differ in: a) nature of the aromatic residues or residues with unsaturated ring; b) sequence sense (R-Ar1-X vs. X-Ar1-R); c)

N- and C-termination, as all combinations of free, single- and double-protected (by acetylation and amidation) termini were tested on selected peptides; d) possible elongation at either peptide termini by a Arg-Ala sequence. This latter sequence was tested to include another structurally-conserved basic residue (Arg8 in SDF-1, Lys11 in vMIP-II), potentially representing a further anchoring site to CXCR4 binding, Ala only acting as a spacer.

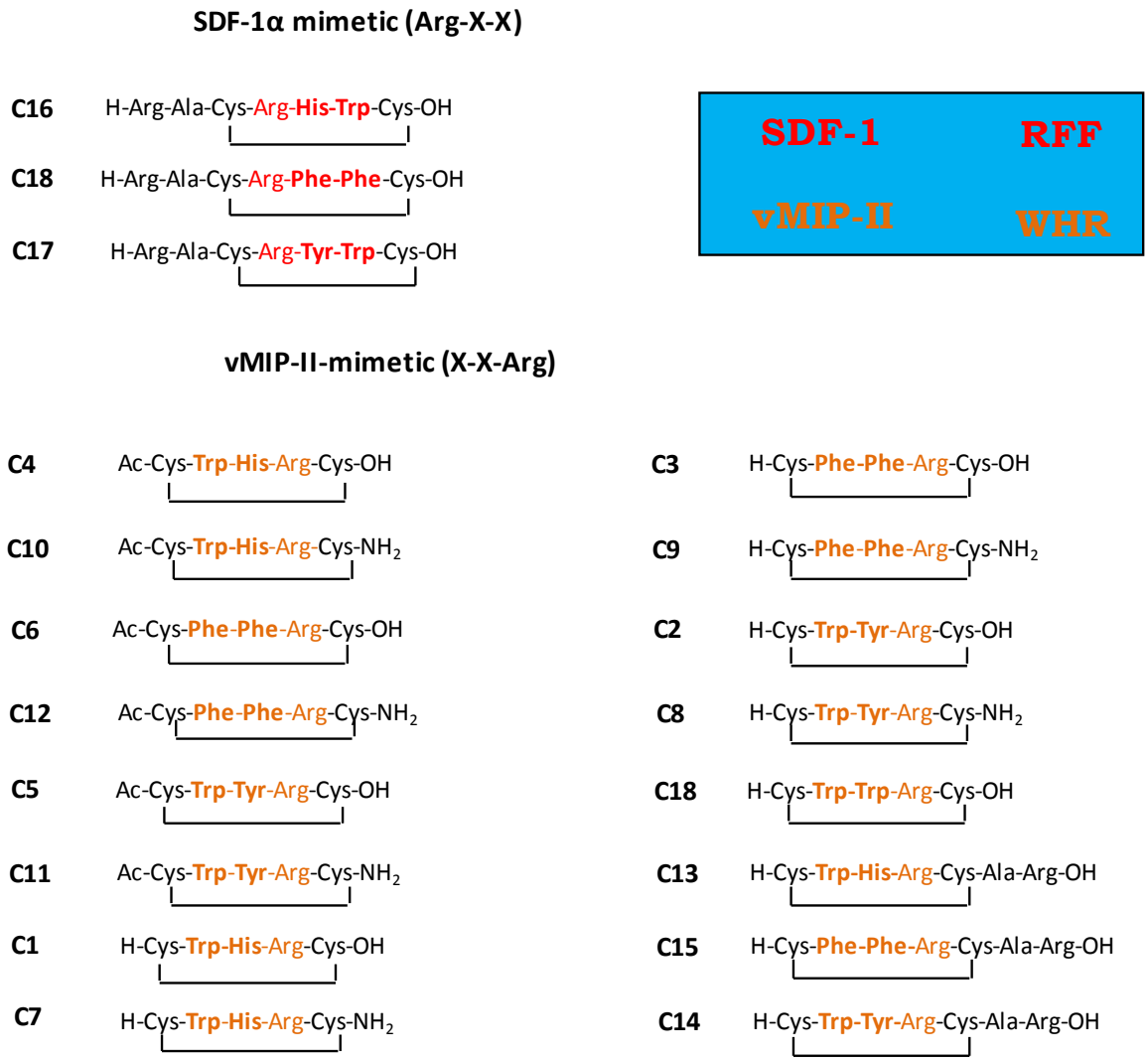

Figure 19 Amino acid sequence of synthesized peptides divided into SDF-1 mimetic and vMIP-II mimetic.

Peptides were designed with the following general scaffolds: (*nf*/*nac*)-C-Ar-X-R-C-(A-R-*cf*/*cf*/*cam*) and (*nf*-R-A/*nf*/*nac*)-C-R-X-Ar-C-(*cf*/*cam*), where Ar represent aromatic residues, X represent aromatic residues or residues with an unsaturated ring , *naf* and *nac* are respectively free amino or acetyl group peptide N-terminations, *cf* and *cam* are free carboxylate or amide group C-terminations, slash-separated sequences in parenthesis represent alternative options, and underlining denotes the cyclic part of the peptides. For brevity, *nf* and *cf* terminations are omitted in the following sequence notations. The Ar1-X sequences occurring in biologically assayed peptides are WH, WY and FF, while peptides containing the WW sequence exhibited, in general, a too low solubility to be reliably assayed. Starting structures were obtained using the experimental SDF-1 backbone conformation for the R-Ar1-X motif and by mutating the preceding and following residues

with cysteine residues, while the sense of peptide sequence was alternatively derived from vMIP-II or SDF-1. The choice of using SDF-1 backbone but with the sequence order of vMIP-II was guided by the better ring closure propensity of the former, combined to potentially antagonist behavior of the latter, inferred by the observed binding properties of vMIP-II N-terminal peptides [142]. The sequence reversal in RACRHWC (C16), RACRYWC (C17) and RACRFFC (C18) peptides was introduced to try to factorize the influence of sequence nature vs. sense on observed experimental properties. All peptides originate from the same scaffold with aromatic side chains mutated opportunely. Other than the natural sequences, also variant with Tyr and Trp residues at second position were designed to test the effect and the modularity of bulkiness and hydrogen bonding capability.

5 ns molecular dynamics (MD) simulations in solution were carried out to evaluate the effects of cyclization mode, elongation and termination on both side chains orientation and backbone conformation of the putative motif. The most evident feature emerging from trajectory analysis, common to all simulated peptides, is the relatively high conformational stability during the 5ns simulated time, the r.m.s.d. of final snapshot from average structure calculated on backbone atoms for the four peptides variants, namely CWHRC (C1), CWYRC (C2) and CFFRC (C3) being .0.41, 0.30, 0.62 Å, respectively. The final peptide conformation well fit onto the experimental conformation of vMIP-II at level of both central core and side-chain spatial orientation. However, local conformational differences and, especially, presence of the cycle closure sequence, may affect the rotamer distribution of WHR sidechains, potentially altering the relative stability of the different substates observed during the simulation, in comparison with vMIP-II and SDF-1.

The lack of direct information about the true bioactive conformations of our templates prevents any simple evaluation of these effects, but, as explained in the “Discussion” section, further activity is planned to address this issue.

Potentially destabilizing effects of partial or full protection at peptide termini were also investigated by MD simulations on CWHRC, but no appreciable modification on overall peptide conformation was observed, the r.m.s.d. respect to the average structure being less than 0.25 Å for all combinations of terminal protection. MD simulations carried out on CFFRCAR (C15) and RACRFFC (C18), selected as probe peptides to investigate the conformational propensities of seven residues peptides, showed an opposite behavior in H-bond capability both between each other and in comparison with their corresponding template proteins: in fact, only CFFRCAR (C15) is able to form a stable interaction between Arg4 side chain and the C-terminal oxygen atoms, that reproduces the H-bond between Arg12 side chain and the carbonylic oxygen of Cys9 in SDF-1 structure, even if its sequence order derives from vMIP-II, where such H-bond is absent. The substantial preservation of the relative sidechain orientation observed in template structures and the overall small conformational variations (compared to both linear and cyclic peptides of comparable size) during the MD simulations suggest a major role for this motif in the high structural stability experimentally observed for the vMIP-II(5-8) peptide [142]. In addition, the high conformational similarity shared by all simulated peptides suggests that most of the differences observed in biological properties among the peptides may be ascribed to local interactions of single atoms or groups with the receptor, rather than to intrinsic conformational preferences of each peptide.

The main goal in the design of this new class of peptides with potential agonist/antagonist activity toward CXCR4 receptor was to test a hypothesis about the activity of a short motif, identified, in reversed sequence order, both in SDF-1 and in vMIP-II N-terminal regions.

2.2 Peptide synthesis

A rational designed 18-membered library, consisting of different cyclic peptides, was synthesized on solid phase by using Fmoc chemistry standard protocols. Different solid supports were employed to construct the peptidic moieties. Rink Amide resin was employed as solid support to synthesize C7, C8, C9, C10, C11, and C12 (Figure 20) bearing an amido group at the C terminus, while Wang resin was employed to synthesize all the other linear compounds (Figure 21).

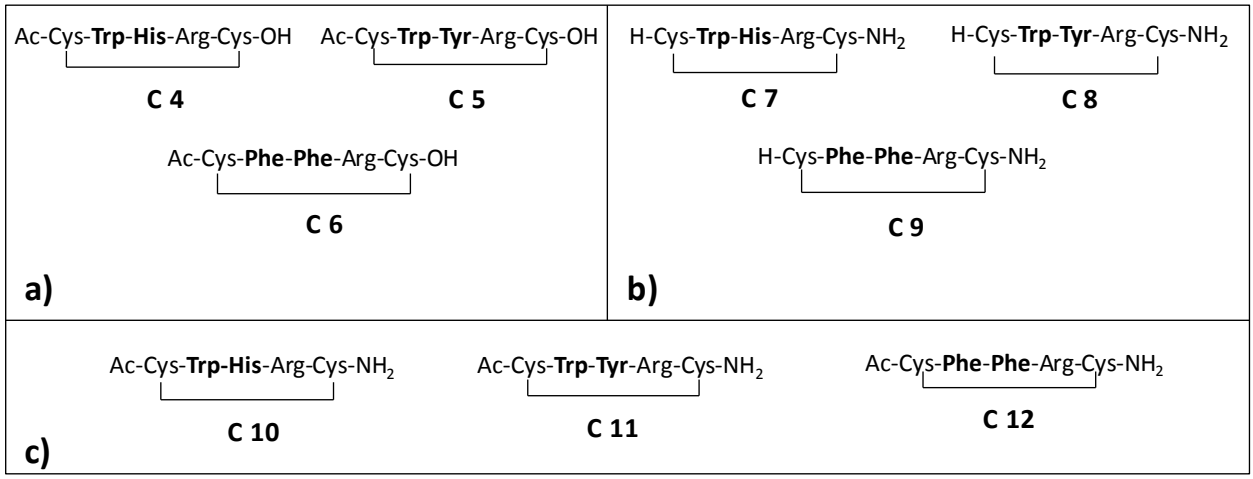

Figure 20 Amino acid sequence of synthesized peptides divided into: a) peptides acetylated at N-teminus; b) peptides with an amido group at the C-terminus and c) peptides acetylated at N-teminus and with an amido group at the C terminus.

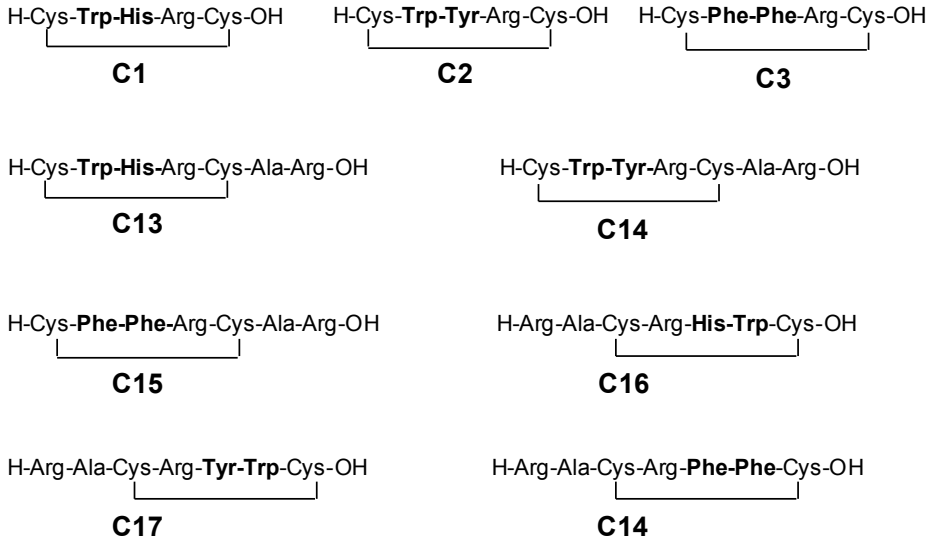

Figure 21 Amino acid sequence of synthesized peptides with free C- and N-terminus.

As shown in scheme 1, for all coupling reaction were used PyBop e HOBt as activating agents. N-terminal amino of peptide C4, C5, C6, C10, C11 and C12 (Figure 20) were acetylated on solid support with a mixture of 4.7% acetic anhydride and 4% pyridine in

DMF. The peptide cleavage from the solid support and the deprotection of all amino acid residues were obtained upon treatment with high percentage of trifluoroacetic acid, H_2O and triisopropylsilane (TFA/H_2O/EDT 94:4:2). The cyclisation reaction was performed by disulphide bridge formation between two cysteine residues. In particular the oxidation reaction was performed dissolving the crude products in aqueous solution (0.1 M) of NH_4HCO_3 . All compounds were obtained in good yield and with high purity grade (>95%) after RP-HPLC purification. They were fully characterized for their identity by mass spectrometry.

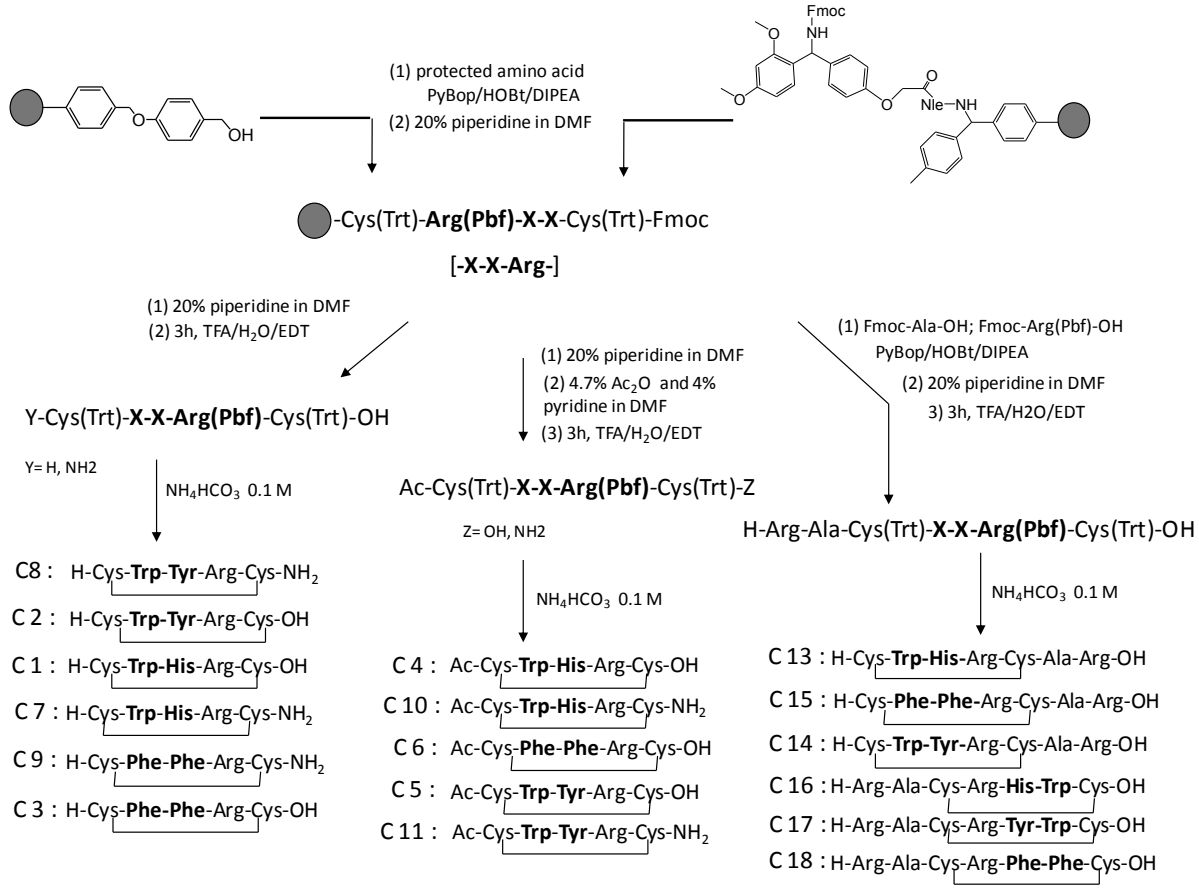

Scheme 1 Peptide ligands synthetic strategy.

3. Biological evaluation

In order to evaluate the peptide ability to modulate CXCR4/SDF-1α axis activation and to understand singular event concerning receptor activation, different biological assays were performed.
In particular peptides biological studies consist in evaluate:

- Binding through flow cytometry
- Modulation of intracellular Ca^{2+} release.
- Modulation of cell migration in presence or without specific ligand SDF-1
- Modulation of P-Erk activation.

In these studies two cellular lines were employed: CCRF-CEM, T-leukemia cell lines and PES43, human melanoma cell line.
For In vivo studies B16 melanoma cells were engineered to express human CXCR4 and then were demonstrated striking lung metastases inhibition of mouse melanoma B16-CXCR4 cells were inoculated into the tail vein of C57/BL mice.

CXCR4 cyclic peptides impaired CXCR4 binding.

The cyclic peptides binding to CXCR4 was evaluated through flow cytometry. Briefly, CCRF-CEM cells were incubated with the CXCR4 inhibitor, AMD3100 10 μM or the ligand peptides (10 μM for 30 minutes). In Figure 22 A, CXCR4 binding was impaired by the peptide C16 (10 μM) compared to AMD3100 10 μM. Figure 22B showed that the seven-residue peptides with sequence derived from CXCL12 (C16, C17, C18) reduced the binding PE-CXCR4 antibody to the receptor (respectively 17, 22 and 21%); peptide C1 also inhibited CXCR4 binding (55% versus 10-30% AMD3100). The interaction with the other peptides minimally affected the binding.

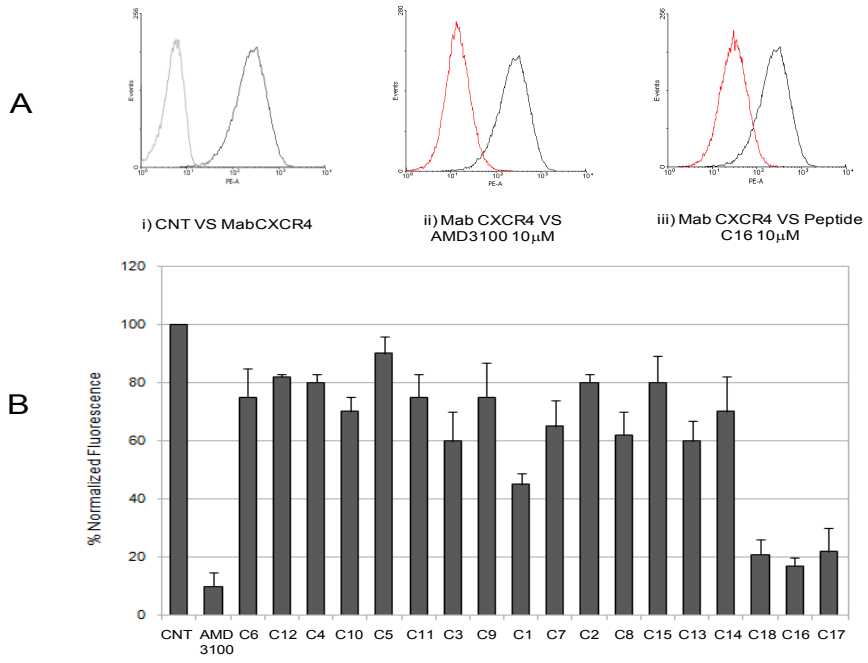

Figure 22 Indirect CXCR4 binding: Assessment of Peptides binding to CXCR4. Experiments were conducted using CCRF–CEM cells. The amount of AMD3100/peptides bound was assessed indirectly by flow cytometry using the PE-labelled anti-CXCR4 antibody. **A** Example experiment, i) CNT VS MabCXCR4 ii) Mab CXCR4 VS AMD3100 10 μM iii) Mab CXCR4 VS Peptide C16 10μM; **B** The results are expressed as the percent antibody bound in the presence of AMD3100/peptides;

CXCR4 cyclic peptides inhibited calcium release CXCL12 induced.

CCRF-CEM pretreated for 1 hour with 10 µM of ligand peptides, were loaded with Fluo-3AM. In figure 23A the effect of peptide C17 was evaluated; ionomicyn value being the positive control. As showed in Figure 23B peptide C17 (33.65%), C9 (49.1%), C16 (49.75%), C18 (51.25%) and C10 (57.35%) clearly reduced the calcium efflux in comparison to the AMD3100 effect (32.85%). Other peptides have a moderately antagonist (>60) up to weakly agonist (<106) effect; peptide C5 (110.35%) and C4 (125.25%) increasing calcium efflux.

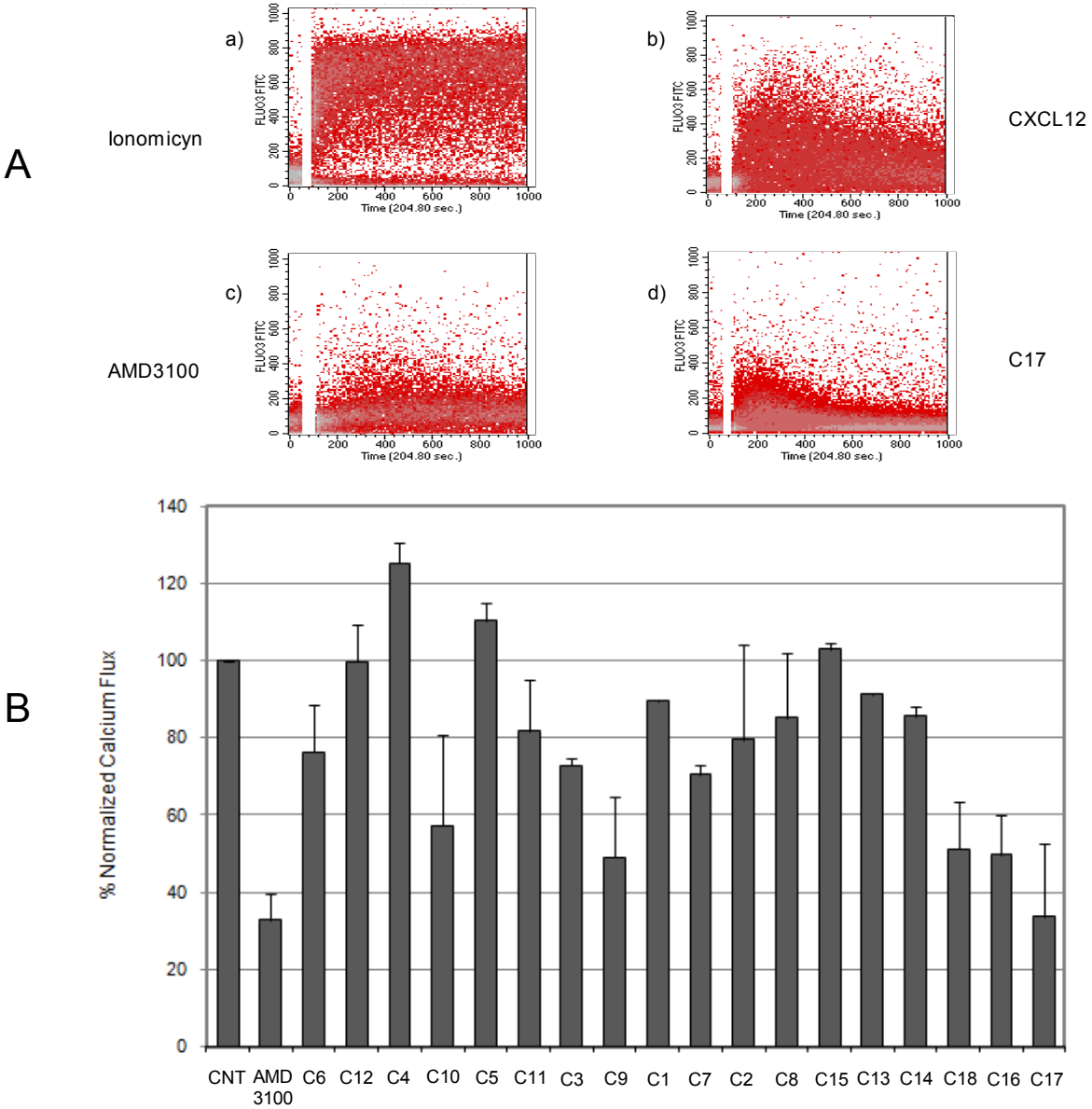

Figure 23 Calcium Efflux: Inibhition of SDF-1 medieted calcium efflux. The assay was performed using CCFR-CEM and Fluo-3 AM calcium indicator. CCFR-CEM were incubated 30'min. at 37°C with Fluo-3 AM and 15'min with AMD/peptides and then treathed with Ionomicyn/SDF-1 before get analyzed. **A** CEM treated with ionomicyn (a) rapresent the maximun calcium efflux; in b), c) and d) the misuration of CXCL12 mediated calcium efflux alone and in presence of AMD3100/C17 as example; **B** The result are expressed as the percent of Fluo-3 AM fluorescence in presence of CXCL12 alone.

CXCR4 cyclic peptides inhibited P-Erk induction, cell migration and wound healing CXCL12 induced.

To further evaluate the effect of cyclic peptides on CXCR4, P-Erk induction and migration CXCL12 induced were analyzed in PES43, human melanoma cells pretreated with the cyclic peptides. Briefly migration was conducted in 8 μm transwell. PES43, human melanoma cells [143] were seeded in the upper well and allowed to migrate toward FBS, BSA, CXCL12 (100ng/ml) in the presence of peptides. Migration index was defined as the number of cells migrating toward CXCL12. Figure 24A demonstrated an efficient inhibition of migration in the presence of peptides C14, C18 and C17. Peptides C10, C1 and C16 also reduced CXCL12-induced migration (50%). Interestingly, five peptides determined convincing migration increase. Peptides C7, C8, C11, C13 and C9 increased migration 1.5-; 1.55-; 1.55-; 1.7- and 1.9-fold higher than CXCL12.
Moreover wound healing assay was conducted in PES43 cells in the presence of CXCL12. Figure 24B shows the delay in wound healing in the presence of peptide C1, C16, C17 and C18. Since functional CXCR4 transduce the signal activating P-Erk CXCL12 dependent induction was evaluated in PES43 cells in the presence or absence of the CXCR4 cyclic peptides. In Figure 25A an example of P-Erk induction in the presence of peptides is shown. Peptide C18 reduced p-ERK-CXCL12-induced after 5 minutes compared to AMD3100 while it does not affect p-ERK in absence of CXCL12. In Figure 25B p-ERK modulation induced by cyclic peptides is shown. In particular peptides C1, C2, C18 and C16 clearly reduced p-ERK induction; peptides C12, C10, C11, C3 and C14 demonstrated weak activity while peptides C6 and C17 did not interfere with P-ERK induction. Interestingly peptides C4, C5, C9, C7, C8, C15 and C13 showed increased p-ERK induction.

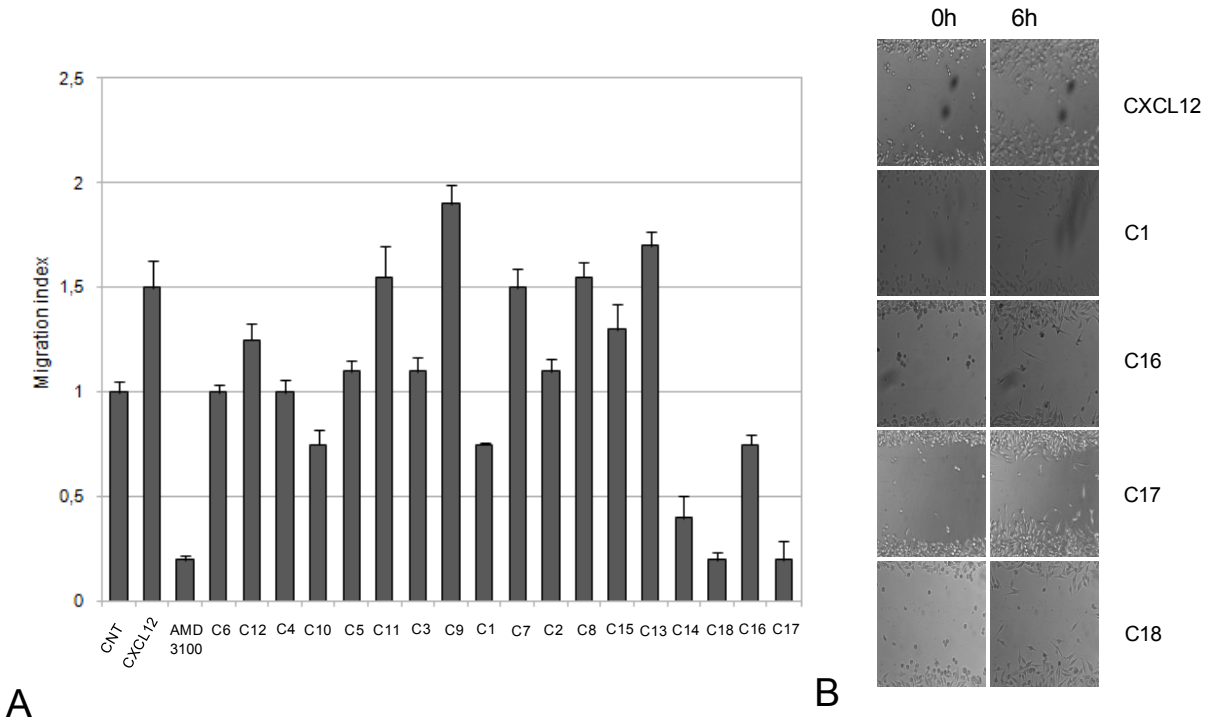

Figure 24 Migration Assay: Migrated cells on the lower surface were fixed, stained with H&E and counted microscopically. In order to study the cell shape, cells were treated at 37°C with or without CXCL12 (100 ng/ml) and AMD3100/peptides. **A** The results are expressed as the migration index respect to migration in presence of CXCL12 alone. **B** Delay in wound healing after 6 hours in presence of C1, C16, C17 and C18 compared with CXCL12. Images were acquired with OKO Time Lapse.

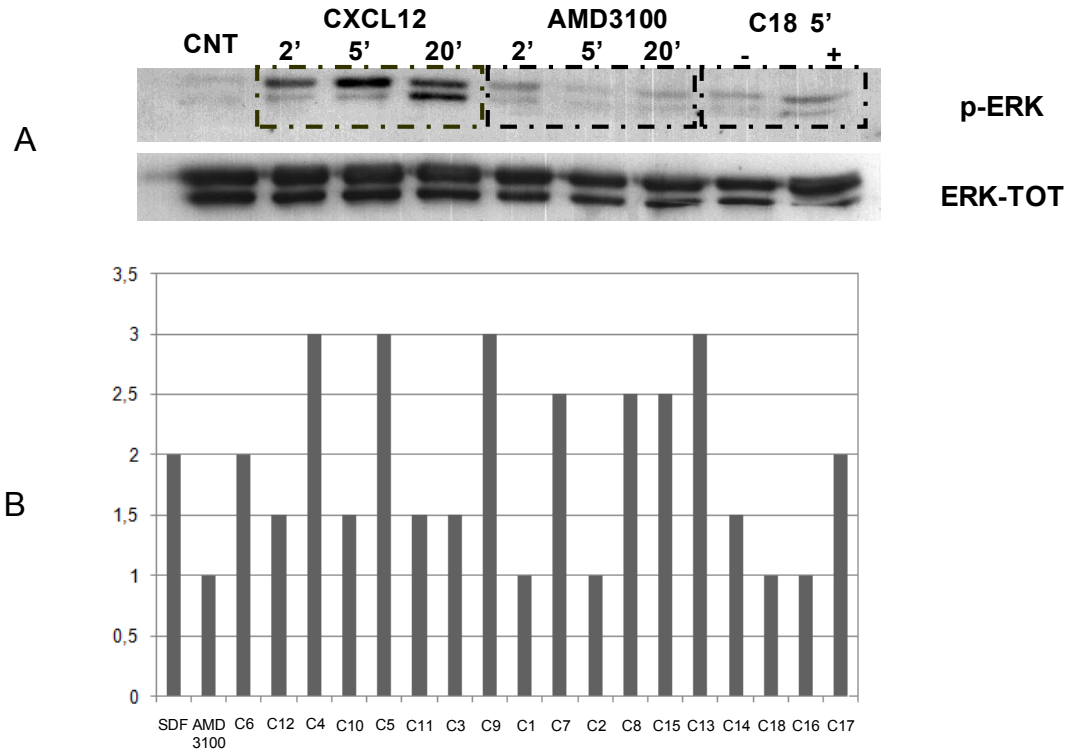

Figure 25 P-ERK induction: CXCL12 induces phosphorylation of extracellular signal regulated kinases (ERK) 1 and 2 in PES43 cells. To study the inibition of CXCL12 mediated ERK phosphorylation in presence of AMD/peptides PES43 were serum-starved for 24 h and then incubated with CXCL12 (100 ng/ml) alone or in presence of AMD3100/peptides. Changes in the phosphorylation of p44/ 42 (Erk1/2) kinases were analysed by Western blotting using antibodies specific for the following proteins: phospho-ERK1 and 2, total ERK. **A** Example experiment. CXCL12 p-ERK induction was evaluated at 2, 5 and 20 minutes and was establish that the maximum is reached at 5 minutes. Peptide C18 inhibitory capability on p-ERK induction was at 5 minutes in presence and in absence of CXCL12. AMD3100 was used as negative control. **B** p-ERK induction evaluated in presence of inhibitory peptides plus CXCL12.

CXCR4 inhibiting peptides C1, C18 and C16 inhibited melanoma metastases.

The "in vitro" screening of twenty CXCR4 cyclic peptides promoted to investigate in vivo activity of 3 selected peptides. To this aim B16 melanoma cells were engineered to express human CXCR4. Then $5x10^5$ B16-CXCR4 cell, pre-incubated with AMD3100 (10 μM) or peptide C1, C18 or C16 (10 μM) were inoculated into the tail vein of C57/BL mice. Mice were treated intraperitoneally once a day for 10 days (2 weeks) with 2mg/kg peptide C1, C18 and C16, 1.25mg/kg AMD3100 or PBS alone. Mice were euthanized after 4 weeks and macroscopic inspection of lungs and H&E were performed. As showed in Figure 26 the lung derived from peptides C1, C18 and C16 treatment presented a dramatic decrease in metastases number compared to untreated mice.

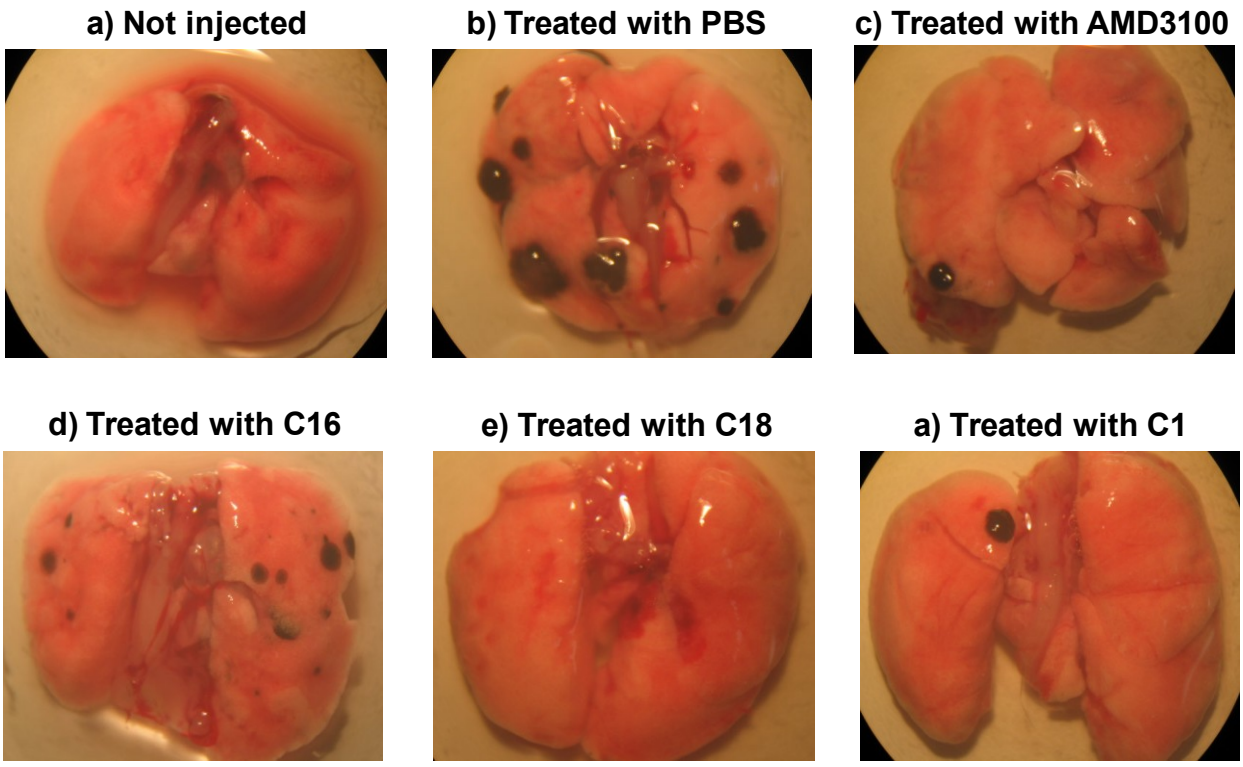

Figure 26 Metastases Formation assay: We injected B16-CXCR4 tumor cells into the tail vein of 25 C57/B female mice and divided them in 5 groups with 5 mouse each goup: goup n°1 treated with PBS (b), and groups n° 2-3-4-5 treated rispectively with AMD3100 1.25mg/kg (c), C16 (c), C18 (d) and C1 (e). We injected 2mg/kg of CXCR4 peptide antagonist for mouse 5 day weekly for 2 weeks i.p. We also have 1 mouse not injected as negative control. Tumor cells were 30' min pre-treated with antagonist and injected on the first day of treatment. Mouse injected with B16-CXCR4 cells and treated with control peptide developed big lung metastasis (4 animals on 5). On the other hand, animals treated with CXCR4 antagonist developed significantly fewer metastases or no metastasis.

3.1 Discussion

The role of CXCR4/SDF1 in tumour progression prompted to the discovery of CXCR4 inhibitors. The best known CXCR4 antagonist is AMD3100, a bicyclam molecule initially used in the treatment of AIDS. Intratumoral AMD3100 inhibits the growth of glioblastoma, breast and prostatic cancers[22, 71, 77, 144-151]. Despite promising results AMD3100 has considerable toxicity, mainly cardiac and is not orally bioavailable [119, 152]. Inibitory peptides were also described such as T22, T140 and TN14003 [52, 131, 132, 153]. These peptides were synthesized by combinatorial synthesis where, given a model compound, the changes are randomly implemented. More recently aimed at an antagonist with molecular-size smaller than T140 led to discovery CXCR4 antagonist with a cyclic pentapeptide template, FC131 with an high HIV-entry inhibition capability [137].
The aim was to identify CXCR4-antagonist clinically suitable. The RFFESH CXCL12's domain was the starting point. In detail, a common structural domain was identified between CXCL12 N-terminal region and vMIP-II N terminal domain and a new library of cyclic peptide molecules was generated and tested through *in vitro* assays.
The main goal in the design of this new class of peptides with potential agonist/antagonist activity toward CXCR4 receptor was to test a hypothesis about the activity of a short motif, identified, in reversed sequence order, both in SDF-1 and in vMIP-II N-terminal regions. In this view, the design was successful, producing peptides endowed with biological activity

in several assays addressing some of the many physiological and pathological functions of CXCR4 receptor.
The biological assays on synthesized peptides revealed an unusual behavior of both the single peptides in different assays, and of the whole set of peptides in each assay. In addition, dramatic and non-additive effects of terminal protective groups were also observed.
Looking at each assay in more detail, Q-Brite results show some degree of regularity, as seven-residue peptides with sequence order derived from SDF-1 (C16, C17 and C18) all exhibited substantially lower values (respectively 17, 22 and 21, comparable to the 10-30 measured for AMD3100) than all other peptides, ranging from 60 to 90, with the only partial exception of C1, which scored an intermediate value of 45.
Also in migration assay, the strongest inhibitory effect was observed for two of the seven-residue peptides more active in Q-Brite test, namely C17 and C18, which exhibited the same 0.20 value measured for AMD3100, a strong antagonist activity being also associated to C14 (0.40). Other tested peptides exhibited behaviors varying from moderately antagonist, to weakly agonist. However, five peptides exhibited strong agonist behavior, with migration values equal or higher than 1.5 (the value measured for SDF-1): C7 (1.5), C8 (1.55), C11 (1.55), C13 (1.7) and C9 (1.9).
A similar variance is also observed in calcium flux experiments, where C10 exhibited the strongest antagonism (40.7 vs. 32.85 measured for AMD3100), followed by C3 (53.3), C17 (56.0) and C9 (59.9). Other peptides have a moderately antagonist (>60) up to weakly agonist (<106) behavior, with two peptides, C5 (113.7) and C4 (121.4) showing strong agonism in this assay.
An even more complex response was obtained in compared P.ERK assays in presence and absence of SDF-1. In fact, while some peptides exhibited values apparently compatible with either strong antagonism (C1, C9), or strong agonism, (C4, C13, C5, C8, C11 and C15) or strong partial agonism (C14, C3 and C15), or weak partial agonism (C2, C17 and C6), in one case (C12) the peptides in the absence of SDF-1 behaves as an agonist with the same value measured for SDF-1, thus making ambiguous any interpretation of the value obtained in the presence of SDF-1. However, the most striking results are obtained for C10 and C16, where an apparently weak to medium agonist behavior in the absence of SDF-1 turn into strong antagonism in the presence of SDF-1, and C7, for which an apparent synergy with SDF-1 is observed. The peptides (C1, C16 and C18) significantly inhibited melanoma metastases and preliminary results showed that renal cancer cells xenograft SN12C-pEGFP was significantly reduced in growth in the presence of peptides C1, C16 and C18.
The pattern of biological responses elicited by these peptides was, however, very various, the behavior varying from agonism to antagonism, to inactivity for a same compound in different tests, and, more intriguingly, showing hints of non-additivity for their interaction with CXCR4 receptor in the presence of SDF-1. These results can not be explained by simple models for receptor activation/inhibition and suggest more complex interpretations, possibly involving direct SDF-1-peptide interactions and/or influence on symmetry, stoichiometry or structural variations of the homo- or hetero-oligomeric state of CXCR4 receptor. These features, while prompting for new studies aimed at unraveling such a complex plot, open new perspectives in obtaining more selective compounds toward different biological pathways involving CXCR4 receptor.

4. Synthesis of peptide-chelating agent conjugates

Small radiolabelled compounds such as peptides are very attractive tools for the diagnosis of several different pathologies [154]. With this idea in our mind, as a subsequent step, it was evaluated the possibility to develop peptide C18 derivative bearing a chelating agent able to coordinate radioactive metals for applications in cancer diagnosis by nuclear medicine techniques. In order to investigate the chelating agent site of linkage which does not interfere on the peptide-receptor interaction, two diethylentriaminopentacetic acid (DTPA)-C18 conjugates were synthesized: one carrying DTPA moiety covalently bound to petide N-terminus (C20) and one carrying the chelating moiety DTPA covalently bound to the ε-NH_2 of a lysine residue which replaced Ala2 of C18 (C19).
The DTPA chelating agent is routinely used to give in vitro and in vivo stable complexes of the radioactive isotope ^{111}In(III).
Scheme 2 shows synthetic process in order to obtain the compound C19 and C20 in good yield and with high purity. For compound C20, the DTPA$(OtBu)_4$ was coupled, through its free carboxyl function, to the α-NH_2 of the Arg residue, after the last Fmoc deprotection step. This coupling step was performed using 2.0 equiv. of DTPA$(OtBu)_4$ and HATU, and 4 equiv. of DIPEA (DMF was used as solvent). The coupling time, compared with the classical solid phase peptide synthesis protocol, was increased to 2 h and completion of the reaction was checked by Kaiser test [155]. The conjugate cleavage from the solid support, the deprotection of all amino acid residues and cyclisation reaction were performed following the same protocol described in Peptide Synthesis paragraph.
Concerning compound C19, after selective removal of the Metyltrityl group on the ε-NH_2, the chelating agent DTPA$(OtBu)_4$ was ancored to Lys2 side chain as described for C20. As final step, the N-terminal Fmoc was removed and the conjugate obtained detached from the solid support and freed from its protective groups (see Peptide synthesis paragraph). The final cyclisation was performed as always described for each synthesized peptide.
The successful synthesis of the two conjugates C19 and C20 allows the subsequent labelling of the peptide derivative with the radioactive isotope^{111}In(III).
Before performing nuclear medicine imaging studies, C19 and C20 were evaluated for their ability to inhibit the specific antibody binding to CXCR4. As shown in Figure 27, both conjugates exhibited a reduced inhibiting activity, compared with that exerted by the only peptide sequence (C18). These results highlighted that the introduction of the chelating agent on the N-terminus, as well as on the lysine ε-NH2 group, can affect the binding process with the receptor target. We are currently exploring other peptide positions where to anchor the DTPA moiety.

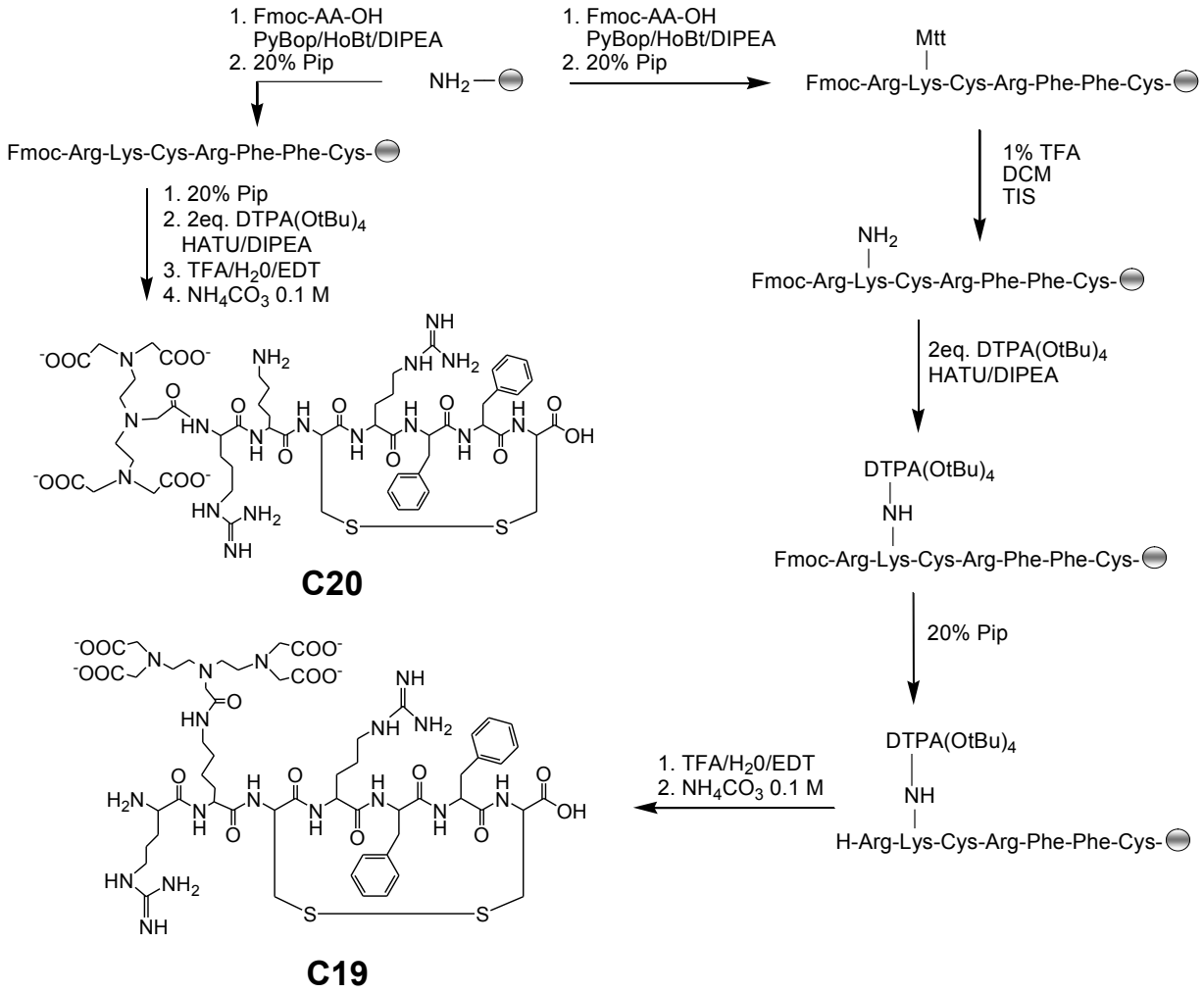

Scheme 2 Synthetic strategy to obtain (DTPA)-C18 conjugates: C19, carrying the chelating moiety DTPA covalently bound to the ε-NH_2 of a lysine residue and C20 carrying DTPA moiety covalently bound to petide N-terminus.

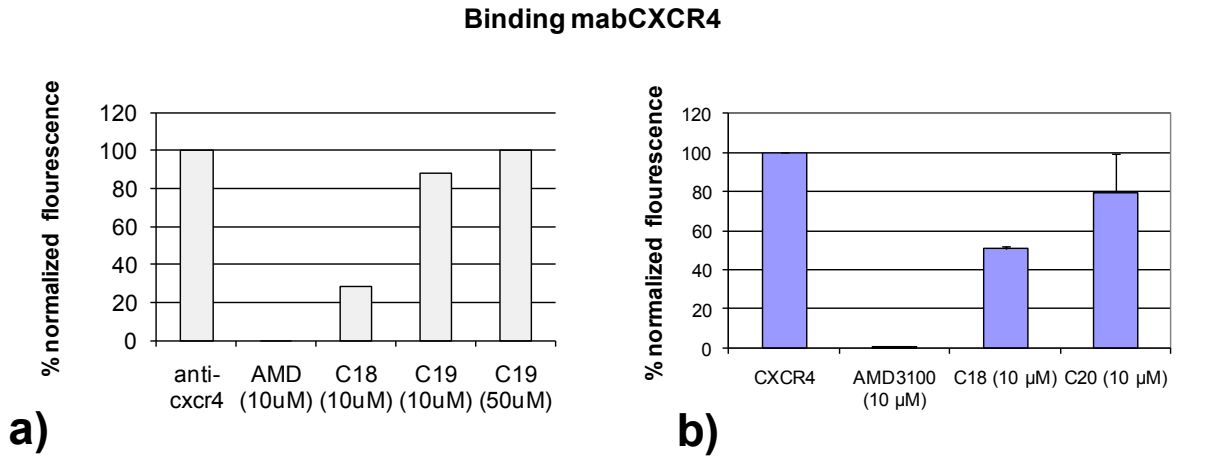

Figure 27 Indirect CXCR4 binding: Assessment of (DTPA)-C18 conjugates binding to CXCR4.

5. Peptidomimetics design

Therapeutically relevant peptides themselves are seldom used in the clinic because of their poor biostability, unfavorable absorption properties, as well as poor receptor subtype selectivity. Nevertheless, they can be used as a template in order to synthesize modified peptides, called peptidomimetics, which are endowed with increased pharmacological activities.

In a successfully designed peptidomimetic, two structural factors must have been taken into account: 1) a favorable docking in the binding site of the receptor target, if necessary the conformation can be stabilized by introduction of elements conferring rigidity such as bridges of various length between different parts of the molecule; 2) the spatial orientation of certain structural motifs (e.g. functional groups, polar and hydrophobic moieties) corresponds to the display in the bioactive conformation of the peptide, so that the required interactions (e.g. hydrogen bonds, electrostatic or hydrophobic interactions) can occur [156].

One possible strategy to favor the formation of bioactive conformations is modifying the side chain of amino acids [157]. In fact, the field of amino acids modifications has gained a big relevance in recent years, particularly with the emergence of new building blocks that allow introducing chemical and functional diversity into molecules with therapeutic potential.

Since the pharmacophoric motif of the most active peptide sequence (**C18**) is characterized by aromatic rings and idrofobic residues, it is possible to project peptidomimetics in order to modulate the aromatic rings distance from the peptide backbone. In particular, Phe3 and Phe4 residues of C18 can be replaced by aminobenzilic derivatives, such as N^{ε}-benzylated Lys and its shorter homologues, in order to evaluate the influence of the more flexible pharmacoforic motif on the binding process.

With these ideas in our mind, we focused on the development of an efficient synthetic route to obtain modified on their side chain, via N-alkylation reaction, N^{α}-Fmoc amino acids suitable to be introduced into a peptide sequence. The aim has been to set out a mild and general N-alkylation procedure which does not affect the stereochemistry of the amino acids chiral center, neither other sensitive functional/protective groups (i.e: the α-COOH and Fmoc/Boc groups) also present on the substrate.

5.1 New N-alkylation procedure of Fmoc-amino acid derivatives

Many different strategies [158-162] have been developed to obtain N^{α}-Alkyl amino acids, including reductive methods, Mitsunobu condition, direct alkylation by halides in presence of strong bases DBU [163, 164], NaOH [165], NaH [165, 166], LiOH [167] and usage of diazomethane in some case of methylation [168]. At the best of our knowledge, there are only few examples in literature that describe the side chain N-alkylation of amino acids [169, 170]. Yan-Mei Li method employs reductive conditions in order to obtain the N^{ε}-methyl lysine. The most cited Kessler protocol employs alkyl halides in presence of DBU or Mitzunobu condition in order to N^{δ}-alkylate the ornithine in solid phase. Both Kessler's procedures require the protection of the ornithine N^{α}-NH_2 with an Alloc group and this is performed by an additional synthetic step.

Most of the cited protocols protect the amino group as sulfonamide, by using the nitrobenzensulfonyl group (Ns) [171-173] in order to synthesis mono-N-alkylated peptides [174]. In fact, the Nosyl group require mild conditions for its deprotection and is compatible with Fmoc solid phase synthesis [175], due to its stability under acidic (HCl) as well as basic (NaOH) conditions.

We have previously described an efficient synthetic strategy to prepare *o*-Ns protected Fmoc-amino acids under mild conditions, in a rapid way and without resorting to any purification step. The products obtained (Fmoc-Lys(Ns)-OH, Fmoc-Orn(Ns)-OH, Fmoc-Dab(Ns)-OH and Fmoc-Dap(Ns)-OH) were successfully employed as building blocks in solid phase synthesis [176]. Starting from these results, as next step we focused on the development of a synthetic procedure for N-alkylation of the above mentioned Fmoc-amino acids derivatives. In this contest, it is worth noting that the reaction conditions of the cited N-alkylation protocols are not compatible with Fmoc-group, since they employs quite strong basic conditions. So, we tried the traditional approach (K_2CO_3, halide, DMF) on the above mentioned amino acid derivatives previously synthesized [176]. This method hardly provided the mono-N-alkylated amino acids, moreover the separation of the product from salts was totally unsuccessful.

Therefore, we developed an alternative and more practical synthetic route which employs only 4 Å molecular sieves in order to promote the N-alkylation with halides in absence of any other base.

Next, we performed the alkylation reaction on several Fmoc-amino acids previously protected on their side chain with Ns group (Fmoc-Lys(Ns)-OH, Fmoc-Orn(Ns)-OH, Fmoc-Dab(Ns)-OH Fmoc-Dap(Ns)-OH) [176]. As shown in Scheme 3, each amino acid derivative was dissolved in DMF at room temperature and treated with the appropriate alkyl halide in presence of activated 4 Å molecular sieves.

The optimized N-alkylation procedure was explored toward a wide range of alkyl halides and, for each of them, the reaction time and the relative yield are summarized in Table 2.

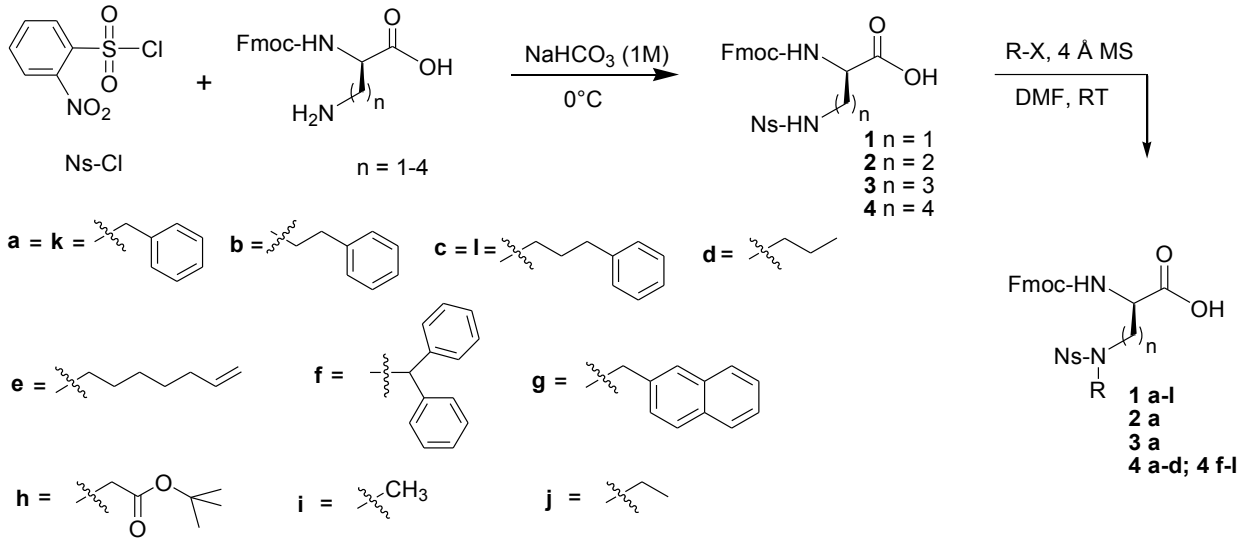

Scheme 3 Synthetic strategy of mono-N-alkylated amino acids

In particular, the N-alkylation reactions with benzyl and 3-phenylpropyl groups were performed by using the appropriate bromide and then repated by using the corresponding chloride. As expected, the employed halides did not react equally [177, 178]. After 24 h we could recover compound 1k and 4k with a yield around 50% (Table 2), while 1a and 4a were obtained in almost quantitative yield (>95%). Concerning 1l and 4l, the chlorides promoted a minimal conversion, which was characterized by a reaction yield lower than 5% (Table 2), while the bromides were successful in producing 1c and 4c (yield of 90-95%).

It is known that while the side chain pKa of Lys, Orn and Dab is very similar, this value for Dap is lower by one unit [179]. Nevertheless, as suggested by the similar reaction yield

obtained for all amino acid derivatives (Lys, Orn, Dab and Dap) alkylated by the same halides, the same nucleofilicity toward the same alkylating agent has been shown by Lys, Orn and Dab as well as Dap (in Table 2, compare yield of 1a, 2a, 3a, 4a; 1b and 4b; 1g and 4g; 1h and 4h; 1i and 4i).

Table 2. Mono-N-Alkylation efficiency of each Fmoc-amino acids with respect to the employed halides.

compound	time (h)	yield (%)	R-X	compound	time (h)	yield (%)	R-X
1a	15	>95	Br-Bn	**3a**	18	>95	Br-Bn
1b	15	95	Br-$(CH_2)_2$-Ph	**4a**	22	>95	Br-Bn
1c	15	95	Br-$(CH_2)_3$-Ph	**4b**	22	90	Br-$(CH_2)_2$-Ph
1d	24	90	Br-$(CH_2)_2$-CH_3	**4c**	24	<70	Br-$(CH_2)_3$-Ph
1e	35	60	Br-$(CH_2)_5$-CH_2=CH_2	**4d**	28	75	Br-$(CH_2)_2$-CH_3
1f	38	70	Br-$CH(Ph)_2$	**4f**	48	50	Br-$CH(Ph)_2$
1g	18	95	Br-CH_2-Naph	**4g**	22	90	Br-CH_2-Naph
1h	15	>95	Br-CH_2-CO_2-$C(CH_3)_3$	**4h**	18	95	Br-CH_2-CO_2-$C(CH_3)_3$
1i	15	>95	I-CH_3	**4i**	18	95	I-CH_3
1j	15	95	I-CH_2-CH_3	**4j**	22	80	I-CH_2-CH_3
1k	24	50	Cl-Bn	**4k**	24	50	Cl-Bn
1l	24	<5	Cl-$(CH_2)_3$-Ph	**4l**	24	<5	Cl-$(CH_2)_3$-Ph
2a	18	>95	Br-Bn				

It is worth noting a decrease of reaction rate with the increase of the amino acid side chain length, for instance, the substitution reaction for compounds like 4c, 4d and 4f proceeds so slowly that by-products formation was also observed. Several effects are likely to contribute to a great decrease in reaction rate and yield (4c < 4d, 4f < 1f), like the presence of not particularly electron-rich (4d) or sterically hindered (4f) substituents on the alkyl bromide central carbon. As a consequence, the reaction yields observed for these compounds were lower than what expected.

In general, the highest yield values were found for the most electron-rich alkyl bromides (see Table 2, yield of 1a, 1b, 1c, 1g, 2a, 3a, 4a, 4b, 4g). In any case of yield around 90%, the compound obtained can be used as crude product for the subsequent peptide synthesis, after centrifugation that allows elimination of the molecular sieves, while for all compounds characterized by a yield lower than 75%, it was necessary to purify the final product by RP-HPLC. In these cases, the purification also allows to recover any unreacted amino acid which can be employed again for alkylation reactions.

In order to further study the developed N-alkylation procedure promoted by molecular sieves, we performed the N-benzylation of the following Fmoc-diaminopropionic acid derivatives, Fmoc-Dap(Boc)-OH, Fmoc-Dap(Mtt)-OH and Fmoc-Dap(Dde)-OH (Figure 28), which are among the most used in peptide solid phase synthesis. As showed in Figure 28, the reaction was successful for each of these differently protected diaminopropionic acid derivative, even though it proceeded slower (24 h) than the same N-benzylation performed on Fmoc-Dap(Ns)-OH (15 h). Moreover, the formation of 5a and 6a is also characterized by a slightly lower yield (75 %), compared with 1a (>95 %). In fact, the synthesis of 5a resulted incomplete, while the synthesis of 6a produced some by-products, as a

consequence for these building blocks a purification step is required before being employed in peptide synthesis. All in all, the proposed N-alkylation methodology resulted validated for different amino protecting groups.

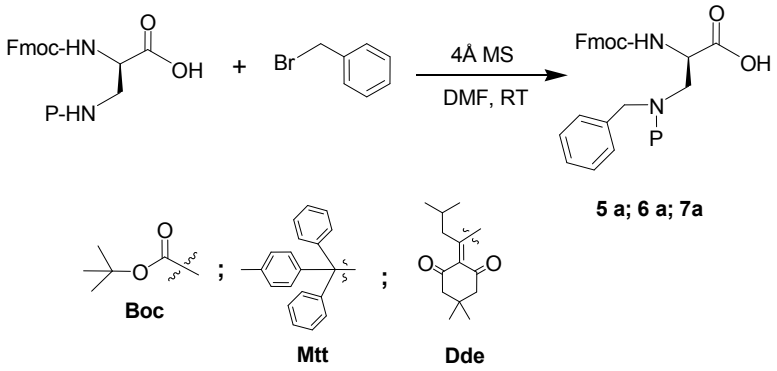

Figure 28 N-benzylation of differently protected Fmoc-diaminopropionic acid derivatives and relative reaction times and yields.

compound	time (h)	yield (%)	P
5a	24	75	Boc
6a	24	75	Mtt
7a	24	95	Dde

5.2 Synthetic strategy to incorporate amino-alkylated building blocks into a peptide sequence

In order to demonstrate the practical applicability of the functionalized amino acids as building blocks, we decided to introduce 1a, into a peptide sequence by using the standard Fmoc-based solid phase protocol (Scheme 4).

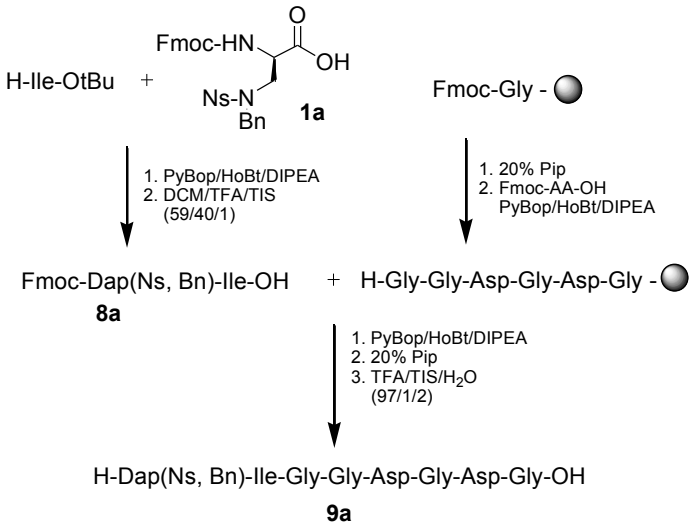

Scheme 4 Introduction of N-alkylated aminoacids into solid supported generic peptide (Fmoc-Gly Wang Resin, 0.8 mmol g^{-1}. TFA = trifluoroacetic acid; TIS = triisopropylsilane).

As preliminarily shown by Kaiser test result and confirmed by LC-MS analysis on the crude products obtained upon cleavage from the resin, the desired alkylated peptide was found with a low yield (data not shown). It is likely that the sterical hindrance of the introduced substituent and the nitrobenzensulfonyl (nosyl) groups on the side amino group makes the coupling of N-alkylated amino acid with the peptide sequence on the resin difficult.

Therefore, a solution phase coupling, in DMF with standard carboxyl activation PyBop/HOBt/DIPEA, of 1a with H-Ile-OtBu was performed (Scheme 4). The corresponding dipeptide 8a was recovered with quantitative yield and high purity, after treatment with trifluoroacetic acid in order to remove tBu group. As subsequent step, 5a was introduced into a peptide sequence in solid phase using standard Fmoc-chemistry (Scheme 4). After cleavage from resin, the alkylated peptide 9a, fully characterized by LC-MS analysis, was obtained with a yield of around 70% (Figure 29). This result confirmed the reliability of the alkylation method developed, since it was proven to fit well with Fmoc chemistry.

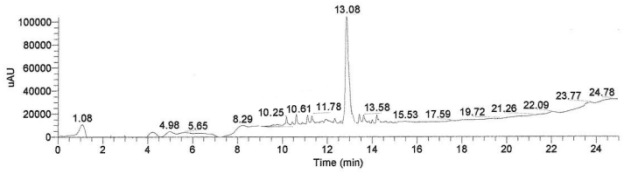

Figure 29 HPLC profile of **9a** crude product.

In conclusion, by using only molecular sieves to promote the reaction, a mild, scaleable and efficient solution phase procedure for side chain N-alkylation of Fmoc-amino acids was developed. It results completely innovative, since in literature, at the best of our knowledge, it is not described any example of N-alkylation reaction performed with halides and molecular sieves as base. The proposed N-alkylation methodology was validated for different amino protecting groups, but the best results were obtained by using *o*-Ns protected Fmoc-amino acids, which represent readily available starting materials. In fact, the employed Fmoc-amino acids are rapidly and efficiently protected with Ns group, and affords the desired mono N-alkylated compound in high yield.
For the majority of the employed halides, the procedure is a one-pot synthesis which avoids the purification after each reaction step. Moreover, it allowed the production of the desired compound in synthetically useful yield for the subsequent peptide chain assembly. Thus, the developed mothodology enables to introduce different substituents on the side chain of peptides C18 and to synthesize a great number of peptidomimetics, with the final goal of modulating the type and the distance of the aromatic pharmacophoric groups from the peptide backbone.

6. Conclusions and future perspectives

On the basis of a three-dimensional structures of both SDF-1 protein and vMIP-II N-terminal segment, a sequence-structure comparison between the N-terminal regions of this two proteins led to the design and synthesis of 18-membered peptide library. Each of this compound were evaluated for their ability to modulate CXCR4/SDF-1 axis function, in order to understand singular event concerning receptor activation. The pattern of biological responses elicited by these peptides was, however, very various, the behavior varying from agonism to antagonism, to inactivity for a same compound in different tests, and, more intriguingly, showing hints of non-additivity for their interaction with CXCR4 receptor in the presence of SDF-1. The lack of direct information about the true bioactive conformations of our templates prevents any simple evaluation of these effects, but further activity is planned to address this issue.

In fact, the results obtained can not be explained by simple models for receptor activation/inhibition and suggest more complex interpretations, possibly involving direct SDF-1-peptide interactions and/or influence on symmetry, stoichiometry or structural variations of the homo- or hetero-oligomeric state of CXCR4 receptor. These features, while prompting for new studies, open new perspectives in obtaining more selective compounds toward different biological pathways involving CXCR4 receptor. In this regard, the forthcoming activity will be focused on the development of peptidomimetics that allow stabilizing the so-called 'bioactive' conformation, that is the peptide conformation required for receptor binding and activation. Moreover, dimers of the most active peptides will be also synthesized and tested for their biological activity, in order to evaluate any potential improvement of it compared with the activity exerted by the corresponding monomeric peptide sequence.

Concerning the in vivo biological assay, it was found a dramatic decrease in mice metastases number induced by the treatment with three of the newly developed peptides. These results strongly suggested to continue the animal experimentation in order to select potential therapeutics among the already available molecules.

7. Material and methods

7.1 Computational methods

The designed peptides were energy minimized with NAMD [180] package using Charmm22 force field [181] and then subjected to Molecular dynamics (MD) simulations in solvent by confining each peptide in rectangular TIP3P water boxes, with a minimal distance from the solute atoms to the box walls of 12 Å. Counterions (Na+ or Cl-) were added to neutralize the system. Particle mesh Ewald method was applied to calculate long-range electrostatics interactions, setting to 14 Å the nonbonded cutoff. The solvated molecules were then energy minimized through 1000 steps with solute atoms restrained to their starting positions using a force constant of 1 kcal mol-1Å-1 prior to MD simulations. After this, the molecules were submitted to 125 ps of equilibration at constant pressure, to adjust water density, and gradually heated to 310 K, keeping the peptide fixed in the first 50 ps and restrained, with stepwise (25 ps) decreasing force constant from 100 to 1 kcal mol-1Å-1 during the last 75 ps. Production runs were carried out for 5 ns using a timestep of 1 fs. Snapshots from production run were saved every 1000 steps and analyzed with NAMD program. Model figures were made with MOLMOL program [182].

7.2 Peptide synthesis

Solid-phase peptide synthesis was performed on a fully automated Multisyntech Syro I synthesizer. Analytical RP-HPLC runs were carried out on a HP Agilent Series 1100 apparatus using a Phenomenex (Torrance, CA) C18 column, 4.6 · 250 mm with a flow rate of 1.0 mL min^{-1}. Preparative RP-HPLC was carried out on a Shimadzu 8A apparatus equipped with an UV Shimadzu detector using a Phenomenex (Torrance, CA) C18 column, 22 · 250 mm with a flow rate of 20 mL min^{-1}. For all the RP-HPLC procedures the system solvent used was H_2O 0.1% TFA (A) and CH_3CN 0.1% TFA (B), with a linear gradient from 5% to 70% B in 30 min. Mass spectral analyses were carried out on Finnigan Surveyor MSQ single quadrupole electrospray ionisation mass spectrometer coupled with a Finnigan Surveyor HPLC (Finnigan/Thermo Electron Corporation San Jose, CA, USA).
The peptide synthesis was performed by solid phase method using the standard Fmoc procedures. PyBOP, HOBt, all Fmoc-amino acid derivatives were purchased from Calbiochem-Novabiochem (Laufelfingen, Switzerland). All other chemicals were obtained from Aldrich (St. Louis, MI), Fluka (Milwaukee, WI) or LabScan (Stillorgan, Dublin, Ireland) and were used without further purification, unless otherwise stated.
The first amino acid was loaded on Wang resin according to literature protocol [183] and the loading was evaluated by Fmoc test. All couplings were performed twice for 30 min in DMF, by using an excess of 4 equiv for each amino acid coupling.
The peptide cleavage from the solid support and the simultaneous removal of all protecting groups from the amino acid residues was carried out by suspending the fully protected compound-resins in TFA/H_2O/EDT (94:4:2) for 3 h followed by filtration. The solution was then concentrated and the crude product isolated by precipitation into cold diethyl ether. The precipitate was collected by centrifugation and dried in vacuo (over KOH pellets). The cyclisation reaction, by disulphide bond formation between the two Cys residues, was performed by dissolving the crude peptide (final concentration 10^{-4}M) in 0.1M solution of NH_4HCO_3 in water to promote the oxidation reaction. After 4 h the reaction mixture was concentrated and the desired compound isolated by chromatographic purification.

Compounds C1-C6 and C13-C18

Fmoc-Arg(Pbf)-OH was the first amino acid derivative attached to the Wang resin (0.80 mmol/g calcd substitution; 0.100 g resin; 0.080 mmol scale) for compounds C13, C14 and C15, while Fmoc-Cys(Trt)-OH was loaded on the same resin as first amino acid residue (0.80 mmol/g calcd substitution; 0.100 g resin; 0.080 mmol scale) for all other molecules. The peptide chains were then elongated by sequential coupling and Fmoc deprotection of appropriate amino acid derivatives (Fmoc-Ala-OH; Fmoc-Tyr(tBu)-OH; Fmoc-Phe-OH; Fmoc-His(Trt)-OH; Fmoc-Trp(Boc)-OH). The synthesis was ended with the acetylation (4.7% acetic anhydride and 4% pyridine in DMF) of the N-terminal amino acid residue for compounds C4, C5, and C6. Following the protocol described in the general procedures paragraph, the peptides were cleaved from the solid support and freed from all the protecting groups at the same time. The final oxidation reaction led to cyclised peptides by disulphide bond formation between the two cysteine residues.

RP-HPLC purification and mass spectrometry analysis confirmed the presence of the desired compounds. C1: t_R =13.83 min; $[M+H]^+$=702.30 (calcd=702.27); C2: t_R=15.20 min; $[M+H]^+$ =728.96 (calcd=728.27); C3: t_R=17.12 min; $[M+H]^+$ =672.95 (calcd=673.27); C4: t_R=16.23 min; $[M+H]^+$ =744.50 (calcd= 744.83); C5: t_R=17.12 min; $[M+H]^+$ =770.50 (calcd=770.27); C6: t_R=19.22 min; $[M+H]^+$ =715.36 (calcd=715.27); C13: t_R =12.30 min; $[M+H]^+$=929.58 (calcd=929.41); C14: t_R =13.60 min; $[M+H]^+$=955.58 (calcd=955.41); C15: t_R =15.30 min; $[M+H]^+$=900.58 (calcd=900.41); C16: t_R =13.70 min; $[M+H]^+$=929.35 (calcd=929.41); C17: t_R =14.30 min; $[M+H]^+$=955.68 (calcd=955.41); C18: t_R =15.70 min; $[M+H]^+$=900.09 (calcd=900.41).

Compounds C7-C12

For each compound 0.200 g of Rink Amide MBHA resin (0.28 $mmolg^{-1}$ substitution; 0.056 mmol scale) were used. The synthesis of the peptide chains was performed by sequential coupling and Fmoc deprotection of the appropriate amino acid derivatives. The acetylation procedure, the same described for the other molecules, was performed at the N-terminal amino acid residue of compounds C10, C11 and C12. After completion of the synthesis, the peptide cleavage from the solid support and the deprotection of all amino acid residues were carried out as described in the previous paragraph.

The crude products obtained were then cyclised by disulphide bond formation, fully purified by RP-HPLC and characterized by mass spectrometry. C7: t_R=14.22 min; $[M+H]^+$ =701.37 (calcd=701.27); C8: t_R=16.90 min; $[M+H]^+$ = 727.09 (calcd=727.27); C9: t_R=18.21 min; $[M+H]^+$ =672.42 (calcd=672.27); C10: t_R=17.84 min; $[M+H]^+$ =743.40 (calcd=743.83); C11: t_R=19.22 min; $[M+H]^+$ =769.70 (calcd=769.27); C12: t_R=19.22 min; $[M+H]^+$ =769.70 (calcd=769.27);

7.3 Biological test

Cell Culture

PES43, human melanoma cell line were grown at 37 °C in 5% CO_2 in IMDM with 10% fetal calf serum (FCS), 2 mM glutamine, 1 mM sodium pyruvate, 50 µg/ml penicillin, 50 µg/ml streptomycin. CCRF-CEM, human T-Leukemia cell line were grown in RPMI-1640 with 10% fetal calf serum (FCS) and 2 mM glutamine. B16-CXCR4 murine melanoma cell line, previously transfected with CXCR4 plasmid, were grown at 37 °C in 5% CO_2 in IMDM with 10% fetal calf serum (FCS) and 2 mM glutamine 50 µg/ml penicillin, 50 µg/ml streptomycin and 100 ug/ml G418.

B16 cells were transfected with CXCR4 according to FuGENE 6 protocol (Roche Applied Science, Indianapolis, IN). Briefly, 20 µg/well of CXCR4 plasmid and 30 µl/well of FuGENE 6 were mixed in 500 µl serum free IMDM (B16) medium and incubated at room

temperature for 15 minutes. Following incubation, the plasmid/FuGENE 6 mixture was added to the cells in 6-well plates. 48 hours later and geneticin selection started (500 µg/mL of G418) (Invitrogen, Carlsbad, CA).

Migration assay and wound closure

Migration was assayed in 24-well Transwell chambers (Corning Inc., Corning, NY) using inserts with 8-µm pore membrane. Membranes were precoated with collagen (human collagen type I/III) and fibronectin (20 µg/ml each). PES43 cells were placed in the upper chamber ($2.5x10^5$ cells/well) in IMDM containing 1% BSA (migration media), and 20 ng/ml CXCL12 was added to the lower chamber in triplicate. After 16 hours incubation, cells on the upper surface of the filter were removed using a cotton wool swab; migration of cells in migration media alone was compared with migration in media containing 20 ng/ml CXCL12. The cells were counted in ten differents fields (original magnification x40). The migration index was defined as the ratio between migrating cells in the experimental group and migrated cells in the control group. For the wound closure assay, tested cells were allowed to reach confluence in six-well plates containing serum depleted growth medium and scratched with pipette tips to make wounds. The wound closure was observed microscopically 6 hours post-wounding (OKO Time Lapse).

Flow Cytometry and peptide binding evaluation

CCRF-CEM cells were washed in PBS and incubated for 30 min at 4°C with anti-CXCR4 antibody PE conjugated (FAB 170P, clone 12G5, R&D Systems, Minneapolis, MN, USA) or mouse IgG2a PE conjugated as negative control. After three washes in PBS, the cells were analysed by FACScan cytofluorometer (Becton Dickinson Immunocytometry Systems, Mountain View, CA, USA). CCRF–CEM cells were incubated with 10 µM peptides or AMD3100 in RMPI-1640 with 2mM glutamine for 30min at 37 °C, 5% CO2 and labelled with an anti-CXCR4 PE-antibody. The number of antibody-molecules bound was calculated comparing GeoMean value with standard beads (PE Fluorescence quantification Kit, BD Inc.).

Calcium mobilization assay.

For the calcium flux studies a 2 mg/mL stock solution of Fluo-3 acetoxymethylester (Molecular Probes, Leiden, the Netherlands) in anhydrous DMSO was used. A 20% w/v stock solution of the detergent pluronic acid F-127 (Molecular Probes) was also prepared in DMSO. CCRF–CEM cells were resuspended in cell loading buffer (PBS, 1% FCS, 1 mmol/L MgCl2, and 1 mmol/L CaCl2) at a concentration of 0.5 x106/mL. Four microliters of Fluo-3AM and four microlitres of Pluronic acid were added to each sample to increase Fluo-3 acetoxymethylester solubility and improve dye loading into the cells. Followed one hour in agitation at room temperature. Thereafter, cells were washed twice with cell loading buffer and incubated at 37°C for 15 minutes. First, untreated cells were examined by flow cytometric analysis for 10 seconds in fluorescence versus time to establish a baseline. Then, chemokines were added as indicated and chemokine induced fluorescence was measured.

Immunoblotting

Cells were homogenized in lysis buffer (40 mM Hepes pH 7,5, 120 mM NaCl, 5 mM $MgCl_2$, 1 mM EGTA, 0,5 mM EDTA, 1% Triton X-100) containing protease (Complete Tablets-EDTA-free, Roche) and phosphatase inhibitors (20 mM a-glycerol-phosphate, 2,5 mM Na-pyrophosphate). Total lysate was cleared by centrifugation at 15,000g for 20 min. Protein concentration of supernatant was measured using Bio-Rad protein assay. 30µg of extracts were denatured and resolved by SDS-PAGE (12%) gel electrophoresis, transferred to a Hybond ECL nitrocellulose membrane (Amersham Biosciences, Freiburg, Germany) by

electroblotting at 250 mA for 2 hours. The following primary antibodies were used: anti-P-ERK(sc 7383, Santa Cruz Biotechnology, Inc., Santa Cruz, CA, USA) and anti-ERK2 (sc 154G, Santa Cruz Biotechnology). Anti-mouse and anti-goat IgG coupled to peroxidase were used as secondary antibodies (Sigma-Aldrich Corp., St. Louis, Missouri, USA) and the signal was revealed through Chemoluminescent detection kit (ECL detection kit, Amersham Biosciences, Freiburg, Germany).

In Vivo Assays
Twenty-five 7 to 8 week-old female C57BL/6 mice weighing approximately 20 g were inoculated into the tail vein with 5 x 10^5 B-16 –CXCR4 cells preincubated for 30 minutes with: 1) PBS, 2) AMD3100 (10μM), 3) C16 (10μM), 4) C18 (10μM), 5) C1 (10μM). Six hours later the intraperitoneal treatment started with AMD3100 (1.25mg/kg) and peptides (2mg/kg) in sterile PBS were administered i.p. once daily, 5 days on and two days off, for a period of 2 weeks. Mice were euthanized after 28 days by cervical dislocation for gross inspection of lungs.

7.4 N-alkylation reaction

Chemicals and Equipment
All purchased chemicals and solvents were used without further purification, unless otherwise stated. Solid-phase peptide synthesis was performed on a fully automated Multisyntech Syro I synthesizer. Molecular sieves type 4 Å (beads, diameter 1.6 mm) were activated by heating at 280 °C for 4h under vacuum and atmosphere of Ar.

LC/MS *analysis*
Analytical RP-HPLC runs were carried out using a C18 column, 4.6 × 250 mm with a flow rate of 1.0 mL min^{-1}. Preparative RP-HPLC was carried out using a C18 column, 22 × 250 mm with a flow rate of 20 mL min^{-1}. For all the RP-HPLC procedures the system solvent used was: H_2O 0.1% TFA (A) and CH_3CN 0.1% TFA (B), with a linear gradient from 5% to 70% B in 30 min (gradient 1) or from 40% to 95% B in 30 min (gradient 2) and detection at 210 nm and 280 nm. LC-ES-MS data were obtained using a single quadrupole electrospray ionisation mass spectrometer coupled with an HPLC apparatus. HRMS were run on a Micromass QTOF mass spectrometer.

NMR *analysis*
^1H and ^{13}C NMR spectra were recorded at 400 and 100 MHz respectively on spectrometer equipped with a z-gradient 5 mm triple-resonance probe head. Samples were prepared in tubes with a diameter of 5 mm using 0.5 ml of deuterated solvent. The chemical shifts are reported in units of ppm on the δ scale relative to solvent signal used ($CDCl_3$ 7.26 ppm for ^1H NMR and 77.00 ppm for ^{13}C NMR). ^1H NMR assignments were based on homo-decoupling experiments.
Optical rotations were measured using a 1 mL cell with a 10 mm path length.

General procedure for N-Alkylation promoted by molecular sieves.
A solution of Fmoc-Xaa(Ns)-OH in DMF (50 mg/ml), previously synthesized by using the already published protocol (De Luca et al. 2005), was added under Ar atmosphere in a round-bottom flask containing 4 Å molecular sieves previously activated at 280°C for 4 h under vacuum. After few minutes the alkylating reagent was added (1.5 eq). The reaction was stirred at room temperature and followed by analytical RP-HPLC until disappearance of the starting compound. The mixture was centrifugated and the precipitate was washed with DMF. Then, the surnatant was concentrated under vacuum and the crude product

was purified by HPLC to be fully characterized by mass spettrometry and NMR spectroscopy.

N_α-(9-Fluorenylmethoxycarbonyl)-N_β-benzyl–N'_β-2-Nitrobenzensulfonyl-L-2,3-Diaminopropionic acid **1a, 1k** HPLC: t_R = 23.581 min (gradient 2); ^{1}H NMR (400 MHz, $CDCl_3$): δ 8.07 & 7.81 (2d, J = 7.1 Hz, 2H, Ns-$H_{3,6}$), 7.77 & 7.58 (2d, J = 7.6 Hz, 4H, Fmoc-$H_{1,4,5,8}$), 7.68 (m, 2H, Ns-$H_{4,5}$), 7.41 & 7.32 (2t, J = 7.2 Hz, 4H, Fmoc-$H_{2,3,6,7}$), 7.37 (m, 5H, Ph-$H_{2,3,4,5,6}$), 5.23 (m, 2 H, CH_2-Ph), 4.48 (br, 1 H, Dap-CH^α), 4.36 (d, J = 6.8 Hz, 2 H, Fmoc-CH_2), 4.20 (t, J = 6.8 Hz, 1 H, Fmoc-CH), 3.58 (br, 2 H, Dap-CH_2^β); ^{13}C NMR (100 MHz, $CDCl_3$): δ 45.40; 47.48; 54.48; 67.97; 68.66; 120.50; 125.59; 126.01; 127.64; 128.28; 129.06;129.25; 131.50; 133.39; 134.27; 141.77; 144.10; 156.59; 169.87. ES-MS: calcd (M + H^+), 601.15; found, m/z 601,35; calcd (M + Na^+), 623.15; found, m/z 623,89; HRMS (ESI) Calcd for $C_{31}H_{27}N_3O_8S$, 601.1557; Found, 601.1561; $[\alpha]_D^{25}$ = -15.7 (c = 0.3, $CHCl_3$).

N_α-(9-Fluorenylmethoxycarbonyl)-N_β-2-phenylethyl–N'_β-2Nitrobenzensulfonyl-L-2,3-Diaminopropionic acid **1b** HPLC: t_R = 23.97 min (gradient 2); ^{1}H NMR (400 MHz, $CDCl_3$): δ 8.07 & 7.83 (2d, J = 6.8 Hz, 2H, Ns-$H_{3,6}$), 7.78 & 7.60 (2d, J = 7.6 Hz, 4H, Fmoc-$H_{1,4,5,8}$), 7.70 (m, 2H, Ns-$H_{4,5}$), 7.42 & 7.23 (2t, J = 7.2 Hz, 4H, Fmoc-$H_{2,3,6,7}$), 7.32 (m, 5H, Ph-$H_{2,3,4,5,6}$), 4.42 (m, 3H, Dap-CH^α & CH_2-CH_2-Ph), 4.37 (d, J = 6.8 Hz, 2 H, Fmoc-CH_2), 4.21 (t, J = 6.8 Hz, 1 H, Fmoc-CH), 3.51 (br, 2H, Dap-CH_2^β), 3.00 (t, J = 6.8 Hz, 2H, CH_2-CH_2-Ph); ^{13}C NMR (100 MHz, $CDCl_3$):
δ 35.31; 43.88; 47.48; 53.92; 67.12; 67.53;120.51; 125.47; 125.69; 127.35; 127.63; 128.94; 129.23; 131.53; 133.27; 134.07; 135.56; 141.84; 144.15; 144.32; 148.56; 156.43; 172.32. ES-MS: calcd (M + H^+), 615.17; found, m/z 615,52, calcd (M + Na^+), 627.17; found, m/z 627,67; HRMS (ESI) Calcd for $C_{32}H_{29}N_3O_8S$, 615.1749; Found, 615.1754. $[\alpha]_D^{25}$ = -6.2 (c = 0.4, $CHCl_3$).

N_α-(9-Fluorenylmethoxycarbonyl)-N_β-3-phenylpropyl–N'_β-2-Nitrobenzensulfonyl-L-2,3-Diaminopropionic acid **1c, 1l** HPLC: t_R = 25.48 min (gradient 2); ^{1}H NMR (400 MHz, $CDCl_3$): δ 8.08 & 7.82 (2br, 2H, Ns-$H_{3,6}$), 7.77 & 7.59 (2d, J = 7.6 Hz, 4H, Fmoc-$H_{1,4,5,8}$), 7.70 (m, 2H, Ns-$H_{4,5}$), 7.41 & 7.19 (2t, J = 7.2 Hz, 4H, Fmoc-$H_{2,3,6,7}$), 7.31 (m, 5H, Ph-$H_{2,3,4,5,6}$), 4.39 (m, 3H, Dap-CH^α & Fmoc-CH_2), 4.21 (m, 3H, Fmoc-CH and CH_2- CH_2- CH_2-Ph), 3.54 (br, 2H, Dap-CH_2^β), 2.70 (t, J = 6.8 Hz, 2H, -CH_2-CH_2-CH_2-Ph), 2.01 (m, 2H, -CH_2-CH_2-CH_2-Ph); ^{13}C NMR (100 MHz, $CDCl_3$):δ 30.34; 32.57; 45.40; 47.49; 54.37; 66.38; 67.92; 120.52; 125.57; 126.01; 126.65; 127.65; 128.30; 128.88; 129.02; 131.51; 133.40; 134.28; 141.79; 144.12; 156.02; 169.65. ES-MS: calcd (M + H^+), 629.18; found, m/z 629.41, calcd (M + Na^+), 651.18; found, m/z 651.80; HRMS (ESI) Calcd for $C_{33}H_{31}N_3O_8S$, 629.1867; Found, 629.1895. $[\alpha]_D^{25}$ = -5.8 (c = 0.3, $CHCl_3$).

N_α-(9-Fluorenylmethoxycarbonyl)-N_β-propyl–N'_β-2-Nitrobenzensulfonyl-L-2,3-Diaminopropionic acid **1d** HPLC: t_R = 22.14 min (gradient 2); ^{1}H NMR (400 MHz, $CDCl_3$): δ 8.11 & 7.83 (2br, 2H, Ns-$H_{3,6}$), 7.78 & 7.60 (2d, J = 7.6 Hz, 4H, Fmoc-$H_{1,4,5,8}$), 7.71 (m, 2H, Ns-$H_{4,5}$), 7.41 & 7.33 (2t, J = 7.2 Hz, 4H, Fmoc-$H_{2,3,6,7}$), 4.45 (br, 1H, Dap-CH^α), 4.37 (d, J = 7.2 Hz, 2 H, Fmoc-CH_2), 4.22 (t, J = 6.8 Hz, 1H, Fmoc-CH), 4.18 (t, J = 6.8 Hz, 2H, -CH_2-CH_2-CH_3), 3.58 (br, 2H, Dpr-CH_2^β), 1.71 (m, 2H, -CH_2-CH_2-CH_3), 0.96 (t, J = 7.6, 3H, -CH_2-CH_2-CH_3); ^{13}C NMR (100MHz,$CDCl_3$):δ 10.76; 22.31; 45.51; 47.50; 67.95; 68.56; 120.53; 125.61; 126.03; 127.65; 128. 31; 131.53; 133.42; 134.29; 141.79; 144.14; 156.76; 170.06. ES-MS: calcd (M + H^+), 553.15; found, m/z 553.21, calcd (M + Na^+), 575,15 found, m/z 575,75; HRMS (ESI) Calcd for $C_{27}H_{27}N_3O_8S$, 553.1498; Found, 553.1503. $[\alpha]_D^{25}$ = -8.3 (c = 0.1, $CHCl_3$).

N_α-(9-Fluorenylmethoxycarbonyl)-N_β-1-heptenyl–N'_β-2-Nitrobenzensulfonyl-L-2,3-Diaminopropionic acid **1e** HPLC: t_R = 26.20 min (gradient 2); ^{1}H NMR (400 MHz, $CDCl_3$): δ

8.10 & 7.83 (2br, 2H, Ns-$H_{3,6}$), 7.77 & 7.59 (2d, J = 7.6 Hz, 4H, Fmoc-$H_{1,4,5,8}$), 7.71 (m, 2H, Ns-$H_{4,5}$), 7.41 & 7.33 (2t, J = 7.2 Hz, 4H, Fmoc-$H_{2,3,6,7}$), 5.77 (m, 1H, -CH_2-CH=CH_2), 5.00 & 4.95 (2m, 2H, -CH_2-CH=C$H_{a,b}$), 4.44 (m, 1 H, Dap-+-CH^{α}), 4.36 (d, J = 7.2 Hz, 2 H, Fmoc-CH_2), 4.21 (m, 3 H, Fmoc-CH and -CH_2-$(CH_2)_4$-CH=CH_2), 3.57 (br, 2 H, Dpr-CH_2^{β}), 2.06 (m, 2H, -$(CH_2)_4$-CH_2-CH=CH_2),1.69 & 1.40 (2m, 8H, -$(CH_2)_4$- CH_2-CH=CH_2); ^{13}C NMR (100 MHz, $CDCl_3$): δ 25.67; 28.72; 28.83; 33.96; 45.45; 47.46; 54.38; 67.032; 67.93; 115.09; 120.49; 125.58; 125.97; 127.61; 128.27; 128.84; 128.98; 131.48; 133.38; 134.24; 139.04; 141.76; 144.11; 156.33; 170.04. ES-MS: calcd (M + H^+), 607.20; found, m/z 607.64, calcd (M + Na^+), 629.20; found, m/z 630.00; HRMS (ESI) Calcd for $C_{31}H_{33}N_3O_8S$, 607.1988; Found, 607.1996. $[\alpha]_D^{25}$ = -6.9 (c = 0.9, $CHCl_3$).

N_{α}-(9-Fluorenylmethoxycarbonyl)-N_{β}-diphenylmethyl–N'_{β}-2-Nitrobenzensulfonyl-L-2,3-Diaminopropionic acid **1f** HPLC: t_R = 26.09 min (gradient 2); ^{1}H NMR (400 MHz, $CDCl_3$): δ 8.00 & 7.79 (2d, J = 7.1 Hz, 2H, Ns-$H_{3,6}$), 7.76 & 7.57 (2d, J = 7.6 Hz, 4H, Fmoc-$H_{1,4,5,8}$), 7.66 (m, 2H, Ns-$H_{4,5}$), 7.42-7.31 (m, 14H, Fmoc-$H_{2,3,6,7}$ and CH-$(Ph)_2$-H), 6.90 (br, 1H, CH-$(Ph)_2$), 4.55 (br, 1H, Dap-CH^{α}), 4.35 (d, J = 6.8 Hz, 2H, Fmoc-CH_2), 4.19 (t, J = 6.8 Hz, 1H, Fmoc-CH), 3.59 (br, 2H, Dap-CH_2^{β}); ^{13}C NMR (100 MHz, $CDCl_3$): δ 45.37; 47.48; 54.54; 68.07; 79.76; 120.51; 125.64; 126.03; 127.53; 127.65; 128.31; 128.85; 128.92; 129.19; 129.28; 131.57; 133.38; 134.27; 139.52; 141.78; 144.12; 156.42; 169.29. ES-MS: calcd (M + H^+), 677.18; found, m/z 677,54; calcd (M + Na^+), 699.18; found, m/z 700,02; HRMS (ESI) Calcd for $C_{37}H_{31}N_3O_8S$, 677.1831; Found, 677.1847. $[\alpha]_D^{25}$ = -6.4 (c = 0.5, $CHCl_3$).

N_{α}-(9-Fluorenylmethoxycarbonyl)-N_{β}-naphtylmethyl–N'_{β}-2-Nitrobenzensulfonyl-L-2,3-Diaminopropionic acid **1g** HPLC: t_R = 25.87 min (gradient 2); ^{1}H NMR (400 MHz, $CDCl_3$): δ 8.02 & 7.84 & 7.76 & 7.64 & 7.56 & 7.50 & 7.45 & 7.39 & 7.30 (9m, 19H, Ns-$H_{3,4,5,6}$, Fmoc-$H_{1,2,3,4,5,6,7,8}$, Naph-$H_{2,3,4,5,6,7,8}$), 5.38 (m, 2H, CH_2-Naph), 4.50 (br, 1H, Dap-CH^{α}), 4.36 (d, J = 6.8 Hz, 2H, Fmoc-CH_2), 4.19 (t, J = 6.8 Hz, 1 H, Fmoc-CH), 3.58 (br, 2H, Dap-CH_2^{β});
^{13}CNMR(100MHz,$CDCl_3$):δ 45.40; 47.49; 54.37; 66.38; 67.92; 120.59; 125.39; 125.90; 126.57; 127.23; 127.54; 128.27; 128.56; 129.07; 131.53; 133.20; 133.99; 141.80; 144.35; 156.57; 170.11.
ES-MS: calcd (M + H^+), 651.17; found, m/z 651,32; calcd (M + Na^+), 673.17; found, m/z 673,89; HRMS (ESI) Calcd for $C_{35}H_{29}N_3O_8S$, 651.1764; Found, 651.1783. $[\alpha]_D^{25}$ = -2.4 (c = 0.3, $CHCl_3$).

N_{α}-(9-Fluorenylmethoxycarbonyl)-N_{β}-t-ButylAcetyl–N'_{β}-2-Nitrobenzensulfonyl-L-2,3-Diaminopropionic acid **1h** HPLC: t_R = 22.998 min (gradient 2); ^{1}H NMR (400 MHz, $CDCl_3$): δ 8.12 & 7.83 (2br, 2H, Ns-$H_{3,6}$), 7.77 & 7.63 (1d & 1m, J = 7.6 Hz, 4H, Fmoc-$H_{1,4,5,8}$), 7.68 (m, 2H, Ns-$H_{4,5}$), 7.41 & 7.33 (2t, J = 7.2 Hz, 4H, Fmoc-$H_{2,3,6,7}$), 4.87 & 4.40 (2d, J = 14 Hz, 2H, $CH_2CO_2C(CH_3)_3$), 4.58 (d, J = 6.4 Hz, 2 H, Fmoc-CH_2), 4.38 (m, 1H, Dap-CH^{α}), 4.25 (t, J = 6.8 Hz, 1 H, Fmoc-CH), 3.69 (br, 2 H, Dap-CH_2^{β}), 1.51 (s, 9H, $CH_2CO_2C(CH_3)_3$).
^{13}C NMR (100 MHz, $CDCl_3$): δ 28.44; 45.73; 47.45; 54.25; 62.28; 68.01; 84.55; 120.40; 125.71; 127.59; 128.19; 131.28; 133.14; 133.97; 141.69; 144.11;148.12; 156.29; 167.81; 169.76. ES-MS: calcd (M + H^+), 625.17; found, m/z 625,70; calcd (M + Na^+), 647.17; found, m/z 647,68; HRMS (ESI) Calcd for $C_{30}H_{31}N_3O_{10}S$, 625.1730; Found, 625.1761; $[\alpha]_D^{25}$ = -6.5 (c = 0.4, $CHCl_3$)

N_{α}-(9-Fluorenylmethoxycarbonyl)-N_{β}-methyl–N'_{β}-2-Nitrobenzensulfonyl-L-2,3-Diaminopropionic acid **1i** HPLC: t_R = 18.088 min (gradient 2); ^{1}H NMR (400 MHz, $CDCl_3$): δ 8.10 & 7.84 (2br, 2H, Ns-$H_{3,6}$), 7.77 & 7.59 (2d, J = 7.2 Hz, 4H, Fmoc-$H_{1,4,5,8}$), 7.71 (m, 2H, Ns-$H_{4,5}$), 7.41 & 7.33 (2t, J = 7.2 Hz, 4H, Fmoc-$H_{2,3,6,7}$), 4.44 (m, 1H, Dap-CH^{α}), 4.35 (d, J = 6.4 Hz, 2 H, Fmoc-CH_2), 4.21 (t, J = 6.8 Hz, 1 H, Fmoc-CH), 3.81 (s, 3H, N_{β}-CH_3), 3.56 (br, 2 H, Dap-CH_2^{β}); ^{13}C NMR (100 MHz, $CDCl_3$): δ 45.32; 47.43; 53.60; 54.29; 67.90; 120.46; 125.52; 125.97; 127.59; 128.24; 131.45; 133.37; 134.25; 141.73; 144.02; 157.29; 169.75. ES-MS: calcd (M + H^+), 525.12; found, m/z 525,52; calcd (M + Na^+), 547.12; found, m/z 547,88; HRMS (ESI) Calcd for $C_{25}H_{23}N_3O_8S$, 525.1206; Found, 525.1210; $[\alpha]_D^{25}$ = -5.9 (c = 0.3, $CHCl_3$).

N_α-(9-Fluorenylmethoxycarbonyl)-N_β-ethyl–N'_β-2-Nitrobenzensulfonyl-L-2,3-Diaminopropionic acid **1j** HPLC: t_R = 19.518 min (gradient 2); ^{1}H NMR (400 MHz, $CDCl_3$): δ 8.10 & 7.83 (2br, 2H, Ns-$H_{3,6}$), 7.77 & 7.59 (2d, J = 7.2 Hz, 4H, Fmoc-$H_{1,4,5,8}$), 7.70 (m, 2H, Ns-$H_{4,5}$), 7.40 & 7.32 (2t, J = 7.2 Hz, 4H, Fmoc-$H_{2,3,6,7}$), 4.43 (m, 1H, Dap-CH^α), 4.36 (d, J = 6.8 Hz, 2H, Fmoc-CH_2,), 4.25 (m, 3 H, Fmoc-CH, N_β-CH_2CH$_3$), 3.57 (br, 2 H, Dap-CH_2^β), 1.32(t, J = 6.4 Hz, 3H, N_β-CH$_2$CH_3);
^{13}C NMR (100 MHz, $CDCl_3$): δ 14.58; 30.19; 45.46; 47.49; 54.38; 63.07; 67.93; 120.51; 125.59; 126.00; 127.64; 128.29; 131.50; 133.41; 133.94; 134.27; 141.78; 144.11; 148.49; 156.33; 169.96. ES-MS: calcd (M + H^+), 539.14; found, m/z 539,44; calcd (M + Na^+), 561.14; found, m/z 561,38; HRMS (ESI) Calcd for $C_{26}H_{25}N_3O_8S$, 539.1362; Found, 639.1398; $[\alpha]_D^{25}$ = -6.3 (c = 0.5, $CHCl_3$)

N_α-(9-Fluorenylmethoxycarbonyl)-N_γ-benzyl–N'_γ-2-Nitrobenzensulfonyl-L-2,4-Diaminobutirric acid **2a** HPLC: t_R = 23.41 min (gradient 2); ^{1}H NMR (400 MHz, $CDCl_3$): δ 8.07 & 7.78 (2br, 2H, Ns-$H_{3,6}$), 7.67 & 7.58 (2md, 6H, Fmoc-$H_{1,4,5,8}$, Ns-$H_{4,5}$), 7.41-7.32 (m, 9H, Fmoc-$H_{2,3,6,7}$ Ph-$H_{2,3,4,5,6}$), 5.15 (m, 2 H, CH_2-Ph), 4.47 (d, J = 6.8 Hz, 2 H, Fmoc-CH_2), 4.41 (m, 1 H, Dab-CH^α), 4.18 (t, J = 6.8 Hz, 1 H, Fmoc-CH), 3.32 & 3.02 (2m, 2H, Dab-CH_2^γ), 2.12 & 1.75 (2m, 2H, Dab-CH_2^β);
^{13}CNMR(100MHz,$CDCl_3$):δ 34.12; 40.38; 47.64; 51.79; 67.68; 68.27; 120.52; 125.56; 125.76; 127.62; 128.28; 129.03; 129.23; 131.15; 133.16; 133.89; 135.33; 141.83; 144.00; 144.24; 156.94; 172.05. ES-MS: calcd (M + H^+), 615.65; found, m/z 616.16, calcd (M + Na^+), 637.65; found, m/z 637.85; HRMS (ESI) Calcd for $C_{32}H_{29}N_3O_8S$, 615.6523; Found, 616.6542. $[\alpha]_D^{25}$ = -17.7 (c = 0.3, $CHCl_3$).

N_α-(9-Fluorenylmethoxycarbonyl)-N_δ-benzyl–N'_δ-2-Nitrobenzensulfonyl-L-Ornithine **3a** HPLC: t_R = 23.77 min (gradient 2); ^{1}H NMR (400 MHz, $CDCl_3$): δ 8.11 & 7.80 (2br, 2H, Ns-$H_{3,6}$), 7.78 & 7.59 (2d, J = 7.6 Hz, 4H, Fmoc-$H_{1,4,5,8}$), 7.69 (m, 2H, Ns-$H_{4,5}$), 7.41 & 7.32 (2t, J = 7.2 Hz, 4H, Fmoc-$H_{2,3,6,7}$), 7.37 (m, 5H, Ph-$H_{2,3,4,5,6}$), 5.18 (m, 2H, CH_2-Ph), 4.41 (d, J = 6.8 Hz, 2 H, Fmoc-CH_2), 4.37 (m, 1 H, Orn-CH^α), 4.20 (t, J = 6.8 Hz, 1H, Fmoc-CH), 3.08 (m, 2H, Orn-CH_2^δ), 1.70 (m, 2H, Orn-CH_2^β), 1.55 (m, 2H, Orn-CH_2^γ); ^{13}C NMR (100 MHz, $CDCl_3$): δ 25.95; 30.22; 43.60; 47.66; 53.78; 67.52; 67.96; 1203.52; 125.57; 125.89; 127.62; 128.27; 128.94; 129.23; 131.53; 133.27; 134.07; 135.56; 141.84; 144.15; 144.32; 148.56; 156.43; 172.32. ES-MS: calcd (M + H^+), 629.18; found, m/z 629.52, calcd (M + Na^+), 651.18; found, m/z 651.84; HRMS (ESI) Calcd for $C_{33}H_{31}N_3O_8S$, 629.1812; Found, 629.1822. $[\alpha]_D^{25}$ = -1.3 (c = 0.8, $CHCl_3$).

N_α-(9-Fluorenylmethoxycarbonyl)-N_ε-benzyl–N'_ε -2-Nitrobenzensulfonyl-L-Lysine **4a, 4k** HPLC: t_R = 24.20 min (gradient 2); ^{1}H NMR (400 MHz, $CDCl_3$): δ 8.11 & 7.82 (2br, 2H, Ns-$H_{3,6}$), 7.77 & 7.60 (2d, J = 7.6 Hz, 4H, Fmoc-$H_{1,4,5,8}$), 7.70 (m, 2H, Ns-$H_{4,5}$), 7.40 & 7.31 (2t, J = 7.2 Hz, 4H, Fmoc-$H_{2,3,6,7}$), 7.35 (m, 5H, Ph-$H_{2,3,4,5,6}$), 5.18 (m, 2H, CH_2-Ph), 4.41 (d, J = 6.8 Hz, 2 H, Fmoc-CH_2), 4.38 (br, 1H, Lys-CH^α), 4.22 (t, J = 6.8 Hz, 1 H, Fmoc-CH), 3.04 (m, 2 H, Lys-CH_2^ε), 1.82 & 1.65 (2m, Lys-C$H_{a,b}^\beta$), 1.52 (m, 2H, Lys-C$H_{a,b}^\gamma$) 1.32 (m, 2H, Lys-C$H_{a,b}^\delta$). ^{13}C NMR (100 MHz, $CDCl_3$): δ 22.40; 29.40; 32.60; 43.87; 47.64; 53.97; 67.59; 67.84; 120.49; 125.59; 125.90; 127.59; 128.23; 128.93; 129.19; 131.56; 133.22; 134.02; 141.82; 144.24; 156.46;172.56. ES-MS: calcd (M + H^+), 643.20; found, m/z 643.11, calcd (M + Na^+), 665.20; found, m/z 665.81; HRMS (ESI) Calcd for $C_{34}H_{33}N_3O_8S$, 643.2031; Found, 643.2048. $[\alpha]_D^{25}$ = -6.1 (c = 0.4, $CHCl_3$).

N_α-(9-Fluorenylmethoxycarbonyl)-N_ε-2-phenylethyl–N'_ε-2-Nitrobenzensulfonyl-L-Lysine **4b** HPLC: t_R = 24.73 min (gradient 2); ^{1}H NMR (400 MHz, $CDCl_3$): δ 8.11 & 7.83 (2br, 2H, Ns-$H_{3,6}$), 7.77 & 7.60 (2d, J = 7.6 Hz, 4H, Fmoc-$H_{1,4,5,8}$), 7.70 (m, 2H, Ns-$H_{4,5}$), 7.40 & 7.21 (2t, J = 7.2 Hz, 4H, Fmoc-$H_{2,3,6,7}$), 7.30 (m, 5H, Ph-$H_{2,3,4,5,6}$), 4.48-4.28 (m, 5H, Lys-CH^α , Fmoc-CH_2 ,

CH_2-CH_2-Ph), 4.21 (t, 1H, J = 6.8 Hz, 1 H, Fmoc-C*H*), 3.03 (m, 2 H, Lys-CH_2^{ε}), 2.96 (t, 2H, J = 6.8 CH_2-CH_2-Ph), 1.72 (m, 1H, Lys-CH_2^{β}), 1.55-1.44 (m, 3H, Lys-CH_2^{β} and Lys-CH_2^{γ}), 1.24 (m, 2H, Lys-CH_2^{δ}). ^{13}C NMR (100 MHz, $CDCl_3$): δ 22.33; 29.41; 32.57; 35.41; 43.87; 47.64; 53.94; 66.40; 67.52; 120.50; 125.60; 125.93; 127.24; 127.59; 128.25; 129.07; 129.39; 131.57; 133.25; 134.05; 137.83; 141.82; 144.26; 148.60; 156.41; 172.61. ES-MS: calcd (M + H^+), 657.21; found, m/z 657.61, calcd (M + Na^+), 679.21; found, m/z 679.81; HRMS (ESI) Calcd for $C_{35}H_{35}N_3O_8S$, 657.2162; Found, 657.2182. $[\alpha]_D^{25}$ = -6.8 (c = 0.3, $CHCl_3$).

N_α-(9-Fluorenylmethoxycarbonyl)-N_ε-3-phenylpropyl–N'_ε-2 Nitrobenzensulfonyl-L-Lysine **4c, 4l** HPLC: t_R = 26.22 min (gradient 2); ^{1}H NMR (400 MHz, $CDCl_3$): δ 8.11 & 7.82 (2br, 2H, Ns-$H_{3,6}$), 7.77 & 7.60 (2d, J = 7.6 Hz, 4H, Fmoc-$H_{1,4,5,8}$), 7.70 (m, 2H, Ns-$H_{4,5}$), 7.40 & 7.20 (2t, J = 7.2 Hz, 4H, Fmoc-$H_{2,3,6,7}$), 7.29 (m, 5H, Ph-$H_{2,3,4,5,6}$), 4.41 (d, 2H, J = 6.8 Hz, 2 H, Fmoc-CH_2), 4.32 (m, 1H, Lys-CH^{α}), 4.21 (t, 1H, J = 6.8 Hz, 1 H, Fmoc-C*H*), 4.16 (m, 2H, CH_2-CH_2-CH_2-Ph) 3.09 (m, 2 H, Lys-CH_2^{ε}), 2.68 (t, 2H, J = 7.6 CH_2-CH_2-CH_2-Ph), 1.98 (m, 2H CH_2-CH_2-CH_2-Ph), 1.79 (m, 1H, Lys-CH_2^{β}), 1.68-1.54 (m, 3H, Lys-CH_2^{β} and Lys-CH_2^{γ}), 1.38 (m, 2H, Lys-CH_2^{δ});
^{13}C NMR (100 MHz, $CDCl_3$): δ 18.32; 22.55; 29.47; 30.52; 32.59; 43.90; 47.67; 54.01; 65.51; 67.56; 120.50; 125.61; 125.91; 126.65; 127.61; 128.25; 128.89; 129.03; 131.56; 133.24; 134.05; 141.36; 141.84; 144.28; 148.60; 156.53; 172.76. ES-MS: calcd (M + H^+), 671.23; found, m/z 671.11, calcd (M + Na^+), 693.23; found, m/z 693.81; HRMS (ESI) Calcd for $C_{36}H_{37}N_3O_8S$, 671.2319; Found, 671.2340. $[\alpha]_D^{25}$ = -5.7 (c = 1.1, $CHCl_3$).

N_α-(9-Fluorenylmethoxycarbonyl)-N_ε-propyl–N'_ε-2-Nitrobenzensulfonyl-L-Lysine **4d** HPLC: t_R = 22.95 min (gradient 2); ^{1}H NMR (400 MHz, $CDCl_3$): δ 8.11 & 7.82 (2br, 2H, Ns-$H_{3,6}$), 7.77 & 7.60 (2d, J = 7.6 Hz, 4H, Fmoc-$H_{1,4,5,8}$), 7.71 (m, 2H, Ns-$H_{4,5}$), 7.40 & 7.32 (2t, J = 7.2 Hz, 4H, Fmoc-$H_{2,3,6,7}$), 4.41 (d, J = 6.8 Hz, 2 H, Fmoc-CH_2), 4.33 (br, 1H, Lys-CH^{α}), 4.21 (t, J = 6.8 Hz, 1 H, Fmoc-C*H*), 4.10 (t, J = 6.4 Hz, 2H CH_2-CH2-CH_3) 3.95 (m, 2 H, Lys-CH_2^{ε}), 1.83 (m, 1H, Lys-CH^{β}), 1.73-1.50 (m, 5H, Lys-CH^{β}, CH_2-CH_2-CH_3, Lys-CH_2^{γ}) 1.38 (m, 2H Lys-CH_2^{δ}), 0.94 (t, J = 7.2 Hz, CH_2-CH_2-CH_3).
^{13}CNMR(100MHz,$CDCl_3$):δ 10.26; 22.25; 22.31; 29.74; 32.34; 45.51; 47.43; 54.49; 67.95; 68.56; 120.83; 125.31; 126.03; 127.45; 128.31; 131.84; 133.42; 134.79; 141.80; 144.23; 156.76; 170.26.
ES-MS: calcd (M + H^+), 595.20; found, m/z 595.31, calcd (M + Na^+), 617.20; found, m/z 617.45; HRMS (ESI) Calcd for $C_{30}H_{33}N_3O_8S$, 595.2022; Found, 595.2056. $[\alpha]_D^{25}$ = -7.4 (c = 0.5, $CHCl_3$).

N_α-(9-Fluorenylmethoxycarbonyl)-N_ε-diphenylmethyl–N'_ε-2-Nitrobenzensulfonyl-L-Lysine **4f** HPLC: t_R = 27.25 min (gradient 2); ^{1}H NMR (400 MHz, $CDCl_3$): δ 8.08 & 7.79 (2br, 2H, Ns-$H_{3,6}$), 7.76 & 7.58 (2d, J = 7.6 Hz, 4H, Fmoc-$H_{1,4,5,8}$), 7.68 (m, 2H, Ns-$H_{4,5}$), 7.39 & 7.39-7.30 (m, 9H, Fmoc-$H_{2,3,6,7}$, CH-(*Ph*)$_2$), 6.88 (s, 1H, *CH*-(Ph)$_2$), 4.46 (m, 1H, Lys-CH^{α}), 4.40 (d, J = 6.8 Hz, 2 H, Fmoc-CH_2), 4.19 (t, J = 6.8 Hz, 1 H, Fmoc-C*H*), 2.99 (m, 2 H, Lys-CH_2^{ε}), 1.66-1.26 (4m, Lys-C$H_{a,b}^{\beta}$, Lys-CH_2^{γ}, Lys-CH_2^{δ}). ^{13}C NMR (100 MHz, $CDCl_3$): δ 22.27; 29.44; 32.54; 43.89; 47.62; 54.00; 67.59; 66.40; 78.71; 120.48; 125.58; 125.90; 127.45; 127.59; 127.78; 128.23; 128.68; 128.85; 129.14; 131.57; 133.21; 134.02; 139.70; 141.80; 144.25; 156.73; 171.80. ES-MS: calcd (M + H^+), 719.23; found, m/z 719.57, calcd (M + Na^+), 741.23; found, m/z 741.66; HRMS (ESI) Calcd for $C_{40}H_{37}N_3O_8S$, 719.2378; Found, 719.2394. $[\alpha]_D^{25}$ = -12.9 (c = 0.3, $CHCl_3$).

N_α-(9-Fluorenylmethoxycarbonyl)-N_ε-naphtylmethyl–N'_ε-2-Nitrobenzensulfonyl-L-Lysine **4g** HPLC: t_R = 26.92 min (gradient 2); ^{1}H NMR (400 MHz, $CDCl_3$): δ 8.06 & 7.85 (2br, & Ns-$H_{3,6}$), 7.83 & 7.76 & 7.66 & 7.59 & 7.50 & 7.39 & 7.29 (7m, 17H, Ns-$H_{4,5}$, Fmoc-$H_{1,2,3,4,5,6,7,8}$, Naph-$H_{2,3,4,5,6,7,8}$), 5.29 (m, 2H, CH_2-Naph), 4.55-4.40 (m, 3H, Fmoc-CH_2, Lys-CH^{α}), 4.20 (t, 1H, J = 6.8 Hz, 1 H, Fmoc-C*H*), 2.98 (m, 2 H, Lys-CH_2^{ε}), 1.66 (m, 1H, Lys-CH_2^{β}), 1.52-1.46 (m, 3H, Lys-CH_2^{β} and Lys-CH_2^{γ}), 1.30 (m, 2H, Lys-CH_2^{δ}); ^{13}C NMR (100 MHz, $CDCl_3$):

δ 22.40; 29.40; 32.59; 43.82; 47.63; 54.01; 67.58; 68.02; 120.48; 123.15; 125.58; 125.89; 126.37; 126.98; 127.58; 128.22; 128.51; 129.07; 131.53; 133.20; 133.99; 141.80; 144.13; 156.13; 170.25. ES-MS: calcd (M + H^+), 693.21; found, m/z 693.07, calcd (M + Na^+), 715.21; found, m/z 715.73; HRMS (ESI) Calcd for $C_{38}H_{35}N_3O_8S$, 693.2152; Found, m/z 693.2169. $[\alpha]_D^{25}$ = -3.5 (c = 0.4, $CHCl_3$).

N_α-(9-Fluorenylmethoxycarbonyl)-N_ε-t-butylacetyl–N'_ε-2-Nitrobenzensulfonyl-L-Lysine **4h** HPLC: t_R = 23.774 min (gradient 2); ^{1}H NMR (400 MHz, $CDCl_3$): δ 8.12 & 7.81 (2br, 2H, Ns-$H_{3,6}$), 7.76 & 7.60 (2d, J = 7.2 Hz, 4H, Fmoc-$H_{1,4,5,8}$), 7.70 (m, 2H, Ns-$H_{4,5}$), 7.40 & 7.31 (2t, J = 7.2 Hz, 4H, Fmoc-$H_{2,3,6,7}$), 4.68 & 4.44 (2d, J = 10 Hz, 2H, $CH_2CO_2C(CH_3)_3$), 4.56 (d, J = 6.4, 2 H, Fmoc-CH_2), 4.41 (m, 1H, Lys-CH^α), 4.21 (t, J = 6.8 Hz, 1 H, Fmoc-C*H*), 3.11 (m, 2 H, Lys-CH_2^ε), 1.89 & 1.73 (2m, 2H, Lys-$CH_{a,b}^\beta$), 1.58 (m, 2H, Lys-CH_2^γ), 1.47 (m, 11H, $CH_2CO_2(CH_3)_3$, Lys-CH_2^δ). ^{13}C NMR (100 MHz, $CDCl_3$): δ 22.17; 28.45; 29.24; 32.29; 43.69; 47.54; 53.79; 62.11; 67.59; 83.46; 120.42; 125.53; 125.75; 127.53; 128.17; 131.50; 133.11; 133.92; 141.74; 144.13; 148.51; 156.47; 166.79 172.14. ES-MS: calcd (M + H^+), 667.22; found, m/z 667.46, calcd (M + Na^+), 689.22; found, m/z 689.81; HRMS (ESI) Calcd for $C_{33}H_{37}N_3O_{10}S$, 667.2200; Found, 667.2233. $[\alpha]_D^{25}$ = -6.3 (c = 0.4, $CHCl_3$).

N_α-(9-Fluorenylmethoxycarbonyl)-N_ε-methyl–N'_ε-2-Nitrobenzensulfonyl-L-Lysine **4i** HPLC: t_R = 19.577 min (gradient 2); ^{1}H NMR (400 MHz, $CDCl_3$): δ 8.12 & 7.83 (2br, 2H, Ns-$H_{3,6}$), 7.76 & 7.60 (2d, J = 7.2 Hz, 4H, Fmoc-$H_{1,4,5,8}$), 7.70 (m, 2H, Ns-$H_{4,5}$), 7.40 & 7.31 (2t, J = 7.2 Hz, 4H, Fmoc-$H_{2,3,6,7}$), 4.40 (d, J = 7.2 Hz, 2 H, Fmoc-CH_2), 4.31 (m, 1H, Lys-CH^α), 4.21 (t, J = 6.8 Hz, 1 H, Fmoc-C*H*), 3.74 (s, 3H, N_ε-CH_3), 3.09 (m, 2 H, Lys-CH_2^ε), 1.80 & 1.63 (2m, 2H, Lys-$CH_{a,b}^\beta$), 1.56 (m, 2H, Lys-CH_2^γ) 1.37 (m, 2H, Lys-CH_2^δ). ^{13}C NMR (100 MHz, $CDCl_3$): δ 22.42; 29.35; 32.45; 43.78; 47.54; 53.01; 53.91; 67.57; 120.44; 125.51; 125.83; 127.54; 128.19; 131.48; 133.19; 134.01; 141.74; 144.14; 148.49; 156.56; 173.19. ES-MS: calcd (M + H^+), 567.17; found, m/z 567.11, calcd (M + Na^+), 589.17; found, m/z 589.26; HRMS (ESI) Calcd for $C_{28}H_{29}N_3O_8S$, 567.1675; Found, 567.1802. $[\alpha]_D^{25}$ = -6.7 (c = 0.5, $CHCl_3$).

N_α-(9-Fluorenylmethoxycarbonyl)-N_ε-ethyl–N'_ε-2-Nitrobenzensulfonyl-L-Lysine **4j** HPLC: t_R = 20.94 min (gradient 2); ^{1}H NMR (400 MHz, $CDCl_3$): δ 8.12 & 7.83 (2br, 2H, Ns-$H_{3,6}$), 7.77 & 7.60 (2d, J = 7.2 Hz, 4H, Fmoc-$H_{1,4,5,8}$), 7.71 (m, 2H, Ns-$H_{4,5}$), 7.41 & 7.32 (2t, J = 7.2 Hz, 4H, Fmoc-$H_{2,3,6,7}$), 4.41 (d, J = 6.8 Hz, 2 H, Fmoc-CH_2), 4.31 (m, 1H, Lys-CH^α), 4.21 (m, 3 H, Fmoc-C*H*, N_ε-CH_2CH_3), 3.10 (m, 2 H, Lys-CH_2^ε), 1.80 & 1.64 (2m, 2H, Lys-$CH_{a,b}^\beta$), 1.58 (m, 2H, Lys-CH_2^γ) 1.39 (m, 2H, Lys-CH_2^δ), 1.29 (t, J = 7.2 Hz, 3H, N_β-CH_2CH_3). ^{13}C NMR (100 MHz, $CDCl_3$): δ 14.64; 22.47; 29.43; 32.61; 43.87; 47.61; 53.99; 62.23; 67.62; 120.50; 125.58; 125.90; 127.59; 128.24; 131.56; 133.24; 134.05; 141.81; 144.21; 148.57; 156.62; 172.78. ES-MS: calcd (M + H^+), 581.18; found, m/z 581.39, calcd (M + Na^+), 603.18; found, m/z 603.61; HRMS (ESI) Calcd for $C_{29}H_{31}N_3O_8S$, 581.1832; Found, 581.1864. $[\alpha]_D^{25}$ = -7.1 (c = 0.3, $CHCl_3$).

N_α-(9-Fluorenylmethoxycarbonyl)-N_β-benzyl–N'_β-t-Butoxicarbonyl-L-2,3-Diaminopropionic acid **5a** HPLC: t_R = 24.608 min (gradient 2); ^{1}H NMR (400 MHz, $CDCl_3$): δ 7.77 & 7.60 (2d, J = 7.6 Hz, 4H, Fmoc-$H_{1,4,5,8}$), 7.40 & 7.30 (2t, J = 7.6 Hz, 4H, Fmoc-$H_{2,3,6,7}$), 7.35 (m, 5H, Ph-$H_{2,3,4,5,6}$), 5.20 (m, 2H, CH_2-Ph), 4.38 (m, 3H, Fmoc-CH_2, Dap-CH^α), 4.24 (t, J = 6.8 Hz, 1 H, Fmoc-C*H*), 3.59 (br, 2 H, Dap-CH_2^β), 1.44 (s, 9H, $C(CH_3)_3$);

^{13}C NMR (100 MHz, $CDCl_3$): δ 28.70; 42.66; 47.57; 55.61; 67.59; 68.03; 80.53; 120.40; 125.58; 127.50; 128.15; 128.82; 128.98; 129.08; 141.74; 144.16; 156.45; 170.73. ES-MS: calcd (M + H^+), 516.23; found, m/z 516,49; calcd (M + Na^+), 538.23; found, m/z 538,73; HRMS (ESI) Calcd for $C_{30}H_{32}N_2O_6$, 516.2260; Found, 516.2291; $[\alpha]_D^{25}$ = -8.3 (c = 0.3, $CHCl_3$).

N_α-(9-Fluorenylmethoxycarbonyl)-N_β-benzyl–N'_β-Methylthrityl-L-2,3-Diaminopropionic acid **6a** HPLC: t_R = 29.639 min (gradient 2); ^{1}H NMR (400 MHz, $CDCl_3$): δ 7.68 & 7.58 (1d & 1m, J = 8 Hz, 4H, Fmoc-$H_{1,4,5,8}$), 7.33-7.13 (m, 23H, Mtt-$(Ph)_3$, Ph-$H_{2,3,4,5,6}$, Fmoc-$H_{2,3,6,7}$), 5.07 (dd, 2 H, CH_2-Ph), 4.30 (m, 1 H, Dap-CH^α), 4.22 (d, J = 6.4 Hz, 2 H, Fmoc-CH_2), 4.05 (t, J = 6.4 Hz, 1 H, Fmoc-C*H*), 3.47 & 3.29 (2br, 2 H, Dap-CH_2^β), 2.35 (s, 3H, Mtt-CH_3);
^{13}C NMR (100 MHz, $CDCl_3$): δ 21.45; 41.46; 47.19; 52.41; 68.20; 68.66; 82.43; 120.34; 125.53; 127.61; 128.16; 128.32; 128.71; 128.99; 129.06; 134.88; 137.38; 141.62; 143.89; 147.42; 157.25; 169.35. ES-MS: calcd (M + H^+), 672.30; found, m/z 672,54; calcd (M + Na^+), 694.30; found, m/z 694,08; HRMS (ESI) Calcd for $C_{31}H_{27}N_3O_8S$, 672.2988; Found, 672.3005; $[\alpha]_D^{25}$ = -11.6 (c = 0.3, $CHCl_3$).

N_α-(9-Fluorenylmethoxycarbonyl)-N_β-benzyl–N'_β-1-(4,4-dimethyl-2,6-dioxocycloex-1-ylidene)-3-methylbutyl-L-2,3-Diaminopropionic acid **7a** HPLC: t_R = 26.381 min (gradient 2); ^{1}H NMR (400 MHz, $CDCl_3$): δ 8.10 (br, 1H, N*H*α), 7.76 & 7.60 (2d, J = 8 Hz, 4H, Fmoc-$H_{1,4,5,8}$), 7.40 & 7.30 (2t, J = 7.2 Hz, 4H, Fmoc-$H_{2,3,6,7}$), 7.35 (m, 5H, Ph-$H_{2,3,4,5,6}$), 5.25 (br, 2 H, CH_2-Ph), 4.64 (d, J = 6.4 Hz, 2 H, Fmoc-CH_2) 4.39 (m, 1H, Dap-CH^α), 4.22 (t, J = 6.4 Hz, 1 H, Fmoc-C*H*), 3.97 (br, 2 H, Dap-CH_2^β), 2.91 (m, 2H, Dde-CH_2CH$(CH_3)_2$), 2.42 (s, 4H, Dde-CH_2C$(CH_3)_2$), 1.89 (m, 1H, Dde-C*H*$(CH_3)_2$), 1.04 (s, 6H, Dde-C(CH_3)$_2$, 0.92 (d, J = 6.8 Hz, 6H, Dde-CH(CH_3)$_2$);
^{13}CNMR(100MHz,$CDCl_3$):δ 22.87; 28.54; 29.59; 30.45; 37.96; 45.51; 47.40; 52.65; 54.19; 68.09; 68.85; 107.68; 120.46; 125.52; 125.58; 127.56; 128.24; 129.19; 129.23; 129.40; 134.81; 141.72; 143.98; 156.21; 169.32; 178.87; 199.43. ES-MS: calcd (M + H^+), 622.30; found, m/z 622,19; calcd (M + Na^+), 644.30; found, m/z 644,69; HRMS (ESI) Calcd for $C_{38}H_{48}N_2O_6$, 622.3043; Found, 622.3083; $[\alpha]_D^{25}$ = -9.8 (c = 0.4, $CHCl_3$).

Fmoc-Dap(Ns, Bn)-Ile-OH **8a** HPLC: t_R = 22.35 min (gradient 2); ES-MS: calcd (M + H^+), 714.23; found, m/z 714.08;

H-Dap(Ns, Bn)-Ile-Gly-Gly-Asp-Gly-Asp-Gly-OH **9a** Yield: 35%; HPLC: t_R = 11.92 min (gradient 1); ES-MS: calcd (M + H^+), 950.36; found, m/z 950.71;

References

1) D. Rossi, A. Zlotnik, The biology of chemokines and their receptors. Annu. Rev. Immunol. 18, (2000) 217–242.

2) P.M. Murphy, M. Baggiolini, I.F. Charo, C. A. Hébert, R. Horuk, K. Matsushima, L. H. Miller, J.J. Oppenheim, C.A. Power, International union of pharmacology. XXII. Nomenclature for chemokine receptors. *Pharmacol. Rev*. 52, (2000) 145–176.

3) A. Zlotnik, O. Yoshie, Chemokines: a new classification system and their role in immunity. *Immunity* 12, (2000) 121–127.

4) M. Locati, U. Deuschle, M.L. Massardi, F.O. Martinez, M. Sironi, S. Sozzani, T. Bartfai, A. Mantovani Analysis of the gene expression profile activated by the CC chemokine ligand 5/RANTES and by lipopolysaccharide in human monocytes. *J. Immunol*. 168, (2002) 3557–3562.

5) R.M. Strieter, P.J. Polverini, S.L. Kunkel, D.A. Arenberg, M.D. Burdick, J. Kasper, J. Dzuiba, J. Van Damme, A. Walz, D. Marriott, S.-Y. Shan, S. Roczniak, A.B. Shanafelt, The functional role of the ELR motif in CXC chemokine-mediated angiogenesis. *J. Biol. Chem.* 270, (1995) 27348–27357.

6) I. Clark-Lewis, B. Dewald, T. Geiser, B. Moser, M. Baggiolini, Platelet factor 4 binds to interleukin 8 receptors and activates neutrophils when its N terminus is modified with Glu-Leu-Arg. *Proc. Natl. Acad. Sci.* 90, (1993) 3574–3577.

7) C.A. Hebert, R.V. Vitangcol, J.B. Baker, Scanning mutagenesis of interleukin-8 identifies a cluster of residues required for receptor binding. *J. Biol. Chem.* 266, (1991) 18989–18994.

8) R.M. Strieter, P.J. Polverini, D.A. Arenberg, S.L. Kunkel. The role of CXC chemokines as regulators of angiogenesis. *Shock* 4, (1995) 155–160.

9) A. Rot, U.H. von Andrian, Chemokines in innate and adaptive host defense: basic chemokinese grammar for immune cells. *Annu. Rev. Immunol.* 22, (2004) 891–928.

10) M. Thelen, Dancing to the tune of chemokines. *Nat. Immunol.* 2, (2001) 129–134.

11) P. Loetscher, B. Moser, M. Baggiolini, Chemokines and their receptors in lymphocyte traffic and HIV infection. *Adv Immunol.* 74, (2000) 127-180.

12) M. Baggiolini, Chemokines and leukocyte traffic. *Nature* 392, (1998) 565-568.

13) B. Moser, P. Loetscher, Lymphocyte traffic control by chemokines. *Nat Immunol.* 2, (2001) 123-128.

14) E.C. Butcher, L.J. Picker, Lymphocyte homing and homeostasis. *Science* 272, (1996) 60-66.

15) T.A. Springer, Traffic signals for lymphocyte recirculation and leukocyte emigration: the multistep paradigm. *Cell* 76, (1994) 301-314.

16) J.J. Campbell, J. Hedrick, A. Zlotnik, M.A. Siani, D.A. Thompson, E.C. Butcher, Chemokines and the arrest of lymphocytes rolling under flow conditions. *Science* 279, (1998) 381-384.

17) C.L. Addison, T.O. Daniel, M.D. Burdick, H. Liu, J.E. Ehlert, Y.Y. Xue, L. Buechi, A. Walz, A. Richmond, R.M. Strieter, The CXC chemokine receptor 2, CXCR2, is the putative receptor for ELR+ CXC chemokine-induced angiogenic activity. *J. Immunol.* 165, (2000) 5269–5277.

18) P. Romagnani, F. Annunziato, L. Lasagni, E. Lazzeri, C. Beltrame, M. Francalanci, M. Uguccioni, G. Galli, L. Cosmi, L. Maurenzig, M. Baggiolini, E. Maggi, S. Romagnani, M. Serio, Cell cycle-dependent expression of CXC chemokine receptor 3 by endothelial cells mediates angiostatic activity. *J. Clin. Invest.* 107, (2001) 53–63.

19) S.K. Gupta, P.G. Lysko, K. Pillarisetti, E. Ohlstein, J.M. Stadel, Chemokine receptors in human endothelial cells. *J. Biol. Chem*. 273, (1998) 4282–4287.

20) A. Muller, *et al.* Involvement of chemokine receptors in breast cancer metastasis. *Nature* 410, (2001) 50–56.

21) C.J. Scotton, J.L. Wilson, D. Milliken, G. Stamp, F.R. Balkwill, Epithelial cancer cell migration: a role for chemokine receptors? *Cancer Res*. 61, (2001) 4961–4965.

22) F. Balkwill, The significance of cancer cell expression of CXCR4. *Semin. Cancer Biol*. 14, (2004) 171–179.

23) F. Balkwill, Cancer and the chemokine network. *Nat. Rev. Cancer* 4, (2004) 540–550.

24) A. Mantovani, P. Allavena, S. Sozzani, A. Vecchi, M. Locati, A. Sica, Chemokines in the recruitment and shaping of the leukocyte infiltrate of tumors. *Semin. Cancer Biol.* 14, (2004) 155–160.

25) G. Opdenakker, J. Van Damme, The countercurrent principle in invasion and metastasis of cancer cells. Recent insights on the roles of chemokines. *Int. J. Dev. Biol.* 48, (2004) 519–527.

26) S.K. Biswas, A. Sica, C.E. Lewis, Plasticity of macrophage function during tumor progression: regulation by distinct molecular mechanisms. *J. Immunol.* 180, (2008) 2011–2017.

27) M.E. Wallace, M.J. Smyth, The role of natural killer cells in tumor control-effectors and regulators of adaptive immunity. *Springer Semin. Immunopathol.* 27, (2005) 49–64.

28) P. Carmeliet, Angiogenesis in life, disease and medicine. *Nature* 438, (2005) 932–936.

29) F. Hillen, A.W. Griffioen, Tumour vascularization: sprouting angiogenesis and beyond. *Cancer Metastasis Rev.* 26, (2007) 489–502.

30) S. Liekens, E. De Clercq, J. Neyts, Angiogenesis: regulators and clinical applications. *Biochem. Pharmacol.* 61, (2001) 253–270.

31) S. Liekens, A. Bronckaers, M.J. Perez-Perez, J. Balzarini, Targeting platelet-derived endothelial cell growth factor/ thymidine phosphorylase for cancer therapy. *Biochem. Pharmacol.* 74, (2007) 1555–1567.

32) B. Homey, A. Muller, A. Zlotnik, Chemokines: agents for the immunotherapy of cancer?. *Nat Rev Immunol* 2, (2002) 175-184.

33) T. Murakami, A.R. Cardones, S.T. Hwang, Chemokine receptors and melanoma metastasis, *J Dermatol Sci* 36, (2004) 71-78.

34) P.M. Murphy, Chemokines and molecular basis of cancer metastasis. *N Engl J Med* 345, (2001) 833-835.

35) P. Allavena, *et al.* The chemokine receptor switch paradigm and dendritic cell migration: its significance in tumor tissues. *Immunol. Rev*. 177, (2000) 141–149.

36) K. Kawada, M. Sonoshita, H. Sakashita, A. Takabayashi, Y. Yamaoka, T. Manabe, K. Inaba, N. Minato, M. Oshima, M.M. Taketo, Pivotal Role of CXCR3 in Melanoma Cell Metastasis to Lymph Nodes. *Cancer Res* 64, (2004) 4010-4017.

37) M.M. Robledo, R.A. Bartolome, N. Longo, J.M. Rodriguez-Frade, M. Mellado, I. Longo, G.N. van Muijen, P. Sanchez-Mateos, J. Teixido, Expression of Functional Chemokine Receptors CXCR3 and CXCR4 on Human Melanoma Cells**.** *J Biol Chem* 276, (2001) 45098-45105.

38) H.W. van Deventer, W. O'Connor, W.J. Jr., Brickey, R.M. Aris, J.P .Ting, J.S. Serody, C-C Chemokine Receptor 5 on Stromal Cells Promotes Pulmonary Metastasis. *Cancer Res* 65, (2005) 3374-3379.

39) Y.M. Li, Y. Pan, Y. Wei, X. Cheng, B.P. Zhou, M. Tan, X. Zhou, W. Xia, G.N. Hortobagyi, D. Yu, M.C. Hung, Upregulation of CXCR4 is essential for HER2-mediated tumor metastasis. *Cancer Cell* 6, (2004) 459-469.

40) J.A. Burger, T.J. Kipps, CXCR4: a key receptor in the crosstalk between tumor cells and their microenvironment. *Blood* 107, (2006) 1761–1767.

41) K.E. Luker, G.D. Luker, Functions of CXCL12 and CXCR4 in breast cancer. *Cancer Lett* 238, (2006) 30–41.

42) Y. Oda, H. Yamamoto, S. Tamiya, S. Matsuda, K. Tanaka, R. Yokoyama, Y. Iwamoto, M. Tsuneyoshi, CXCR4 and VEGF expression in the primary site and the metastatic site of human osteosarcoma: analysis within a group of patients, all of whom developed lung metastasis. *Mod Pathol*. 19, (2006) 738-745.

43) S. Woo, J. Bae, C. Kim, J. Lee, B. Koo, A significant correlation between nuclear CXCR4 expression and axillary lymph node metastasis in hormonal receptor negative breast cancer. *Ann Surg Oncol* 15, (2008) 281–285.

44) Q.D. Chu, L. Panu, N.T. Holm, B.D. Li, L.W. Johnson, S. Zhang, High chemokine receptor CXCR4 level in triple negative breast cancer specimens predicts poor clinical outcome. *J Surg Res* 159, (2010) 689-695.

45) D. Zagzag, M. Esencay, O. Mendez, et al. Hypoxia- and vascular endothelial growth factor-induced stromal cell-derived factor-1α/ CXCR4 expression in glioblastomas: one plausible explanation of Scherer's structures. *Am J Pathol* 173, (2008) 545–560.

46) N.T. Holm, K. Byrnes, B.D. Li, et al. Elevated levels of chemokine receptor CXCR4 in HER-2 negative breast cancer specimens predict recurrence. *J Surg Res* 141, (2007) 53–59.

47) N.T. Holm, F. Abreo, L.W. Johnson, B.D. Li, Q.D. Chu, Elevated chemokine receptor CXCR4 expression in primary tumors following neoadjuvant chemotherapy predicts poor outcomes for patients with locally advanced breast cancer (LABC). *Breast Cancer Res Treat* 113, (2009) 293–299.

48) A. Khan, J. Greenman, S.J. Archibald, Small molecule CXCR4 chemokine receptor antagonists: developing drug candidates. *Curr Med Chem* 14, (2007) 2257-2277.

49) H. Kang, G. Watkins, A. Douglas-Jones, R.E. Mansel, W.G. Jiang, The elevated level of CXCR4 is correlated with nodal metastasis of human breast cancer. *Breast* 14, (2005) 360–367.

50) D. Wong, W. Korz, Translating an antagonist of chemokine receptor CXCR4: from bench to bedside. *Clin Cancer Res* 14, (2008) 7975–7980.

51) M. Darash-Yahana, E. Pikarsky, R. Abramovitch, et al. Role of high expression levels of CXCR4 in tumor growth, vascularization, and metastasis. *Faseb J* 18, (2004) 1240–1242.

52) Z. Liang, T. Wu, H. Lou, et al. Inhibition of breast cancer metastasis by selective synthetic polypeptide against CXCR4. *Cancer Res* 64, (2004) 4302–4308.

53) Z. Liang, Y. Yoon, J. Votaw, M.M. Goodman, L. Williams, H. Shim, Silencing of CXCR4 blocks breast cancer metastasis. *Cancer Res* 65, (2005) 967–971.

54) S. Scala, A. Ottaiano, P.A. Ascierto, M. Cavalli, E. Simeone, P. Giuliano, M. Napolitano, R. Franco, G. Botti, G. Castello, Expression of CXCR4 predicts poor prognosis in patients with malignant melanoma. *Clin Cancer Res.* 11, (2005) 1835-1841.

55) S. Scala, C. Ieranò, A. Ottaiano, R. Franco, A. La Mura, G. Liguori, M. Mascolo, S. Staibano, P.A. Ascierto, G. Botti, G. De Rosa, G. Castello, CXC chemokine receptor 4 is expressed in uveal malignant melanoma and correlates with the epithelioid-mixed cell type. *Cancer Immunol Immunother.* 56, (2007) 1589-1595.

56) C. D'Alterio, C. Consales, M.N. Polimeno, R. Franco, L. Cindolo, L. Portella, M. Cioffi, R. Calemma, S. Scala, Concomitant CXCR4 and CXCR7 Expression Predicts Poor Prognosis in Renal Cancer. *Curr Cancer Drug Targets.* (2010) [Epub ahead of print].

57) T. Kijima, Gautam Maulik, Patrick C. Ma, Elena V. Tibaldi, Ross E. Turner, Barrett Rollins, Martin Sattler, Bruce E. Johnson, Ravi Salgia, Regulation of cellular proliferation, cytoskeletal function, and signal transduction through CXCR4 and c-Kit in small cell lung cancer cells. *Cancer Res*. 62, (2002) 6304–6311.

58) T. Nagasawa, H. Kikutani, T. Kishimoto, Molecular cloning and structure of a pre-B-cell growth-stimulating factor. *Proc. Natl Acad. Sci.* 91, (1994) 2305–2309.

59) G. Dontu, W. Abdallah, J. Foley, K. Jackson, M. Clarke, M. Kawamura, et al., In vitro propagation and transcriptional profiling of human mammary stem/progenitor cells. *Genes Dev.* 17, (2003) 1253–1270.

60) M. Al-Hajj, M. Wicha, A. Benito-Hernandez, S. Morrison, M. Clarke, Prospective identification of tumorigenic breast cancer cells. *Proc. Natl Acad. Sci.* 100, (2003) 3983–3988.

61) R. Phillips, M. Burdick, M. Lutz, J. Belperio, M. Keane, R. Strieter, The stromal derived factor-1/CXCL12–CXC chemokine receptor 4 biological axis in non-small cell lung cancer metastases. *Am. J. Respir. Crit. Care Med.* 167, (2003) 1676–1686.

62) M.Crump, J.-H.Gong, P.Loetscher,K.Rajarathnam,A.Amara, F. Arenzana-Seisdedos, et al., Solution structure and basis for functional activity of stromal cell-derived factor-1; dissociation of CXCR4 activation frombinding and inhibition ofHIV-1. *Eur. Mol. Biol. Organ. J.* 16, (1997) 6996–7007.

63) A. Amara, O. Lorthioir, A. Valenzuela, A. Magerus, M. Thelen, M. Montes, et al., Stromal cell-derived factor-1alpha associates with heparan sulfates through the first beta-strand of the chemokine. *J. Biol. Chem.* 274, (1999) 23916–23925.

64) F. Barbieri, A. Bajetto, C. Porcile, A. Pattarozzi, A. Massa, G. Lunardi, G. Zona, A. Dorcaratto, J.L. Ravetti, R. Spaziante, G. Schettini, T. Florio, CXC receptor and chemokine expression in human meningioma: SDF1/ CXCR4 signaling activates ERK1/2 and stimulates meningioma cell proliferation. *Ann. N.Y. Acad. Sci.* 1090, (2006) 332–343.

65) K. Hattori, B. Heissig, K. Tashiro, T. Honjo, M. Tateno, J.H. Shieh, N.R. Hackett, M.S. Quitoriano, R.G. Crystal, S. Rafii, M.A. Moore, Plasma elevation of stromal cellderived factor-1 induces mobilization of mature and immature hematopoietic progenitor and stem cells. *Blood* 97, (2001) 3354–3360.

66) W.J. Lane, S. Dias, K. Hattori, B. Heissig, M. Choy, S.Y. Rabbany, J. Wood, M.A. Moore, S. Rafii, Stromal-derived factor 1-induced megakaryocyte migration and platelet production is dependent on matrix metalloproteinases. *Blood* 96, (2000) 4152–4159.

67) I. Petit, D. Jin, S. Rafii, The SDF-1-CXCR4 signaling pathway: a molecular hub modulating neo-angiogenesis. *Trends Immunol.* 28, (2007) 299–307.

68) Q. Ma, D. Jones, P.R. Borghesani, R.A. Segal, T. Nagasawa, T. Kishimoto, R.T. Bronson, T.A. Springer, Impaired B-lymphopoiesis, myelopoiesis, and derailed cerebellar neuron migration in CXCR4- and SDF-1-deficient mice. *Proc. Natl. Acad. Sci.* 95, (1998) 9448–9453.

69) Y. Feng, C.C. Broder, P.E. Kennedy, E.A. Berger, HIV-1 entry cofactor: functional cDNA cloning of a seventransmembrane, G protein-coupled receptor. *Science* 272, (1996) 872–877.

70) M.C. Smith, K.E. Luker, J.R. Garbow, J.L. Prior, E. Jackson, D. Piwnica-Worms, G.D. Luker, CXCR4 regulates growth of both primary and metastatic breast cancer. *Cancer Res.* 64, (2004) 8604–8612.

71) C.J. Scotton, J.L. Wilson, K. Scott, G. Stamp, G.D. Wilbanks, S. Fricker, G. Bridger, F.R. Balkwill, Multiple actions of the chemokine CXCL12 on epithelial tumor cells in human ovarian cancer. *Cancer Res.* 62, (2002) 5930–5938.

72) J. Pan, J. Mestas, M.D. Burdick, R.J. Phillips, G.V. Thomas, K. Reckamp, J.A. Belperio, R.M. Strieter, Stromal derived factor-1 (SDF-1/CXCL12) and CXCR4 in renal cell carcinoma metastasis. *Mol. Cancer* 5, (2006) 56.

73) R.S. Taichman, C. Cooper, E.T. Keller, K.J. Pienta, N.S. Taichman, L.K. McCauley, Use of the stromal cell-derived factor-1/CXCR4 pathway in prostate cancer metastasis to bone. *Cancer Res.* 62, (2002) 1832–1837.

74) H. Geminder, O. Sagi-Assif, L. Goldberg, T. Meshel, G. Rechavi, I.P. Witz, A. Ben Baruch, A possible role for CXCR4 and its ligand, the CXC chemokine stromal cellderived factor-1, in the development of bone marrow metastases in neuroblastoma. *J. Immunol.* 167, (2001) 4747– 4757.

75) S. Vlahakis, A. Villasis-Keever, T. Gomez, M. Vanegas, N. Vlahakis, C. Paya, G protein-coupled chemokine receptors induce both survival and apoptotic signaling pathways. *J. Immunol.* 169, (2002) 5546–5554.

76) A. Kayali, K. Van Gunst, I. Campbell, A. Stotland, M. Krittzik, G. Liu, et al., The stromal cell-derived factor-1alpha/CXCR4 ligand–receptor axis is critical for progenitor survival and migration in the pancreas. *J. Cell Biol.* 163, (2003) 859–869.

77) J. Rubin, A. Kung, R. Klein, J. Chan, Y. Sun, K. Schmidt, et al., A small molecule antagonist of CXCR4 inhibits intracranial growth of primary brain tumors. *Proc. Natl Acad. Sci.* 100, (2003) 13513–13518.

78) J. Luo, B. Manning, L. Cantley, Targeting the PI3K-Akt pathway in human cancer: rationale and promise. *Cancer Cell* 4, (2003) 257–262.

79) A. Curnock, Y. Sotsios, K. Wright, S. Ward, Optimal chemotactic responses of leukemic T cells to stromal cellderived factor-1 requires the activation of both class IA and IB phosphoinositide 3-kinases. *J. Immunol.* 170, (2003) 4021–4030.

80) S. Peng, V. Peek, Y. Zhai, D. Paul, Q. Lou, X. Xia, et al., Akt activation, but not extracellular signal-regulated kinase activation, is required for SDF-1alpha/CXCR4-mediated migration of epitheloid carcinoma cells. *Mol. Cancer Res.* 3, (2005) 227–236.

81) L. Chang, M. Karin, Mammalian MAP kinase signalling cascades. *Nature* 410, (2001) 37–40.

82) J. Fresno Vara, E. Casado, J. de Castro, P. Cejas, C. Belda- Iniesta, M. Gonzalez-Baron, PI3K/Akt signalling pathway and cancer. *Cancer Treat. Rev.* 30, (2004).

83) A. Fernandis, A. Prasad, H. Band, R. Klosel, R. Ganju, Regulation of CXCR4-mediated chemotaxis and chemoinvasion of breast cancer cells. *Oncogene* 23, (2004) 157–167.193–204.

84) T. Hartmann, J. Burger, A. Glodek, N. Fujii, M. Burger, CXCR4 chemokine receptor and integrin signaling co-operate in mediating adhesion and chemoresistance in small cell lung cancer (SCLC) cells. *Oncogene* Apr 4 (2005) [Epub ahead of print].

85) T. Schioppa, B. Uranchimeg, A. Saccani, S.K. Biswas, A. Doni, A. Rapisarda, S. Bernasconi, S. Saccani, M. Nebuloni, L. Vago, A. Mantovani, G. Melillo, A. Sica, Regulation of the chemokine receptor CXCR4 by hypoxia. *J. Exp. Med.* 198, (2003) 1391–1402.

86) E. Schutyser, Y. Su, Y. Yu, M. Gouwy, S. Zaja-Milatovic, J. Van Damme, A. Richmond, Hypoxia enhances CXCR4 expression in human microvascular endothelial cells and human melanoma cells. *Eur. Cytokine Netw.* 18, (2007) 59– 70.

87) P. Staller, J. Sulitkova, J. Lisztwan, H. Moch, E.J. Oakeley, W. Krek, Chemokine receptor CXCR4 downregulated by von Hippel-Lindau tumour suppressor pVHL. *Nature* 425, (2003) 307–311.

88) C.Y. Chu, S.T. Cha, C.C. Chang, C.H. Hsiao, C.T. Tan, Y.C. Lu, S.H. Jee, M.L. Kuo, Involvement of matrix metalloproteinase-13 in stromal-cell-derived factor 1 alphadirected invasion of human basal cell carcinoma cells. *Oncogene* 26, (2007) 2491–2501.

89) J. Kijowski, M. Baj-Krzyworzeka, M. Majka, R. Reca, L. Marquez, M. Christofidou-Solomidou, et al., The SDF-1- CXCR4 axis stimulates VEGF secretion and activates integrins but does not affect proliferation and survival in lymphohematopoietic cells. *Stem Cells* 19, (2001) 453–466.

90) R. Bachelder, M. Wendt, A. Mercurio, Vascular endothelial growth factor promotes breast carcinoma invasion in an autocrine manner by regulating the chemokine receptor CXCR4. *Cancer Res.* 62, (2002) 7203–7206.

91) W.J. Fairbrother, D. Reilly, T. Colby, J. Hesselgesser, R. Horuk, The solution structure of melanoma growth stimulating activity. *J. Mol. Biol.* 242, (1994) 252–270.

92) N.J. Skelton, F. Aspiras, J. Ogez, T.J. Schall, Proton NMR assignments and solution conformation of RANTES, a chemokine of the C-C type. *Biochemistry* 34, (1995) 5329–5342.

93) A. Rot, E. Hub, J. Middlenton, F. Pons, C. Rabeck, K. Thierer, J. Wintle, B.Wolff, M. Zsak, P.Dukor, Some aspects of IL-8 pathophysiology. III: Chemokine interaction with endothelial cells. *J. Leukocyte Biol.* 59, (1996) 39–44.

94) C.C. Bleul, R.C. Fuhlbrigge, J.M. Casasnovas, A. Aiuti, T.A. Springer, A highly efficacious lymphocyte chemoattractant, stromal cell-derived factor 1 (SDF-1). *J. Exp. Med.* 184, (1996) 1101–1109.

95) D.L. Farrens, C.Altenbach, K. Yang, W.L. Hubbell, H.G. Khorana, Requirement of rigid-body motion of transmembrane helices for light activation of rhodopsin. *Science* 274, (1996) 768–770.

96) E. De Clercq, The bicyclam AMD3100 story. *Nat. Re*V*. Drug Disco*V*ery* 2, (2003) 581-587.

97) N. Fujii, H. Nakashima, H. Tamamura, The therapeutic potential of CXCR4 antagonists in the treatment of HIV. *Expert Opin. In*V*est. Drugs* 12, (2003) 185-195.

98) Y. Feng, C.C. Broder, P.E. Kennedy, A.E. Berger, HIV-1 entry cofactor: functional cDNA cloning of a seven-transmembrane, G protein-coupled receptor. *Science* 272, (1996) 872-877.

99) E. Oberlin, A. Amara, F. Bachelerie, C. Bessia, J.L. Virelizier, F. Arenzana-Seisdedos, O. Schwartz, J.M. Heard, I. Clark-Lewis, D.F. Legler, M. Loetscher, M. Baggiolini, B. Moser, The CXC chemokine SDF-1 is the ligand for LESTR/fusin and prevents infection by T-cell-line-adapted HIV-1. *Nature* 382, (1996) 833-835.

100) K. Tachibana, S. Hirota, H. Lizasa, H. Yoshida, K. Kawabata, Y. Kataoka, Y. Kitamura, K. Matsushima, N. Yoshida, S. Nishikawa, T. Kishimoto, T. Nagasawa, The chemokine receptor CXCR4 is essential for vascularization of the gastrointestinal tract. *Nature* 393, (1998) 591-594.

101) A. Muller, B. Homey, H.Soto, N. Ge, D. Catron, M.E. Buchanan, T. McClanahan, E. Murphy, W. Yuan, S.N. Wagner, J.L. Barrera, A. Mohar, E. Verastegui, A. Zlotnik, Involvement of chemokine receptors in breast cancer metastasis. *Nature* 410, (2001) 50-56.

102) Z. Liang, T. Wu, H. Lou, X. Yu, R.S. Taichman,; S.K. Lau, S. Nie, J. Umbreit, H.Shim, Inhibition of breast cancer metastasis by selective synthetic polypeptide against CXCR4. *Cancer Res.* 64, (2004) 4302-4308.

103) M. Kucia, K. Jankowski, R. Reca, M. Wysoczynski, L.J. Bandura, D. Allendorf, J. Zhang, J. Ratajczak, M.Z. Ratajczak, CXCR4-SDF-1 signalling, locomotion, chemotaxis and adhesion. *J. Mol. Histol.* 35, (2004) 233-245.

104) J.O. Trent, Z.X.Wang, J.L. Murray, W. Shao, H. Tamamura, N. Fujii, S.C. Peiper, Lipid bilayer simulations of CXCR4 with inverse agonists and weak partial agonists. *J. Biol. Chem.* 278, (2003) 47136-44.

105) S. Ueda, S. Oishi, Z.X. Wang, T. Araki, H. Tamamura, J. Cluzeau, H. Ohno, S. Kusano, H. Nakashima, J.O. Trent, S.C. Peiper, N. Fujii, Structure-activity relationships of cyclic peptide-based chemokine receptor CXCR4 antagonists: disclosing the importance of side-chain and backbone functionalities. *J. Med. Chem.* 50, (2007) 192-198.

106) H. Tamamura, H. Tsutsumi, H. Masuno, S. Mizokami, K. Hiramatsu, Z. Wang, J.O. Trent, H. Nakashima, N. Yamamoto, S.C. Peiper, N. Fujii, Development of a linear type of low molecular weight CXCR4 antagonists based on T140 analogs. *Org. Biomol. Chem.*, 4, (2006) 2354-2357.

107) H. Tamamura, A. Ojida, T. Ogawa, H. Tsutsumi, H. Masuno, H. Nakashima, N. Yamamoto, I. Hamachi, N. Fujii, Identification of a new class of low molecular weight antagonists against the chemokine receptor CXCR4 having the dipicolylamine-zinc(II) complex structure. *J. Med. Chem.* 49, (2006) 3412-3415.

108) H. Tamamura, K. Hiramatsu, S. Ueda, Z. Wang, S. Kusano, S. Terakubo, J.O. Trent, S.C. Peiper, N. Yamamoto, H. Nakashima, A. Otaka, N. Fujii, Stereoselective synthesis of [L-Arg-L/D-3- (2-naphthyl)alanine]-type (*E*)-alkene dipeptide isosteres and its application to the synthesis and biological evaluation of pseudopeptide analogues of the CXCR4 antagonist FC131. *J. Med. Chem.* 48, (2005) 380-391.

109) E. De Clercq, Recent advances on the use of the CXCR4 antagonist plerixafor (AMD3100, Mozobil™) and potential of other CXCR4 antagonists as stem cell mobilizers, Pharmacology & Therapeutics (2010) on line.

110) M. Kioi, H. Vogel, G. Schultz, R.M. Hoffman, G.R. Harsh, J.M. Brown, Inhibition of vasculogenesis, but not angiogenesis, prevents the recurrence of glioblastoma after irradiation in mice. *J Clin Invest.* 120, (2010) 694–705.

111) P.A. Tasker, L. Sklar, *J. Cryst. Mol. Struct.* 5, (1975) 329–344.

112) H.J. Choi, M.P. Suh, Self-Assembly of Molecular Brick Wall and Molecular Honeycomb from Nickel(II) Macrocycle and 1,3,5-Benzenetricarboxylate: Guest-Dependent Host Structures. *J. Am. Chem. Soc.* 120, (1998) 10622–10628.

113) L.O. Gerlach, R.T. Skerlj, G.J. Bridger, T.W. Schwartz, Molecular Interactions of Cyclam and Bicyclam Non-peptide Antagonists with the CXCR4 Chemokine Receptor. *J. Biol. Chem.* 276, (2001) 14153–14160.

114) M.M. Rosenkilde, L.O. Gerlach, J.S. Jakobsen, R.T. Skerlj, G.J. Bridger, T.W. Schwartz, Molecular Mechanism of AMD3100 Antagonism in the CXCR4 Receptor: TRANSFER OF BINDING SITE TO THE CXCR3 RECEPTOR. *J. Biol. Chem.* 279, (2004) 3033–3041.

115) D. Schols, S. Struyf, J. Van Damme, J.A. Este, G. Henson, E. De Clercq, Inhibition of T-tropic HIV Strains by Selective Antagonization of the Chemokine Receptor CXCR4. *J. Exp. Med.* 186, (1997) 1383–1388.

116) S. Hatse, K. Princen, G. Bridger, E. De Clercq, D. Schols, Chemokine receptor inhibition by AMD3100 is strictly confined to CXCR4. *FEBS Lett.* 527, (2002) 255–262.

117) S.K. Gupta , K. Pillarisetti, R.A. Thomas, N. Aiyar, Pharmacological evidence for complex and multiple site interaction of CXCR4 with SDF-1α: implications for development of selective CXCR4 antagonists. *Immunology Letters* 78, (2001) 29–34.

118) C.W. Hendrix, C. Flexner, R.T. MacFarland, C. Giandomenico, E.J. Fuchs, E. Redpath, G. Bridger, G.W. Henson, *Antimicrob. Agents Chemother.* 44, (2000) 1667–1673.

119) C.W. Hendrix, A. Collier, M.M. Lederman, D. Schols, R.B. Pollard, S. Brown, J.B. Jackson, R.W. Coombs, M.J. Glensby, C.W. Flexner, G.J. Bridger, K. Badel, R.T. MacFarland, G.W. Henson, G. Calandra, *J. Acquired Immune Defic. Syndr.* 37, (2004) 1253–1262.

120) R.M. Izatt, K. Pawlak, J.S. Bradshaw, R.L. Bruening, Thermodynamic and kinetic data for macrocycle interactions with cations and anions *Chem. Rev.* 91, (1991) 1721–2085.

121) A. Larochelle, A. Krouse, M. Metzger, D. Orlic, R.E .Donahue, S. Fricker, G. Bridger, C.E. Dunbar, P. Hematti, AMD3100 mobilizes hematopoietic stem cells with long-term repopulating capacity in nonhuman primates *Blood* 107, (2006) 3772–3778.

122) T. Nakamura, H. Furunaka, T. Miyata, F. Tokunaga, T. Muta, S. Iwanaga, M. Niwa, T. Takao, Y. Shimonishi, Tachyplesin, a class of antimicrobial peptide from the hemocytes of the horseshoe crab (Tachypleus tridentatus). Isolation and chemical structure. *J. Biol. Chem.* 263, (1988) 16709–16713.

123) T. Miyata, F. Tokunaga, T. Yoneya, K. Yoshikawa, S. Iwanaga, M. Niwa, T. Takao, Y. Shimonishi Antimicrobial Peptides, Isolated from Horseshoe Crab Hemocytes, Tachyplesin II, and Polyphemusins I and II: Chemical Structures and Biological Activity *J. Biochem.* 106, (1989) 663–668.

124) M. Masuda, H. Nakashima, T. Ueda, A novel anti-HIV synthetic peptide, T-22 ([Tyr^{5,12},Lys^{7}]-polyphemusin II) *Biochem. Biophys. Res. Commun.* 189, (1992) 845–850.

125) H. Nakashima, M. Masuda, T. Murakami, Y. Koyanagi, A. Matsumoto, N. Fujii, N. Yamamoto, Anti-human immunodeficiency virus activity of a novel synthetic peptide, T22 ([Tyr-5,12, Lys-7] polyphemusin II): a possible inhibitor of virus-cell fusion**.** *Antimicrob Agents Chemother.* 36, (1992) 1249–1255.

126) H. Tamamura, Y. Xu, T. Hattori, X. Zhang, R. Arakaki, K. Kanbara, A. Omagari, A. Otaka, T. Ibuka, N. Yamamoto, H. Nakashima N. Fujii, A Low-Molecular-Weight Inhibitor against the Chemokine Receptor CXCR4: A Strong Anti-HIV Peptide T140. *Biochem. Biophys. Res. Commun.* 253, (1998) 877–882.

127) T. Murakami, T. Nakajima, Y. Koyanagi, K. Tachibana, N. Fujii, H. Tamamura, N. Yoshida, M. Waki, A. Matsumoto, O.Yoshie, T. Kishimoto, N. Yamamoto, T. Nagasawa, A Small Molecule CXCR4 Inhibitor that Blocks T Cell Line–tropic HIV-1 Infection. *J. Exp. Med.* 186, (1997) 1389–1393.

128) Y. Xu, H. Tamamura, R. Arakaki, et al. *AIDS Res. Hum. Retroviruses* 15, (1999) 419–427.

129) T. Murakami, T.Y. Zhang, Y. Koyanagi, Y. Tanaka, J. Kim, Y. Suzuki, S. Minoguchi, H. Tamamura, M. Waki, A. Matsumoto, N. Fujii, H. Shida, J.A. Hoxie, S.C. Peiper, N. Yamamoto, Inhibitory Mechanism of the CXCR4 Antagonist T22 against Human Immunodeficiency Virus Type 1 Infection. *J. Virol.* 73, (1999) 7489–7496.

130) K. Kanbara, S. Sato, J. Tanuma, et al. *AIDS Res. Hum. Retroviruses* 17, (2001) 615–622.

131) H. Tamamura, M. Sugioka, Y. Odagaki, A. Omagari, Y. Kan, S. Oishi, H. Nakashima, N. Yamamoto, S.C. Peiper, N. Hamanaka, A. Otaka, No. Fujii, Conformational study of a highly specific CXCR4 inhibitor, T140, disclosing the close proximity of its intrinsic

pharmacophores associated with strong anti-HIV activity**,** *Bioorg. Med. Chem. Lett.*, 11, (2001) 359–362.

132) H. Tamamura, A. Omagari, S. Oishi, Pharmacophore identification of a specific CXCR4 inhibitor, T140, leads to development of effective anti-HIV agents with very high selectivity indexes. *Bioorg Med Chem Lett* 10, (2000) 2633–2637.

133) H. Tamamura, A. Omagari, K. Hiramatsu, Development of specific CXCR4 inhibitors possessing high selectivity indexes as well as complete stability in serum based on an anti-HIV peptide T140. *Bioorg Med Chem Lett*;11, (2001) 1897–1902.

134) H. Tamamura, K. Hiramatsu, S. Kusano, et al. *Org. Biomol. Chem.* 1, (2003) 3656–3662.

135) N. Fujii, S. Oishi, K. Hiramatsu, T. Araki, S. Ueda, H. Tamamura, A. Otaka, S. Kusano, S. Terakubo, H. Nakashima, J.A. Broach, J.O. Trent, Z.Wang, S.C. Peiper, Molecular-Size Reduction of a Potent CXCR4-Chemokine Antagonist Using Orthogonal Combination of Conformation- and Sequence-Based Libraries, *Angew Chem. Int. Ed. Engl.* 42, (2003) 3251–3253.

136) H. Tamamura, A. Esaka, T. Ogawa, T. Araki, S. Ueda, Z. Wang, J.O. Trent, H. Tsutsumi, H. Masuno, H. Nakashima, N. Yamamoto, S.C. Peiper, A. Otaka, N. Fujii. Structure–activity relationship studies on CXCR4 antagonists having cyclic pentapeptide scaffolds. *Org. Biomol. Chem.* 3, (2005) 4392–4394.

137) H. Tamamura, H. Tsutsumi, H. Masuno, S. Mizokami, K. Hiramatsu, Z. Wang, J.O. Trent, H. Nakashima, N. Yamamoto, S.C. Peiper, N..Fujii, Development of a linear type of low molecular weight CXCR4 antagonists based on T140 analogs. *Org Biomol Chem.* 4, (2006) 2354-2357.

138) A. Ojida, Y. Mito-oka, K. Sada, et al. *J. Am. Chem. Soc.* 126, (2004) 2454–2463.

139) H. Tamamura, A.Ojida, T. Ogawa, et al. *J. Med. Chem.* 49, (2006) 3412–3415.

140) T.N. Kledal, M.M. Rosenkilde, F. Coulin, G. Simmons, A.H. Johnsen, S. Alouani, C.A. Power, H.R. Lüttichau, J. Gerstoft, P.R. Clapham, I. Clark-Lewis, T.N. Wells, T.W. Schwartz. A broad-spectrum chemokine antagonist encoded by Kaposi's sarcoma-associated herpesvirus. *Science* 277, (1997) 1656-1659.

141) L. Shan, X. Qiao, E. Oldham, D. Catron, H. Kaminski, D. Lundell, A. Zlotnik, E. Gustafson, J.A. Hedrick, Identification of viral macrophage inflammatory protein (vMIP)-II as a ligand for GPR5/XCR1. *Biochem Biophys Res Commun.* 268, (2000) 938-941.

142) M.P. Crump, E. Elisseeva, J. Gong, I. Clark-Lewis, B.D. Sykes. Structure/function of human herpesvirus-8 MIP-II (1-71) and the antagonist N-terminal segment (1-10). *FEBS Lett.* 489, (2001) 171-175.

143) S. Scala, A. Ottaiano, P.A. Ascierto, et al. Expression of CXCR4 predicts poor prognosis in patients with malignant melanoma. *Clin Cancer Res.* 11, (2005) 1835-1841.

144) E. De Clercq, The AMD3100 story: the path to the discovery of a stem cell mobilizer (Mozobil). *Biochem Pharmacol.* 77, (2009) 1655-1664.

145) S.P. Fricker, V. Anastassov, C. Cox J, M. Darkes, O. Grujic, S.R. Idzan, J. Labrecque, G. Lau, R.M. Mosi, K .L. Nelson, L. Qin, Z. Santucci, R.S.Y. Wong, Characterization of the molecular pharmacology of AMD3100: A specific antagonist of the G-protein coupled chemokine receptor, CXCR4. *Biochemical pharmacology* 72, (2006) 588 – 596.

146) Y.P. Jiang, X.H. Wu, H.Y. Xing, X.Y. DU, Role of CXCL12 in metastasis of human ovarian cancer. *Chin Med J (Engl)* 120, (2007) 1251-1255.

147) J.L. Liesveld, J. Bechelli, K. Rosell, C. Lu, G. Bridger, G. Phillips 2nd, C.N. Abboud, Effects of AMD3100 on transmigration and survival of acute myelogenous leukemia cells. *Leuk Res.* 31 (2007) 1553-1563.

148) R. Philips, M.D. Burdick, M. Lutz, J.A. Belperio, M.P. Keane, R.M. Strieter. The stromal derived factor-1/CXCL12-CXC chemokine receptor 4 biological axis in non-small cell lung cancer metastases. *Am J Respir Crit Care Med*167, (2003) 1676–1686.

149) W.C. Liles, H.E. Broxmeyer, E. Rodger, B. Wood, K. Hubel, S. Cooper, et al. Mobilization of hematopoietic progenitor cells in healthy volunteers by AMD3100, a CXCR4 antagonist. *Blood*; 102, (2003) 2728–2730.

150) K. Hubel, W.C. Liles, H.E. Broxmeyer, E. Rodger, B. Wood, S. Cooper, et al. Leukocytosis and mobilization of CD34+ hematopoietic progenitor cells by AMD3100, a CXCR4 antagonist. *Support Cancer* 1, (2004) 165–172.

151) S.M. Devine, N. Flomenberg, D.H. Vesole, J. Liesveld, D. Weisdorf, K. Badel, et al. Rapid mobilization of CD34+ cells following administration of the CXCR4 antagonist AMD3100 to patients with multiple myeloma and non-Hodgkin's lymphoma. *J Clin Oncol* 22, (2004) 1095–1102.

152) S. Dai, F. Yuan, J. Mu, C. Li, N. Chen, S. Guo, J. Kingery, S.D. Prabhu, R. Bolli, G. Rokosh, Chronic AMD3100 antagonism of SDF-1alpha-CXCR4 exacerbates cardiac dysfunction and remodeling after myocardial infarction. *J Mol Cell Cardiol.* 49, (2010) 587-597.

153) H. Tamamura, Y. Xu, T. Hattori, et al. A low-molecular-weight inhibitor against the chemokine receptor CXCR4: a strong anti-HIV peptide T140. *Biochem Biophys Res Commun* 253, (1998) 877–882.

154) A. Heppeler, S. Froidevaux, A.N. Eberle, H.R. Maecke, Receptor targeting for tumor localisation and therapy with radiopeptides. *Curr Med Chem* 7, (2000) 971–994.

155) E. Kaiser, R.L. Colescott, C.D. Bossinger, P.I. Cook, Color test for detection of free terminal amino groups in the solid-phase synthesis of peptides. *Anal. Biochem* 34, (1970) 595-598.

156) J. Gante, Peptidomimetics—Tailored Enzyme Inhibitors. *Angew. Chem. Int. Ed. Eng.* 33, (1994) 1699-1720.

157) S. Hanessian, G. McNaughton-Smith, H.J. Lombart, W.D. Lubell, Design and Synthesis of Conformationally Constrained Amino Acids as Versatile Scaffolds and Peptide Mimetics. *Tetrahedron* 53, (1997) 12789-12854.

158) C.A. Olsen, H. Franzyk, J.W. Jaroszewski, N-Alkylation and Indirect Formation of Amino Functionalities in Solid-Phase Synthesis. Synthesis (2005) 2631–2653.

159) Y. Sasaki, D.H. Coy, Solid phase synthesis of peptides containing the CH2NH peptide bond isostere. *Peptides* 8, (1987) 119–121.

160) S. Gazal, G. Gellerman, C. Gilon, Novel Gly building units for backbone cyclization: synthesis and incorporation into model peptides. *Peptides* 24, (2003) 1847–1852.

161) L. Yang, K. Chiu, Solid phase synthesis of Fmoc N-methyl amino acids: Application of the Fukuyama amine synthesis. *Tetrahedron Lett* 38, (1997) 7307-7310.

162) S.M. Dankwardt, D.B Smith., J.A. Porco, C.H. Nguyen Solid phase synthesis of N-alkyl sulfonamides. *Synlett.* 25, (1997) 854–856.

163) J.F. Reichwein, R.M.J. Liskamp, Site-specific *N*-alkylation of peptides on the solid phase. *Tetrahedron Lett* 39, (1998) 1243-1246.

164) E. Biron, J. Chatterjee, H. Kessler N-Methylation of Peptides on Solid Support. *J. Pept. Sci.* 12, (2006) 213-219.

165) E. Biron, H. Kessler, Convenient Synthesis of N-Methylamino Acids Compatible with Fmoc Solid-Phase Peptide Synthesis. *J. Org. Chem.* 70, (2005) 5183-5189.

166) M. Stodulski, J. Mlynarski Synthesis of N-alkyl-N-methyl amino acids. Scope and limitations of base-induced N-alkylation of Cbz-amino acids. Tetrahedron: Asymmetry 19, (2008) 970-975.

167) J.H. Cho, B.M. Kim, LiOH-mediated N-monoalkylation of α-amino acid esters and a dipeptide ester using activated alkyl bromides. *Tetrahedron Lett* 43, (2002) 1273-1276.
168) M.L. De Gioia, A. Leggio, A. Liguori N-Methylation of Peptides on Selected Positions during the Elongation of the Peptide Chain in Solution Phase. J. Org. Chem. 70, (2005) 3892-3897.

169) Z.P. Huang, X.Y. Su, J.T. Du, Y.F. Zhao, Y.M. Li, Facile synthesis of Nε-(benzyl, methyl)-lysine as a building block for site-specifically lysine monomethylated peptides. *Tetrahedron Lett.* 47, (2006) 5997–5999.

170) O. Demmer, I. Dijkgraaf, M. Schottelius, H.J. Wester, H. Kessler, Introduction of Functional Groups into Peptides via N-Alkylation H. *Org. Lett.* 10, (2008) 2015-2018.

171) T. Fukuyama, M. Cheung, C.K. Jow, Y. Hidai, T. Kan, 2,4-Dinitrobenzenesulfonamides: A simple and practical method for the preparation of a variety of secondary amines and diamines. *Tetrahedron Lett.* 38, (1997) 583-584.

172) K. Toshiyuki , T. Fukuyama Ns Strategies: A Highly Versatile Synthetic Method for Aminess. *Chem. Commun.* (2004) 353-359.

173) T.W. Greene, P.G.M. Wuts, Protective Groups in Organic Synthesis, 4th ed; John Wiley & Sons: New York, (2007).

174) Y. Rew, M. Goodman Solid-Phase Synthesis of Amine-Bridged Cyclic Enkephalin Analogues via On-Resin Cyclization Utilizing the Fukuyama−Mitsunobu Reaction. *J. Org. Chem.* 67, (2002) 8820-8826.

175) S.C. Miller, T.S. Scanlan oNBS-SPPS: A New Method for Solid-Phase Peptide Synthesis. *J. Am. Chem. Soc.* 120, (1998) 2690-2691.

176) S. De Luca, R. Della Moglie, A. De Capua, G. Morelli New synthetic strategy for o-NBS protected amino acids and their use in synthesis of mono-benzylated peptides. *Tetrahedron Lett.* 46, (2005) 6637-6640.

177) T.F. Andersen, K. Stromgaard, Synthesis of polyamines and polyamine toxins. An improved alkylation procedure. *Tetrahedron Lett.* 45, (2004) 7929–7933.

178) F. Hahn, U. Schepers, Versatile procedure for asymmetric and orthogonal protection of symmetric polyamines and its advantages for solid phase synthesis J. Comb. Chem. 10, (2008) 267-273.

179) A. Isidro-Llobet, M. Alverez, F. Albericio, Amino Acid-Protecting Groups. *Chem. Rev.* 109, (2009) 2455-2504.

180) J.C. Phillips, R.Braun, W. Wang, J. Gumbart, E. Tajkhorshid, E. Villa, C. Chipot, R.D. Skeel, L. Kale, K. Schulten. Scalable molecular dynamics with NAMD. *Journal of Computational Chemistry*, 26, (2005) 1781-1802.

181) A.D. MacKerell Jr.; D. Bashford; M. Bellott; R.L. Dunbrack Jr.; J.D. Evanseck; M.J. Field; S. Fischer; J. Gao; H. Guo; S. Ha; D. Joseph-McCarthy; L. Kuchnir; K. Kuczera; F.T.K. Lau; C. Mattos; S. Michnick; T. Ngo; D.T. Nguyen; B. Prodhom; W.E. Reiher III; B. Roux; M. Schlenkrich; J.C. Smith; R. Stote; J. Straub; M. Watanabe; J. Wiorkiewicz-Kuczera; D. Yin; M. Karplus; "All-Atom Empirical Potential for Molecular Modeling and Dynamics Studies of Proteins", *J. Phys. Chem.* 102, (1998) 3586-3616.

182) R. Koradi, M. Billeter, K. Wu¨thrich, J. MOLMOL: a program for display and analysis of macromolecular structures. *Mol. Graphics* 14, (1996) 51-55.

183) R.C. Sheppard, B.J. Williams, *Int. J. Peptide Protein Res.* 20, (1982) 451–454.

Comunications

1) *Luca Monfregola, Stefania De Luca, Filomena Salapete, Luigi Portella, Rosa Maria Vitale, Piero Amodeo, Stefania Scala.* **New peptide antagonists / agonists as selective ligands for CXCR4 receptor;** 11th Naples Workshop on Bioactive Peptides, Napoli, Italia, Maggio 2008.

2) *Luca Monfregola, Stefania De Luca, Luigi Portella, Rosa Maria Vitale, Piero Amodeo, Stefania Scala.* **New peptide antagonists / agonists as selective ligands for CXCR4 receptor.** Scuola Nazionale di Chimica Bioinorganica, Napoli, Italia, Settembre 2008.

3) Portella L., Mauro F. Napolitano M., Ieranò C., D'Alterio C., Vitale R., Amodeo P., De Luca S., Monfregola L., Castello G. and Scala S. **Design, Synthesis and functional characterization of new peptides inhibitors for C-X-C chemokine receptor-4 (CXCR4).** 50th Annual Meeting of the Italian Cancer Society, Naples, Ottobre 2008

4) Luca Monfregola, Rosa Maria Vitale, Pietro Amodeo, Stefania De Luca. **A SPR strategy for high-throughput ligand screenings based on synthetic peptides mimicking a selected subdomain of the target protein: A proof of concept on HER2 receptor;**12th Naples Workshop on Bioactive Peptides, Napoli, Italia, Giugno 2010

Pubblications

1) Monfregola L., De Luca S. The Role of HER2 in Target Cancer Therapy and Hypothesized Future Perspectives. *HER2 and Cancer, Chapter IV* **2011** *Nova Science Publishers, Inc.* (In press)

2) Monfregola L., De Luca S. Synthetic Strategy for Side Chain mono-N-Alkylation of Fmoc-amino Acids Promoted by Molecular Sieves. *Amino Acids,* **2010**, published on line: 11 November 2010 [DOI 10.1007/s00726-010-0798-6]

3) Verardi R., Traaseth N.J., Shi L., Porcelli F., Monfregola L., De Luca S., Amodeo P., Veglia G., Scaloni A. Probing membrane topology of the antimicrobial peptide distinctin by solid-state NMR spectroscopy in zwitterionic and charged lipid bilayers. *Biochim Biophys Acta,* **2010**, Aug 16. [Epub ahead of print])

4) Monfregola L.,Saviano M.and De Luca S. Synthesis and Characterization of a Selective Alpha(v)Beta(3) Receptor Cyclic Peptide Antagonist Functionalized with a Chelating Group for Metal Labelling. *International Journal of Peptide research and therapeutics,* **2009**,16(1):1-5;

5) Monfregola L., Vitale R.M., Amodeo P. and De Luca S. A SPR strategy for high-throughput ligand screenings based on synthetic peptides mimicking a selected subdomain of the target protein: A proof of concept on HER2 receptor. *Bioorganic & Medicinal Chemistry,* **2009**, 17(19): 7015-20;